

การประชุมความร่วมมือระหว่างอุปกรณ์เติมอากาศเชิงกลที่ผิวน้ำและอุปกรณ์กระจายฟองอากาศในด้าน  
ประสิทธิภาพการถ่ายเทออกซิเจนและประสิทธิภาพเชิงพลังงาน



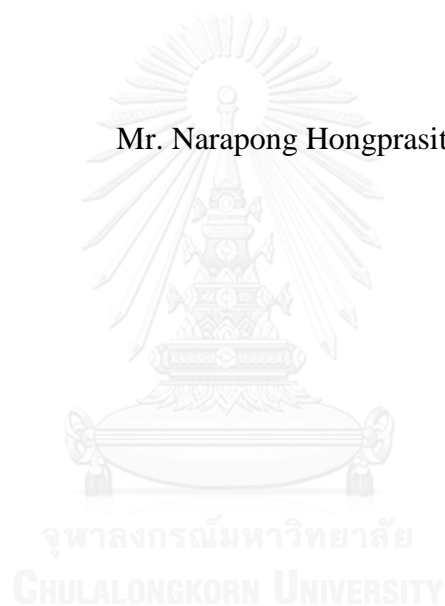
บทคัดย่อและแฟ้มข้อมูลฉบับเต็มของวิทยานิพนธ์ตั้งแต่ปีการศึกษา 2554 ที่ให้บริการในคลังปัญญาจุฬาฯ (CUIR)  
เป็นแฟ้มข้อมูลของนิสิตเจ้าของวิทยานิพนธ์ ที่ส่งผ่านทางบัณฑิตวิทยาลัย

The abstract and full text of theses from the academic year 2011 in Chulalongkorn University Intellectual Repository (CUIR)  
are the thesis authors' files submitted through the University Graduate School.

วิทยานิพนธ์นี้เป็นส่วนหนึ่งของการศึกษาตามหลักสูตรปริญญาวิศวกรรมศาสตรดุษฎีบัณฑิต  
สาขาวิชาวิศวกรรมสิ่งแวดล้อม ภาควิชาวิศวกรรมสิ่งแวดล้อม  
คณะวิศวกรรมศาสตร์ จุฬาลงกรณ์มหาวิทยาลัย  
ปีการศึกษา 2559  
ลิขสิทธิ์ของจุฬาลงกรณ์มหาวิทยาลัย

COMBINATION OF SURFACE AND DIFFUSED AERATORS IN TERM OF  
OXYGEN TRANSFER EFFICIENCY AND ENERGY PERFORMANCE

Mr. Narapong Hongprasith



A Dissertation Submitted in Partial Fulfillment of the Requirements  
for the Degree of Doctor of Philosophy Program in Environmental Engineering  
Department of Environmental Engineering  
Faculty of Engineering  
Chulalongkorn University  
Academic Year 2016  
Copyright of Chulalongkorn University

Thesis Title	COMBINATION OF SURFACE AND DIFFUSED AERATORS IN TERM OF OXYGEN TRANSFER EFFICIENCY AND ENERGY PERFORMANCE
By	Mr. Narapong Hongprasith
Field of Study	Environmental Engineering
Thesis Advisor	Associate Professor Pisut Painmanakul, Ph.D.
Thesis Co-Advisor	Professor Tsuyoshi IMAI, Ph.D.

---

Accepted by the Faculty of Engineering, Chulalongkorn University in  
Partial Fulfillment of the Requirements for the Doctoral Degree

..... Dean of the Faculty of Engineering  
(Associate Professor Supot Teachavorasinskun, Ph.D.)

#### THESIS COMMITTEE

..... Chairman  
(Assistant Professor Chaiyaporn Puprasert, Ph.D.)

..... Thesis Advisor  
(Associate Professor Pisut Painmanakul, Ph.D.)

..... Thesis Co-Advisor  
(Professor Tsuyoshi IMAI, Ph.D.)

..... Examiner  
(Assistant Professor On-anong Larpparisudthi, Ph.D.)

..... Examiner  
(Associate Professor Patiparn Punyapalakul, Ph.D.)

..... External Examiner  
(Marupatch Jamnongwong, Ph.D.)

นราพงศ์ หงส์ประสิทธิ์ : การประยุกต์ร่วมระหว่างอุปกรณ์เติมอากาศเชิงกลที่ผิวน้ำและอุปกรณ์กระจายฟองอากาศในด้านประสิทธิภาพการถ่ายเทออกซิเจนและประสิทธิภาพเชิงพลังงาน (COMBINATION OF SURFACE AND DIFFUSED AERATORS IN TERM OF OXYGEN TRANSFER EFFICIENCY AND ENERGY PERFORMANCE) อ.ที่ปรึกษาวิทยานิพนธ์หลัก: รศ. ดร.พิสุทธิ เพ็ชรมนกุล, อ.ที่ปรึกษาวิทยานิพนธ์ร่วม: ศ. ดร.ซีโยชิ อิโมอิ, 108 หน้า.

งานวิจัยนี้มีจุดประสงค์ในการศึกษาแนวทางการพัฒนาประสิทธิภาพของระบบเติมอากาศทั้งในด้านการถ่ายเทออกซิเจนและประสิทธิภาพเชิงพลังงาน โดยการประยุกต์ใช้ท่ออย่างยืดหยุ่นเป็นอุปกรณ์กระจายฟองอากาศ (Diffuser) โดยจากการศึกษาสมบัติทางกายภาพของท่ออย่างยืดหยุ่น ได้แก่ ขนาดรูพรุน (Orifice diameter,  $d_{OR}$ ) ความทนต่อแรงดึง (Tensile strength) และ ความยืด (Elongation) เป็นต้น เพื่อศึกษาความสัมพันธ์ระหว่างสมบัติทางกายภาพของตัวอุปกรณ์ ต่อกลไกการสร้างฟองอากาศซึ่งจะส่งผลไปยังประสิทธิภาพการถ่ายเทออกซิเจน หลังจากนั้นจึงศึกษาแนวทางการเพิ่มประสิทธิภาพโดยอุปกรณ์สร้างฟิล์มของเหลวที่ผิวน้ำ (Liquid Film Forming Apparatus, LFFA) ที่เป็นอุปกรณ์ที่ติดตั้งและใช้งานได้ง่าย โดยมีความสามารถในการสร้างพื้นผิวสัมผัสจำเพาะ (a) ได้อย่างมากและสามารถเพิ่มประสิทธิภาพการถ่ายเทออกซิเจนได้มากถึงร้อยละ 37

อย่างไรก็ตาม จากผลการศึกษาทำให้ทราบว่า การกวนผสมเป็นอีกกลไกหนึ่งที่สำคัญในการกระจายออกซิเจนละลายในน้ำให้ทั่วถึง และมีความสัมพันธ์ต่อประสิทธิภาพเชิงพลังงานอีกด้วย จึงเป็นที่มาของการศึกษาระบบเติมอากาศแบบร่วม (Combination aeration system) ซึ่งเป็นการประยุกต์ร่วมกันระหว่างอุปกรณ์กระจายฟองอากาศและอุปกรณ์กวนผสม (เครื่องสูบน้ำ)

จากผลการทดลอง พบว่า ขนาดรูพรุนของท่ออย่างยืดหยุ่นมีความสัมพันธ์ต่อขนาดฟองอากาศที่สร้างได้ในขณะที่ความทนต่อแรงดึงและความยืดแสดงถึงความเหนียวซึ่งส่งผลต่อการสูญเสียประสิทธิภาพเชิงพลังงาน หากมีค่าดังกล่าวมากจนเกินไป สำหรับการประยุกต์ใช้อุปกรณ์สร้างฟิล์มของเหลวที่ผิวน้ำในบ่อเพาะเลี้ยงสัตว์น้ำพบว่าสามารถเพิ่มประสิทธิภาพเชิงพลังงานของระบบกระจายฟองอากาศจนสูงกว่าระบบแบบใบพัดตีน้ำถึง 3 เท่า แต่ยังคงมีความจำเป็นในการเพิ่มประสิทธิภาพการกวนผสมเพื่อให้เพาะเลี้ยงสัตว์น้ำได้จริง

สำหรับระบบเติมอากาศแบบร่วม พบว่าการกวนผสมโดยการสร้างกระแสในแนวราบ ช่วยเพิ่มประสิทธิภาพการถ่ายเทออกซิเจนในบ่อเติมอากาศที่มีพื้นที่กว้างได้สูงถึงร้อยละ 100 เมื่อเปรียบเทียบกับระบบใบพัดตีน้ำแบบจำลอง นอกจากนี้ การรวบรวมผลการทดลองต่างๆยังสามารถสร้างเป็นแบบจำลองทางคณิตศาสตร์เพื่อใช้ทำนายค่าสัมประสิทธิ์การถ่ายเทออกซิเจน ( $k_L a$ ) ได้โดยมีความคลาดเคลื่อนไม่เกินร้อยละ 10 ซึ่งสามารถใช้เป็นเกณฑ์ในการออกแบบระบบเติมอากาศต่อไปได้ อย่างไรก็ตาม ยังมีความจำเป็นที่ต้องศึกษาเพิ่มเติมเพื่อพัฒนาให้แบบจำลองดังกล่าวสามารถใช้งานได้หลากหลายและมีความแม่นยำมากขึ้นด้วย

ภาควิชา วิศวกรรมสิ่งแวดล้อม

ลายมือชื่อนิติต .....

สาขาวิชา วิศวกรรมสิ่งแวดล้อม

ลายมือชื่อ อ.ที่ปรึกษาหลัก .....

ปีการศึกษา 2559

ลายมือชื่อ อ.ที่ปรึกษาร่วม .....

# # 5471441521 : MAJOR ENVIRONMENTAL ENGINEERING

KEYWORDS: COMBINATION AERATION SYSTEM / HORIZONTAL WATER VELOCITY / VOLUMETRIC MASS TRANSFER COEFFICIENT / AERATION EFFICIENCY / BUBBLE HYDRODYNAMIC PARAMETERS / FLEXIBLE RUBBER TUBE DIFFUSER / PHYSICAL DIFFUSER PROPERTIES / LIQUID FILM FORMING APPARATUS (LFFA)

NARAPONG HONGPRASITH: COMBINATION OF SURFACE AND DIFFUSED AERATORS IN TERM OF OXYGEN TRANSFER EFFICIENCY AND ENERGY PERFORMANCE. ADVISOR: ASSOC. PROF. PISUT PAINMANAKUL, Ph.D., CO-ADVISOR: PROF. TSUYOSHI IMAI, Ph.D., 108 pp.

Paddle wheels are widely used in aquaculture pond in Thailand due to convenient installation and operation, with an ability to supply oxygen together with making water circulation as their advantage. But the low oxygen transfer efficiency (OTE) and energy performance (Aeration efficiency, AE) should be considered as the main drawback of this aerator type, because they can make a contacting area between air (oxygen) and water at the water surface only. While diffused aerators present a high OTE and AE. However, their mixing performance in the vertical direction is not enough for a large aquaculture pond. Then it is necessary to apply another equipment to perform water flow or horizontal water circulation, such as axial propellers, water pump, or paddle wheels. To fulfill this gap, a combination aeration system was setup by combining the diffused aerators and water pumps: diffused aerators play the role for an oxygen transfer mechanism, while water pumps creating a horizontal circulation for the oxygen distribution. It was found that the highest AE (0.47 kg-O<sub>2</sub>/kW-hr) was obtained when applying 57 mm/s of the horizontal water velocity during the aeration by 2 sets of the flexible rubber tube diffuser. This AE value was closed to 0.51 kg-O<sub>2</sub>/kW-hr of 3 sets of diffusers, and higher than a system contained by 2 units of 60W water pumps, (which represented as a paddle wheels system) up to 47 times. The uniform DO distribution was obtained by 57 mm/s of the horizontal water velocity, and the improvement of oxygen transfer was obtained by reducing of bubble size ( $d_B$ ) and their rising velocity ( $U_B$ ) which can produce more interfacial area (a-area) up to 278%. Moreover, both of oxygen transfer parameters and bubble hydrodynamic parameters can be predicted accurately by the theoretical prediction models with an error lower than 10% for the combination aeration system that can be used as a criterion for the aeration system design.

Department: Environmental Engineering

Field of Study: Environmental Engineering

Academic Year: 2016

Student's Signature .....

Advisor's Signature .....

Co-Advisor's Signature .....

## ACKNOWLEDGEMENTS

This Thesis has the financial support from the Ratchadapisek Sompoch Endowment Fund (2016), Chulalongkorn University (Project Number CU-59-022-FW) and research funding of Faculty of Engineering, Chulalongkorn University. The authors would like to acknowledge the Graduate school of Chulalongkorn University, Center of Excellence for Environmental and Hazardous Waste Management (EHWM) of Chulalongkorn University for additional financial and technical support, as well as, the Faculty of Marine Technology of Burapha University at their Chanthaburi campus for location support, and the CHAREON PHATARA PANICH CO., LTD. for materials supply.

I would like to express my special thanks of gratitude to my advisor, and co-advisor: Assoc. Prof. Pisut Painmanakul, Ph.D. and Prof. Tsuyoshi Imai, Ph.D., respectively, who gave me the valuable opportunity to do this thesis topic, which also helped me, suggested me in doing a lot of research and I came to know about so many new things, I am really thankful to them.

I would like to thank my friends for their feedback, cooperation and of course friendship. Last but not the least, I would like to thank my family: my parents and to my brothers and sister for supporting me spiritually throughout writing this thesis and my life in general.

## CONTENTS

	Page
THAI ABSTRACT .....	iv
ENGLISH ABSTRACT.....	v
ACKNOWLEDGEMENTS.....	vi
CONTENTS.....	vii
List of Tables .....	ix
List of Figures .....	x
CHAPTER 1 INTRODUCTION .....	1
1.1 Introduction .....	1
1.2 Objectives .....	2
1.3 Scope of Research .....	2
CHAPTER 2 EFFECTS OF PHYSICAL PROPERTIES OF DIFFUSED AERATOR ON OXYGEN TRANSFER EFFICIENCY AND BUBBLE HYDRODYNAMIC PARAMETERS.....	5
2.1 Introduction .....	5
2.2 Objectives .....	5
2.3 Literature Review .....	6
2.4 Materials and Methods .....	9
2.5 Results and Discussion .....	13
2.6 Conclusions .....	29
CHAPTER 3 IMPROVEMENT OF OXYGEN TRANSFER EFFICIENCY IN TERM OF INTERFACIAL AREA INCREASE BY LIQUID FILM FORMING APPARATUS (LFFA).....	31
3.1 Introduction .....	31
3.2 Objectives .....	32
3.3 Literature Review .....	32
3.4 Materials and Methods .....	33
3.5 Results and Discussion .....	39
3.6 Conclusions .....	47

	Page
CHAPTER 4 STUDY OF COMBINATION AERATION SYSTEM IN TERM OF OXYGEN TRANSFER EFFICIENCY AND ENERGY PERFORMANCE IN PILOT-SCALE EXPERIMENT .....	49
4.1 Introduction .....	49
4.2 Objectives .....	50
4.3 Literature Review .....	50
4.4 Materials and Methods .....	52
4.5 Results and Discussion .....	60
4.6 Conclusions .....	74
CHAPTER 5 CONCLUSIONS AND RECOMMENDATIONS .....	78
5.1 Effects of physical properties of diffused aerator on oxygen transfer efficiency and bubble hydrodynamic parameters .....	78
5.2 Improvement of oxygen transfer efficiency in term of interfacial area increase by Liquid Film Forming Apparatus (LFFA) .....	79
5.3 Study of combination aeration system in term of oxygen transfer efficiency and energy performance in pilot-scale experiment .....	79
5.4 Recommendations for the future .....	80
REFERENCES .....	82
Appendix A The oxygen transfer performance of the flexible tube diffuser .....	86
Appendix B Liquid Film Forming Apparatus (LFFA) in the aquaculture pond .....	92
Appendix C The combination aeration system performance in 680L of pilot-scale experiment .....	93
Appendix D The oxygen transfer parameters and bubble hydrodynamic parameters calculation .....	100
VITA .....	108



## List of Tables

	Page
Table 2.1 Physical properties of diffused aerators and analytic methods.....	10
Table 2.2 Oxygen transfer performance of flexible aeration diffuser tube.....	13
Table 2.3 Physical characteristic of flexible aeration diffuser tube.....	16
Table 2.4 Bubble hydrodynamic parameters of flexible tube No. 12.....	19
Table 2.5 Bubble hydrodynamic parameters of the studied diffusers: bubble diameter ( $d_B$ ), bubble rising velocity ( $U_B$ ), and specific interfacial area (a).....	23
Table 2.6 RTD result of flexible tube No. 12 in the installation test.....	27
Table 2.7 The recommended operational condition for the flexible aeration diffuser tube .....	30
Table 3.1 The operational conditions of the experiment.....	34
Table 3.2 Oxygen transfer performance of LFFA in the laboratory aeration tank ...	40
Table 3.3 The operation conditions of the experiment .....	47
Table 3.4 The recommended operation condition for the LFFA .....	48
Table 4.1 Existing correlations for predicting bubble diameter ( $d_B$ ) .....	56
Table 4.2 Existing correlations for predicting bubble rising velocity ( $U_B$ ) .....	57
Table 4.3 Residence time distribution study (RTD) results.....	66
Table 4.4 Correlations for bubble diameter ( $d_B$ ) prediction.....	68
Table 4.5 Correlations for bubble rising velocity ( $U_B$ ) prediction.....	68
Table 4.6 Correlations for liquid-side mass transfer coefficient ( $k_L$ ) prediction .....	69
Table 4.7 The recommended installation and operational condition for the combination aeration system.....	75
Table 4.8 The recommended prediction model for the volumetric mass transfer coefficient.....	76

## List of Figures

		Page
Figure 1.1	Diagram of research.....	4
Figure 2.1	Comparison of fouling factor between the used Ethylene–Propylene-Diene Monomer (EPDM) membrane diffuser and the new EPDM membrane diffuser .....	7
Figure 2.2	Comparison of pressure factor between the used EPDM membrane diffuser and the new EPDM membrane diffuser .....	8
Figure 2.3	Experimental set-up for the study of physical properties of diffused aerators.....	9
Figure 2.4	Porous stone tube, Flexible membrane, and Flexible rubber tube diffuser .....	9
Figure 2.5	Capture of bubbles for bubble hydrodynamic analyze .....	11
Figure 2.6	Diagram of physical properties of diffused aerators study .....	13
Figure 2.7	Aeration efficiency of the different flexible tube diffusers .....	15
Figure 2.8	Operational pressure versus gas flow rate for different flexible aeration diffuser tubes.....	17
Figure 2.9	Image analysis results of flexible tube No. 12.....	18
Figure 2.10	Interfacial area of flexible tube No. 12.....	19
Figure 2.11	The conventional diffused aerators.....	22
Figure 2.12	Comparison of the flexible tube to the conventional aerators in term of $k_{La}$ and AE.....	23
Figure 2.13	Experimental set up and installation pattern in the pilot-scale .....	25
Figure 2.14	Comparison of $k_{La}$ coefficient and pressure of the flexible tube No. 12 in the pilot-scale.....	26
Figure 2.15	Comparison of conductivity with time .....	26
Figure 2.16	Comparison of the experimental and predicted $k_{La}$ coefficient of flexible tube No. 12 .....	28
Figure 3.1	Schematic diagrams of the experimental set up for the Liquid-Film-Forming Apparatus (LFFA).....	33

Figure 3.2	The studied aerators in the aquaculture pond.....	34
Figure 3.3	Schematic diagram of the Liquid-Film-Forming Apparatus (LFFA).....	35
Figure 3.4	Top view of the LFFA installation in the laboratory aeration tank.....	36
Figure 3.5	Top view of the Liquid-Film-Forming Apparatus (LFFA) installation ..	37
Figure 3.6	Diagram of improvement of oxygen transfer efficiency by the LFFA....	39
Figure 3.7	Oxygen transfer performance of LFFA in the aquaculture pond. The data was shown as the mean $\pm$ SD, from 12 monitoring positions.....	42
Figure 3.8	Application of the LFFA .....	44
Figure 3.9	Comparison of the oxygen transfer performance. The data was shown as the mean $\pm$ SD, from 12 monitoring positions.....	45
Figure 4.1	Flexible rubber tube diffuser.....	52
Figure 4.2	Water pump.....	52
Figure 4.3	Schematic diagrams of the Experimental set up.....	55
Figure 4.4	Relation of generated bubble diameter ( $d_B$ ) and bubble rising velocity ( $U_B$ ) (Grace and Wairegi) .....	58
Figure 4.5	Diagram of Combination aeration system study.....	60
Figure 4.6	Effects of the horizontal water velocity ( $v_H$ ) on the oxygen transfer performance .....	61
Figure 4.7	Comparison of the aeration systems in term of the oxygen transfer performance .....	62
Figure 4.8	Changing of bubble rising direction by the horizontal water velocity ( $v_H$ ).....	63
Figure 4.9	Effects of the horizontal water velocity ( $v_H$ ) on the bubble hydrodynamic parameter ( $d_B$ and $U_B$ ) .....	64
Figure 4.10	Effects of the horizontal water velocity ( $v_H$ ) on the Interfacial area (a).....	64
Figure 4.11	The effluent residence time distribution curve and the tanks-in-series model .....	66
Figure 4.12	Predicted results of bubble diameter ( $d_B$ ) for the combination aeration system .....	69
Figure 4.13	Predicted results of bubble rising velocity ( $U_B$ ) for the combination aeration system .....	70

Figure 4.14	Comparison of predicted bubble diameter to the experimental result ....	71
Figure 4.15	Comparison of predicted bubble rising velocity to the experimental result.....	72
Figure 4.16	Comparison of predicted liquid side mass transfer coefficient to the experimental result.....	73
Figure 4.17	Comparison of predicted volumetric mass transfer coefficient to the experimental result.....	74
Figure 4.18	The guideline for the combination aeration system design .....	77



# CHAPTER 1

## INTRODUCTION

### 1.1 Introduction

In aeration processes, oxygen is generally introduced by either diffused or mechanical surface aerators. Contacting between the gas phase and the liquid phase is the important factor for the oxygen transfer, due to interfacial area is used as an oxygen transfer pathway. The introduced oxygen will be transferred into the liquid phase as the dissolved oxygen (DO) via that interfacial film between gas phase and liquid phase, after that turbulence or mixing will be needed due to distribution of the DO concentration. The volumetric mass transfer coefficient ( $k_L a$ ) is widely used to evaluate aeration performance, by observing the DO increase with time, after that the oxygen transfer efficiency (OTE) and aeration efficiency (AE) can be calculated, therefore they can describe the oxygen transfer rate per power consumption as an energy performance. Normally, the  $k_L a$  coefficient can be experimentally obtained as a combined parameter, which consists of liquid-side mass transfer coefficient ( $k_L$ ) and interfacial area ( $a$ ). The  $k_L$  coefficient relates with the water properties, which affect on the oxygen transfer mechanism through the interfacial film. The  $a$ -area relates to the bubbles characteristics in term of the interface area per overall volume, which is included by the gas volume and the liquid volume.

Generally, the paddle wheels are widely used in Thailand due to their advantage for applying oxygen and having the horizontal mixing, for the aquaculture pond which has a large-surface area. However, the low oxygen transfer efficiency and energy performance should be considered as the main drawback of this aerator type. Therefore, the diffusers which have the higher oxygen transfer efficiency should be applied for further. The advantage can be obtained as a combination of them: the diffusers for aeration while the paddle wheels for mixing or oxygen distribution. Furthermore, bubble diameter will be reduced by shear force from the water cross-flow that can improve the oxygen transfer rate by increase of the  $a$ -area. The objective of this research is to study the oxygen transfer mechanism and bubble hydrodynamic parameters, which can be occurred by the combination of different aerators (diffusers and paddle wheels), due to improve the aeration system both term of oxygen transfer efficiency and energy performance. Then the optimum operating condition, which can achieve the best oxygen transfer efficiency while consume the lowest of energy, will be investigated. After that the results are expected to be proposed as a design criteria and operation guideline for this alternative aeration system.

## 1.2 Objectives

- 1.2.1 To study and develop aeration process in both terms of oxygen transfer efficiency and energy performance.
- 1.2.2 To propose the suitable theoretical prediction model for predicting bubble hydrodynamic and oxygen transfer parameters, then the prediction parameters can be used as a primary data for aeration process design.

## 1.3 Scope of Research

This research is separated into 3 parts, the first part focuses on the physical properties of the diffusers that affect on oxygen transfer efficiency and mechanism through bubble hydrodynamic parameters. The second part focuses on improvement of oxygen transfer efficiency in term of interfacial area by the Liquid-Film-Forming Apparatus (LFFA). The last part of this research focuses on investigation of the suitable operational condition of the combination aeration system (diffusers and mixing devices), together with the oxygen transfer mechanism study. Then the suitable condition will be validated in the actual-scale of aquaculture pond, and proposed as an operational guideline for this combination aeration system. For details on each part are as follow:

- 1.3.1 Effects of diffused aerator physical properties on oxygen transfer efficiency and bubble hydrodynamic parameters

The different diffused aerators (such as membrane diffusers, flexible tube diffusers, and porous rigid diffusers) will be chosen from their general application, studied and investigated for the relation to oxygen transfer efficiency in the laboratory experiment. The experiment will be set up in 0.6m x 0.6m x 0.6m in dimension of aeration tank. The diffusers will be characterized in term of their orifice size, surface texture and thickness, toughness, and tensile strength, as well as the relation between physical properties and oxygen transfer will be investigated. The oxygen transfer will be evaluated by oxygen transfer rate as a  $k_L a$  coefficient, together with the bubble hydrodynamic parameters observation. Therefore, the suitable diffuser with the suitable properties can be proposed for the aeration system.

- 1.3.2 Improvement of oxygen transfer efficiency in term of interfacial area increase by Liquid Film Forming Apparatus (LFFA)

The Liquid Film Forming Apparatus (LFFA) is applied to improve oxygen transfer efficiency for diffuser systems, through interfacial area increase by foam creating at the water surface. However, the operational condition is still needed to be

investigated. Then the experiment will be set up in 0.6m x 0.6m x 0.6m in dimension of aeration tank, in the same scale as previous part of this research. The condition will be considered on installation pattern (number of equipment, and arrangement), and supplied air flow rate in an actual scale of aquaculture pond, 10m x 10m x 1.5m in dimension. The suitable diffuser from the previous experiment will be applied and combined with LFFA to investigate the suitable operational condition, and propose as an application guideline for the LFFA.

### 1.3.3 Study of combination aeration system in term of oxygen transfer efficiency and energy performance in pilot-scale experiment

This experiment will be set up in the aeration tank, 1m x 2m x 0.6m in dimension, for studying the aeration mechanism and system installation when the diffusers and mixing devices are applied as a combination for aeration system. The diffusers are expected to improve the aeration efficiency, while the mixing devices can improve the oxygen distribution, therefore the combination of them can improve both terms of oxygen transfer efficiency and energy performance. The suitable operating condition will be investigated through the devices installation, air flow rate, and horizontal mixing level, which can be evaluated in term of the OTE, AE, and horizontal water velocity. Moreover, bubble hydrodynamic parameters will be observed for studying aeration mechanism in each experiment condition. And then the suitable operating condition will be applied and validated in actual-scale experiment to propose as an operational guideline for this alternative aeration system.

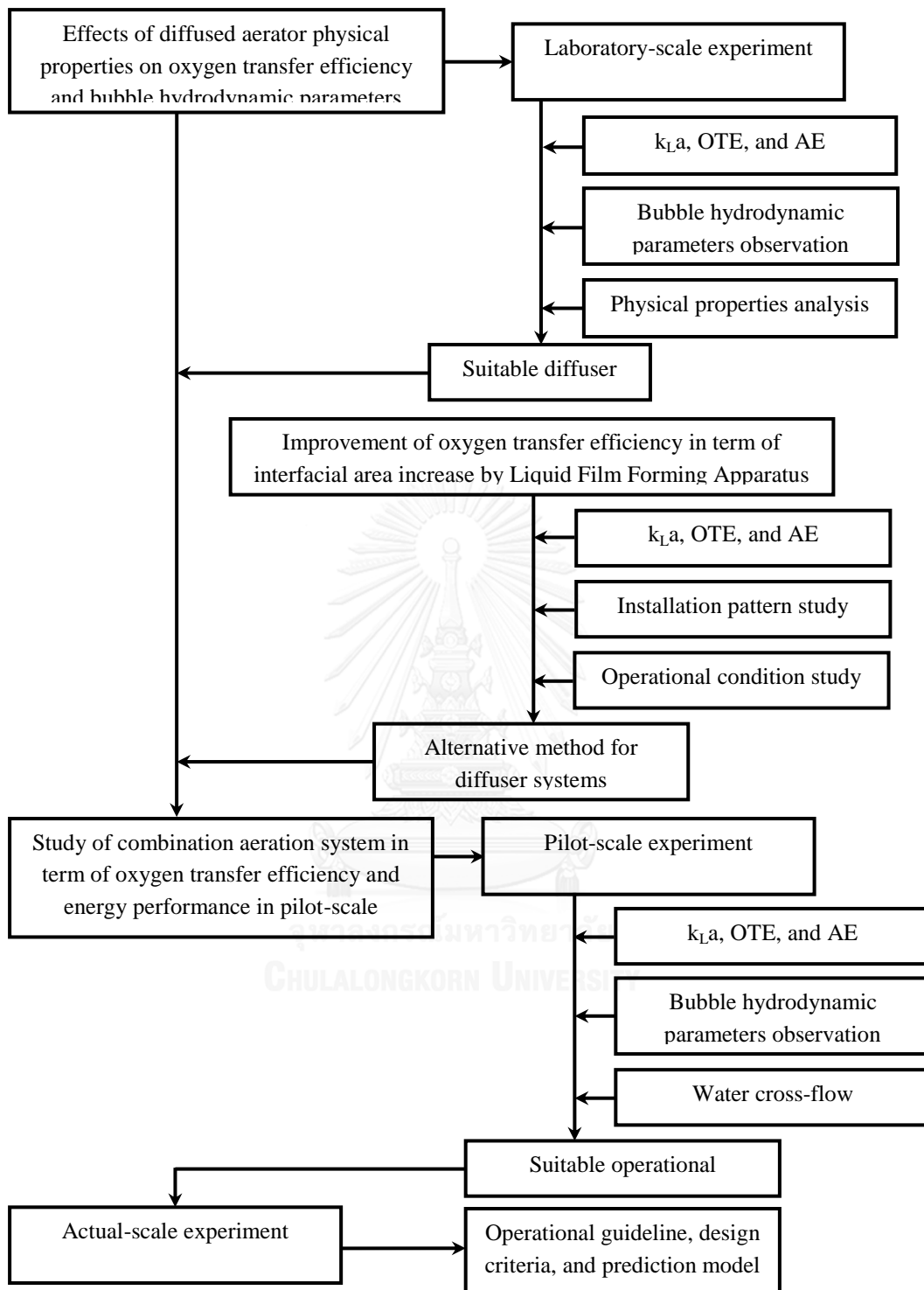


**Figure 1.1** Diagram of research



## **CHAPTER 2**

### **EFFECTS OF PHYSICAL PROPERTIES OF DIFFUSED AERATOR ON OXYGEN TRANSFER EFFICIENCY AND BUBBLE HYDRODYNAMIC PARAMETERS**

#### **2.1 Introduction**

Fine-pore diffused aerators are common used in aeration system in wastewater treatment plant. Porous stone, Punched polymeric membrane, and perforated rubber tube are common used for assembling diffused aerators due to small bubble creation as their advantage. The small bubble size has a large surface of contacting area between bubble (oxygen source) and water that can yield high oxygen transfer rate. However, some type of diffused aerator requires high pressure to create a small bubble because of their physical property that relates to high energy consumption. Even their applications are the same purpose, supplying oxygen for aeration, but they have different physical properties that affect on aeration or oxygen transfer mechanism. Concerning to the aeration system performance and energy consumption, the suitable diffuser should be studied and proposed. This research aims to compare oxygen transfer efficiency and energy performance of the different types of diffused aerator that are always used in any application: wastewater treatment, or aquaculture. Physical property of the diffusers is important factor, which affects on bubble formation and oxygen transfer mechanism that should be studied through observation of bubble formation or movement (bubble hydrodynamic parameters) during the aeration process. Then the suitable diffused aerator can be proposed and recommended for the aeration system.

#### **2.2 Objectives**

- 2.2.1 To compare aeration efficiency of different types of diffused aerators with different physical properties.
- 2.2.2 To study effects of physical properties of diffused aerators on oxygen transfer mechanism, through the bubble hydrodynamic parameters observation.
- 2.2.3 To propose the suitable diffused aerator with the optimum physical properties and aeration efficiency for aeration processes.

### 2.3 Literature Review

In 2008, Rosso and research team found that when fine-pore diffusers are used in aeration systems for long term, fouling and scaling are always occurred and properties of the diffusers would be changed. Fouling by organic matters or scaling by inorganic matters will block introduced air at the pores of diffusers, and affect on pore size reduction or lead to properties change. These effects will increase operational pressure and working load for blowers that may cause an insufficient discharge pressure across the diffusers. The aeration system will produce uneven bubble distribution due to insufficient discharge pressure, which typically associated with uneven dissolved oxygen (DO) concentration, which may lead to odor formation, sludge bulking problems, and poor mixing [1].

In this study, they evaluated the diffusers performance by Standard Oxygen Transfer Efficiency (SOTE) and expressed the ratio of process- to clean-water by  $\alpha$  factor. After that fouling effect was evaluated as a fouling factor and pressure factor, as shown by following equations,

$$\alpha = \frac{\alpha \text{SOTE}}{\text{SOTE}} \quad (2.1)$$

$$F = \frac{\text{SOTE}_{\text{USED}}}{\text{SOTE}_{\text{NEW}}} \quad (2.2)$$

$$P = \frac{\text{DWP}_{\text{USED}}}{\text{DWP}_{\text{NEW}}} \quad (2.3)$$

When it is desirable to differentiate the effects of wastewater contaminants and fouling.  $\text{SOTE}_{\text{USED}}$  is the SOTE of the diffusers when fouling is occurred, and  $\text{SOTE}_{\text{NEW}}$  is the efficiency of the new diffusers without any fouling.  $\text{DWP}_{\text{USED}}$  and  $\text{DWP}_{\text{NEW}}$  are dynamic wet pressure of the used diffusers and the new diffusers, respectively.

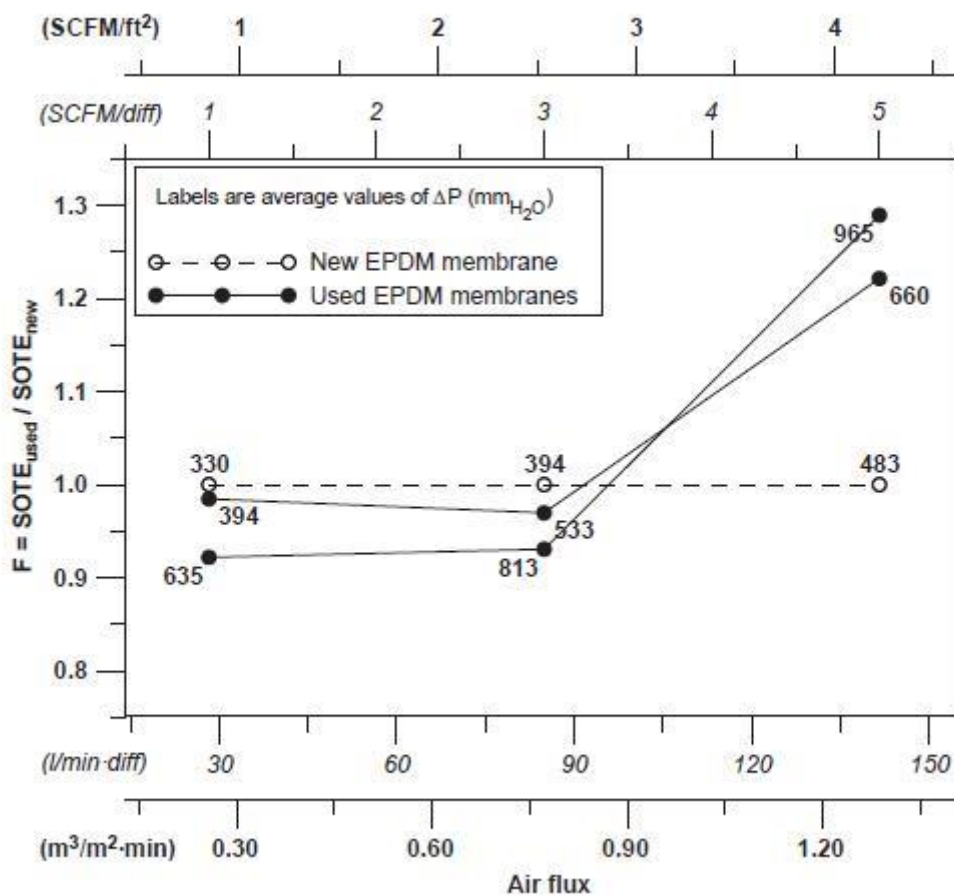


**Figure 2.1** Comparison of fouling factor between the used Ethylene–Propylene-Diene Monomer (EPDM) membrane diffuser and the new EPDM membrane diffuser

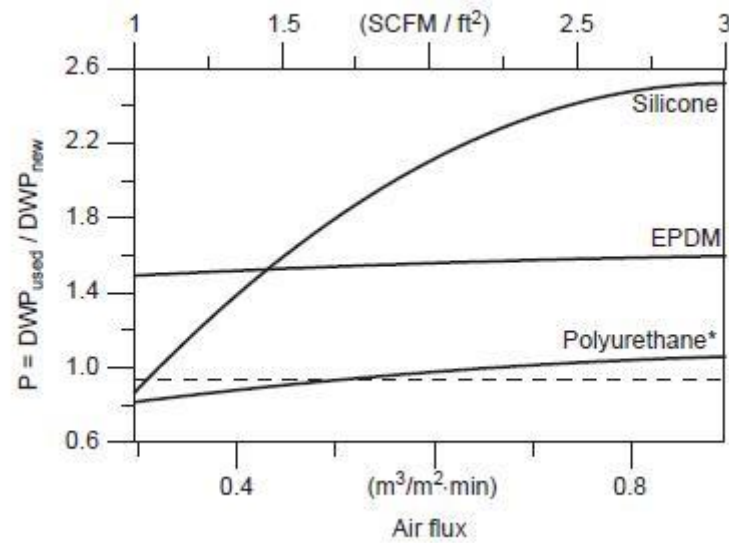


**Figure 2.2** Comparison of pressure factor between the used EPDM membrane diffuser and the new EPDM membrane diffuser

It was found that SOTE of the used membrane diffusers were increased around 20% at high air flow rate when the fouling was occurred, but the operational pressure that was represented by P-factor was increased around 40%-50%. Moreover, some properties of the diffusers were changed by fouling and diffuser ageing itself, some diffuser pore was torn and bubble distribution was affected. This fouling affects on increase of electrical power consumption and leads to failure of the system [1].

From my previous research, the relation between properties of flexible rubber tube diffuser and oxygen transfer efficiency was studied in 10 L of aeration tank. And it was found that:

- Orifice size or diffuser pore relates to generated bubble size directly.
- Thickness wall of the tube relates to bubble formation distribution.
- Toughness and elasticity relate to operational pressure and aeration efficiency.

However, this result is specific for the flexible rubber tube only, so this topic has to be studied for further about oxygen transfer mechanism through bubble hydrodynamic parameters observation, and enlarge scope into other types of diffuser for several applications [2].

## 2.4 Materials and Methods

The experiment will be set-up in 200 L of aeration tank in laboratory scale, 0.6 m in width, 0.6 m in length, and 0.6 m in depth, as shown in the following figure.

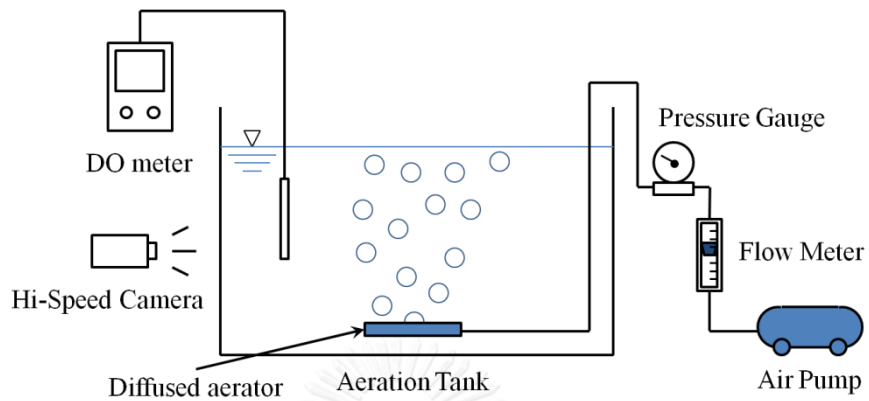


**Figure 2.3** Experimental set-up for the study of physical properties of diffused aerators



a) Porous stone tube diffuser



b) Flexible membrane diffuser



c) Flexible rubber tube diffuser

**Figure 2.4** Porous stone tube, Flexible membrane, and Flexible rubber tube diffuser

The different types of diffuser, which are porous stone diffuser, membrane diffuser, and flexible tube diffuser, will be chosen from several applications with their different physical properties. These properties will be focused on orifice size ( $d_{OR}$ ), wall thickness, rigidity, toughness, and elongation that might affect on the aeration mechanism, as shown by following table,

**Table 2.1** Physical properties of diffused aerators and analytic methods

Parameters		Analytical methods
1.	Orifice diameter	Microscoping
2.	Wall thickness of diffused aerators	Vernier micrometer
3.	Hardness	Durometer
4.	Elasticity	Tensile test

The experiment will be operated in tap water to diminish uncontrolled factors from impurities in the water, with 0-100 L/min of air flow rate. During the aeration period, dissolved oxygen (DO) and operational pressure will be observed to estimate volumetric mass transfer coefficient ( $k_L a$ ), and electrical power consumption. Then the system will be evaluated by oxygen transfer efficiency (OTE) and aeration efficiency (AE) to compare the diffusers both term of efficiency and energy performance. Furthermore, hydrodynamic parameters will be observed during the aeration period to measure generated bubble diameter ( $d_B$ ) and bubble rising velocity ( $U_B$ ) that are the main parameters for calculate interfacial area ( $a$ ), for study and describe the oxygen transfer mechanism.

In this part, the DO during aeration will be measured and converted into the  $k_L a$  coefficient to estimate oxygen mass transfer rate and evaluate the aeration system, by following the American Society of Civil Engineers method (ASCE), and using sodium sulfite ( $Na_2SO_3$ ) for de-oxygenation. The  $k_L a$  coefficient can be estimated by Eq. (2.4), after that it can be rearranged into linear form as Eq. (2.5),

$$\frac{C_S - C_t}{C_S - C_0} = e^{-(k_L a) \times t} \quad (2.4)$$

$$\ln(C_S - C_t) = \ln(C_S - C_0) - k_L a \times t \quad (2.5)$$

Where  $C_S$ ,  $C_t$ , and  $C_0$  are DO in liquid phase in equilibrium, DO at aeration time, and initial DO respectively, and  $t$  is aeration time. After that, the OTE can be calculated by Eq. (2.6),

$$\text{OTE} = \frac{\text{Oxygen}_{\text{Transferred}}}{\text{Oxygen}_{\text{Introduced}}} = \frac{k_L a \times C_S \times V}{\rho_G \times Q_G \times W_{O_2}} \quad (2.6)$$

Where  $V$  is aerated water volume,  $\rho_G$  and  $Q_G$  are the introduced air density and the air flow rate, respectively. Moreover, the energy performance can be evaluated by electrical power consumption ( $P$ ) and AE, which can be calculated by following equations,

$$P = Q_G \times \Delta P_{\text{Total}} = Q_G \times (\rho_L \times g \times H_L + \Delta P) \quad (2.7)$$

$$\text{AE} = \frac{\text{Oxygen transfer rate}}{\text{Power consumption}} = \frac{k_L a \times C_S \times V}{P} \quad (2.8)$$

Where  $\rho_L$  is liquid density,  $g$  is acceleration due to gravity,  $H_L$  is liquid height, and  $\Delta P_{\text{Total}}$  is total head loss through the diffuser [3]. Concerning to the bubble hydrodynamic parameters, the  $d_B$  and  $U_B$  will be experimentally obtained by image analysis system using high speed camera, and then these two parameters can be estimated by following equations,

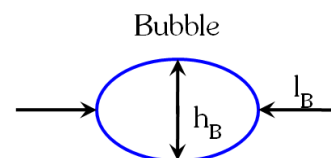
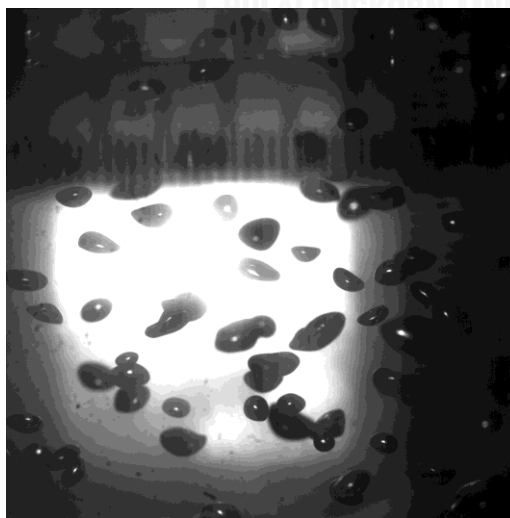


**Figure 2.5** Capture of bubbles for bubble hydrodynamic analyze

$$d_B = (l_B^2 \times h_B)^{1/3} \quad (2.9)$$

$$d_{32} = \frac{\sum d_B^3}{\sum d_B^2} \quad (2.10)$$

$$U_B = \frac{\Delta D}{t_{\text{Frame}}} \quad (2.11)$$

Where  $l_B$  and  $h_B$  are the bubble length and bubble height respectively. Then, Sauter diameter ( $d_{32}$ ) is presented as an averaged bubble size [4].  $\Delta D$  is the bubble spatial displacement between  $t = 0$  and  $t = T_{\text{Frame}}$ , which is 2,000 frames/s of high speed camera in this research. Then, interfacial area ( $a$ ) can be thus expressed as Eq. (2.12)

$$a = \frac{\text{Total surface area}}{\text{Total volume}} = \frac{f_B H_L \pi d_B^2}{U_B (A H_L + N_B V_B)} \quad (2.12)$$

Where  $N_B$  is the generated bubble number,  $f_B$  is the bubble formation frequency,  $H_L$  is the liquid height,  $V_B$  is the bubble volume and  $S_B$  is the bubble surface area and  $A$  is cross-sectional area of the aeration tank [5].

From this study, the relation between physical properties of diffusers, oxygen transfer mechanism, and aeration efficiency are expected to be investigated, through the measurement of volumetric mass transfer coefficient and observation of bubble hydrodynamic parameters. Therefore, comparing the different type of diffusers, and then propose the suitable diffuser with concerning both term of oxygen transfer efficiency and energy performance.



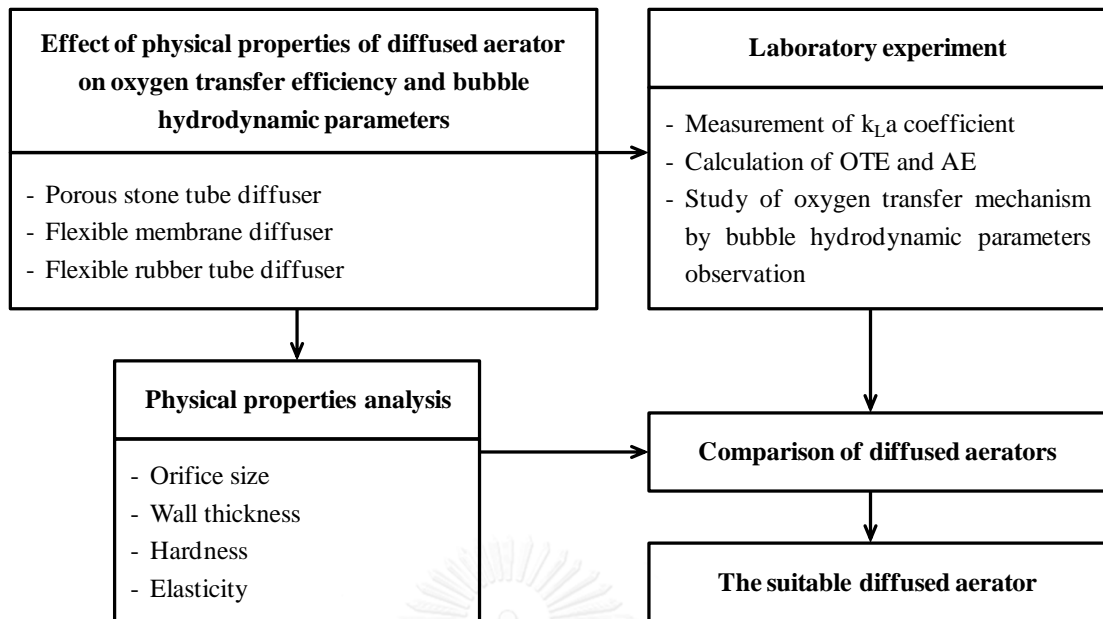


**Figure 2.6** Diagram of physical properties of diffused aerators study

## 2.5 Results and Discussion

### 2.5.1 Volumetric mass (oxygen) transfer coefficients ( $k_L a$ )

**Table 2.2** Oxygen transfer performance of flexible aeration diffuser tube

Tube No.	$k_L a$	OTE	Pressure	AE
	$\times 10^{-3}$ 1/s	%	psi	mg-O <sub>2</sub> /kW-s
1	1.2-5.4	2.1-2.4	3.0-12.0	79-287
2	1.3-3.2	1.4-2.3	1.0-1.4	402-904
3	1.1-2.7	1.2-2.0	0.8-1.2	391-989
4	1.3	2.3	14.0	67
5	1.2-3.0	1.3-2.1	1.0-3.0	178-833
6	1.1-3.0	1.3-1.9	0.8-1.2	441-945
7	1.3-2.2	2.0-2.2	8.0-17.5	45-112
8	1.1-3.7	1.6-2.1	0.8-1.8	366-936
9	1.1-3.8	1.7-1.9	1.0-2.0	334-742
10	1.2-4.7	2.1-2.5	3.2-14.0	59-274
11	1.4-3.4	1.5-2.4	1.8-6.0	99-538
12	1.4-3.9	1.7-2.4	0.8-1.1	631-1,210
13	1.2-3.6	1.6-2.2	1.8-13.0	49-475

14	1.2-3.7	1.6-2.1	0.8-1.2	547-1,059
15	1.3-3.3	1.4-2.3	0.8-1.2	481-1,157
16	1.3-12.2	2.2-5.4	4.0-31.0	69-226
17	1.1-3.7	1.6-2.1	1.0-2.8	234-798
18	1.3-3.3	1.4-2.2	0.8-1.2	480-1,104

The table 2.2 summarized the volumetric mass transfer coefficient ( $k_{La}$ ) of the 18 samples of the flexible aeration tube diffusers, which were different physical properties. From the flexible tube production process, the production condition was varied by changing ingredient (amount of recycled rubber seeds and additional chemicals), melting and casting temperature, casting speed, etc. Until the 18 different tubes were obtained, and compared their oxygen transfer performance by the  $k_{La}$  values. From the result, it was found that no matter what the gas diffusers are, the  $k_{La}$  coefficient increase with the gas flow rate from  $1.2 \times 10^{-3}$  to  $4.0 \times 10^{-3}$  1/s for a gas flow rate varying between 1 and 4 L/min. Except the tube No. 16, the highest  $k_{La}$  values can be observed ( $1.2 \times 10^{-2}$  1/s) but it needed the highest operational pressure (31.0 psi) that represented the highest power consumption was needed, in the same time. For the tube No. 4, it cannot be operated with 2 and 4 L/min of the air flow rate because it required too high of operational pressure that was over range of air pump and pressure gauge (over than 31 psi at 2 L/min of air flow rate). Even the air pump was fully turned on, but it can be operated just only 2 L/min. According to the over range of the operational pressure, the experiments for the tube No. 4 had to be stopped due to the safety concern.

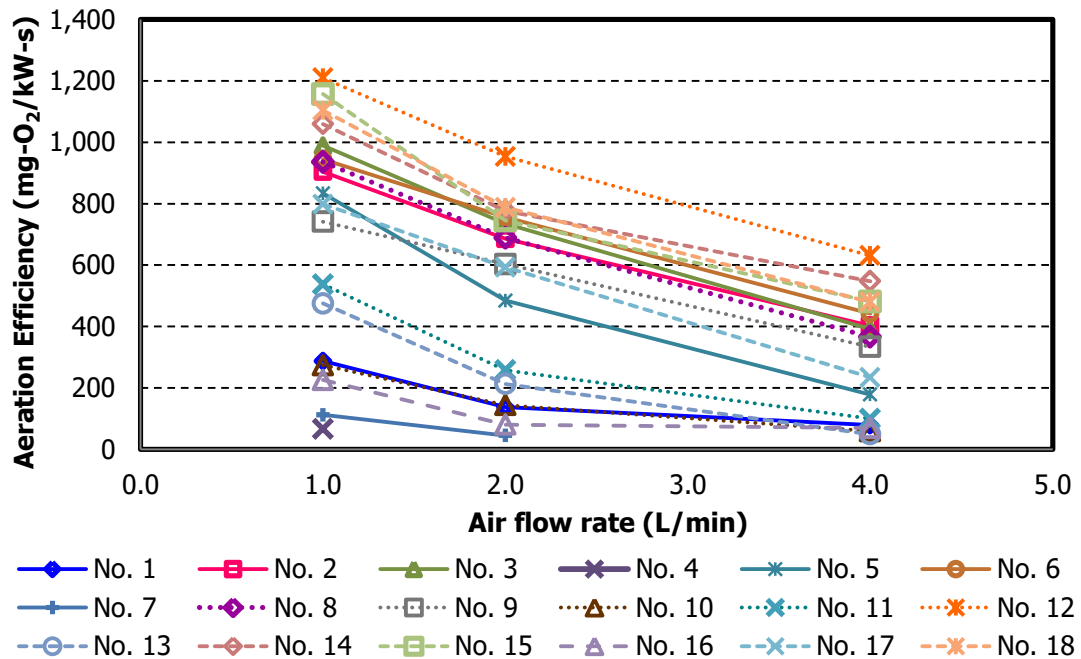


**Figure 2.7** Aeration efficiency of the different flexible tube diffusers

In order to compare the performance of different gas diffusers more clearly, the aeration efficiency (AE) which is an oxygen transfer rate per power consumption should be taken into account. According to Figures 2.7, the values of AE vary between 80 and 1,200 mg-O<sub>2</sub>/kW-s for a gas flow rate varying between 1 and 4 L/min. The highest AE or the highest energy performance was obtained with the tube No. 12 while the  $k_L a$  and OTE were nearly the same value, then the tube No. 12 can be presented as the best flexible tube diffuser. Therefore, in order to provide a better understanding on the oxygen transfer performance from different gas diffusers, the related physical characteristics of different flexible aeration diffuser tubes used in this research will be well studied and presented in the next section.

### 2.5.2 Physical characteristic of flexible aeration diffuser tube

In this part, the 6 samples of the tube diffuser (No. 3, 5, 8, 12, 13, and 16) were chosen in order to analyze the related physical characteristics based on their oxygen transfer performance as previously presented. Table 2.3 shows the summary of the experimental results in terms of tube wall thickness, tensile strength, hardness and elongation. Note that the Vernier micrometer, Durometer and Tensile test were applied in order to measure the tube wall thickness, Tube hardness and Tube elasticity, respectively.

**Table 2.3** Physical characteristic of flexible aeration diffuser tube

Tube No.	Thickness	Tensile strength	Hardness	Elongation
	mm	kN/m <sup>2</sup>	-	%
3	2.85	1,100	50	22
5	2.60	2,900	67	93
8	2.55	2,200	57	65
12	3.15	1,000	63	19
13	2.80	3,000	69	80
16	3.40	3,100	72	75
Tube No.	k <sub>L</sub> a	OTE	Pressure	AE
	x10 <sup>-3</sup> 1/s	%	psi	mg-O <sub>2</sub> /kW-s
3	1.1 - 2.7	1.2 - 2.0	0.8 - 1.2	79 - 287
5	1.2 - 3.0	1.3 - 2.1	1.0 - 3.0	178 - 833
8	1.1 - 3.7	1.6 - 2.1	0.8 - 1.8	366 - 936
12	1.4 - 3.9	1.7 - 2.4	0.8 - 1.1	631 - 1,210
13	1.2 - 3.6	1.6 - 2.2	1.8 - 13.0	49 - 475
16	1.3 - 12.2	2.2 - 5.4	4.0 - 31.0	69 - 226

According to Table 2.3, it can be observed that the increase of tube wall thickness can increase the k<sub>L</sub>a coefficients: more non-uniform porous section presence in diffuser is probably related to the bubble generation phenomena (size and distribution). Moreover, the tube wall thickness can affect directly on the operational pressure (P), power consumption (P<sub>G</sub>), and thus the aeration efficiency (AE). The very high tensile strength and elongation obtained with several diffusers (No. 5, 13, and 16), should relate to elasticity behavior of diffuser tube in this study. These parameters increase

the operational pressure due to the elasticity ( $P_0$ ) that cause the friction on orifice opening mechanism for bubble generation, which resisted the air pass through the orifice. Then it required more pressure to blow the air pass through the orifice, resulting in the increasing of operational pressure as shown in Figure 2.8.

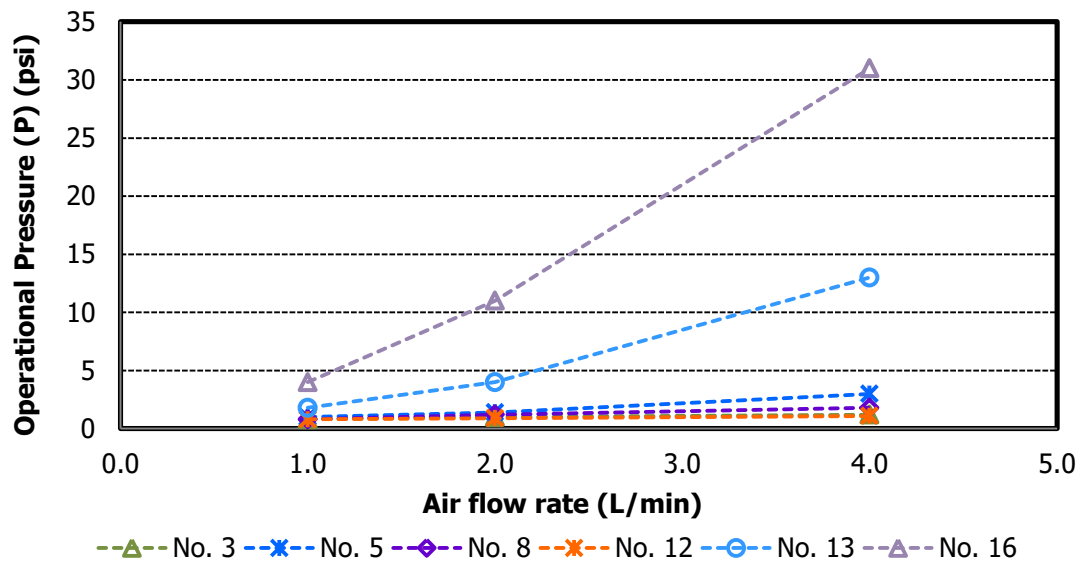
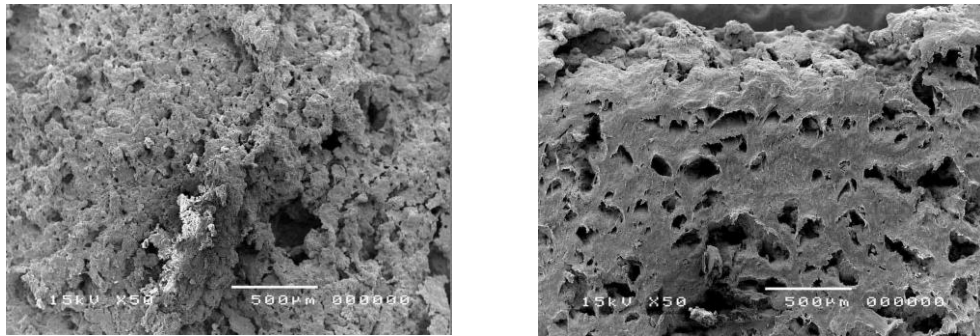


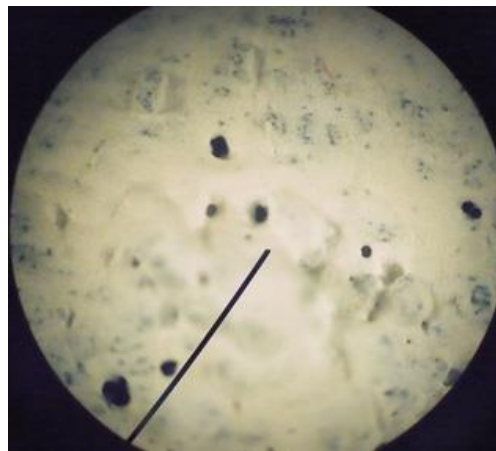
**Figure 2.8** Operational pressure versus gas flow rate for different flexible aeration diffuser tubes

It can be concluded that the physical tube characteristics can be applied in order to describe the oxygen transfer mechanism and thus to select the suitable flexible aeration diffuser tube. For example, the highest  $k_L a$  coefficient and lowest AE obtained with the tube No. 16 should be corresponded to their wall thickness and tensile strength. Considering to the tube hardness obtained in this study, the results obtained with different diffusers were close to 50 and 72: this can possibly affect on the flexible tube structure and orifice size modification at different gas flow rate. From this study, due to the values of  $k_L a$  and OTE, the tube No. 12 should be, therefore, applied in order to produce the practical flexible aeration diffuser tube. Figure 2.9 presents the image analysis results of the tube No. 12. Note that the tube wall and section were obtained with the 50x Scanning Electron Microscopes (SEMs). The orifice size and modification was measure by 4x Microscope.



(a) Flexible tube surface

(b) Section view of tube



(c) Orifice diameter

**Figure 2.9** Image analysis results of flexible tube No. 12

According to Figure 2.9, it can be observed that high amount of porous presence on the tube wall (a): this can serve as the diffuser orifice for bubble generation. Moreover, non-uniform porous and channeling were found in the tube section (b). The average orifice diameter was equal to 0.19 mm and independent to the gas flow rate (1–4 L/min): the characteristic of tube hardness should be responsible for these results. In next section, the bubble hydrodynamic parameters (bubble size, bubble formation frequency and their rising velocity) will be determined, as well as, the interfacial area (a) in order to describe the oxygen transfer mechanism related to the generated bubbles from different flexible aeration diffuser tubes and to confirm the selection of suitable gas diffuser.

### 2.5.3 Bubble hydrodynamic parameters and Interfacial area

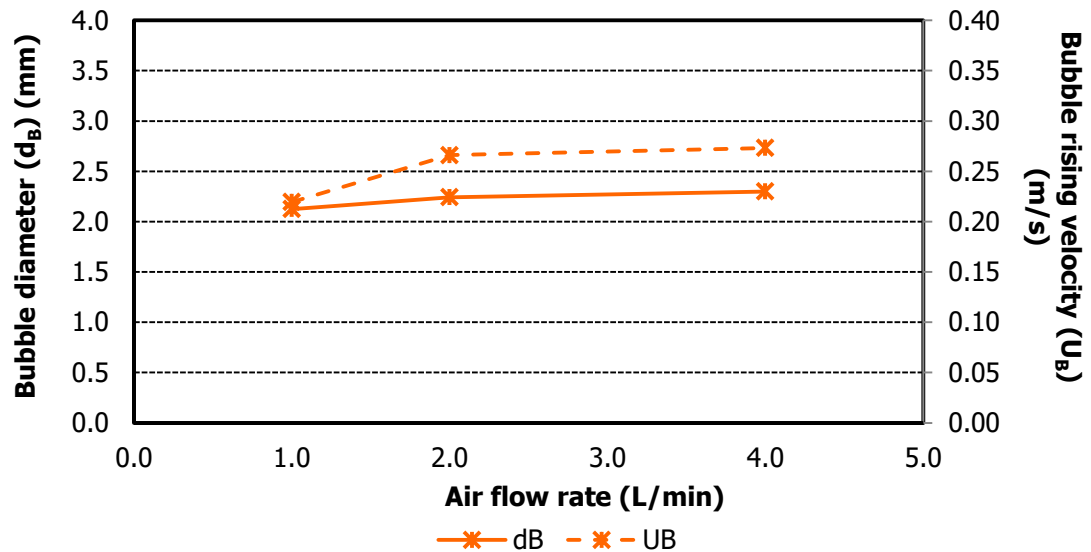


**Figure 2.10** Interfacial area of flexible tube No. 12

According to the best flexible tube diffuser, tube No. 12 was chosen to analyze the detached bubble diameter ( $d_B$ ) and their rising velocity ( $U_B$ ) in the function of the gas flow rate as shown in the figure 2.10.

**Table 2.4** Bubble hydrodynamic parameters of flexible tube No. 12

Tube No. 12	$d_B$	$U_B$	$a$	$k_L$	$k_L a$
	mm	m/s	$m^2/m^3$	$\times 10^{-3}$ m/s	$\times 10^{-3}$ 1/s
	2.1 - 2.3	0.22 - 0.27	2.6 - 7.6	0.51 - 0.60	1.4 - 3.9

As shown in table 2.4, the generated bubble size was roughly constant for whatever the air flow rate: these results relate to the rigid orifice behavior: the bubble size was controlled by the fixed orifice size ( $\approx 0.19$  mm for tube No. 12) [5]. Therefore, it can be stated that the tube hardness characteristics can play the important role on diffuser behavior (flexible or rigid), and thus on the variation of bubble size. For a given gas flow rate, the order is found: the bubble diameter of the tube No. 16 was larger than the tube No. 12 and the tube No. 3, respectively. These results correspond to the tube elasticity characteristic as presented in Table 2. This can be explained that the

increase in the bubble diameter with the elasticity is characteristic of flexible membrane sparger [6]. This is caused by the fact that with higher elasticity, a larger hole (orifice) in the material can bulge and yield the higher bubble size. However, at higher gas flow rate, the bubble size obtained with the tube No. 3 (2.45 mm at 4 L/min of air flow rate) was greater than those obtained with the other diffusers. These results confirm the importance of tube hardness characteristic on the bubble generation phenomena due to the orifice size modification. It can be also noted that the generated bubble sizes obtained in this section were also controlled by the static surface tension ( $\sigma_{\text{Tap water}} = 72.2 \text{ mN/m}$ ) from the same liquid phase used in this study.

For the rising bubble velocities obtained experimentally vary between 0.22 – 0.27 m/s. It can be observed that the  $U_B$  values seem to be increased with the gas flow rate. Moreover, the  $U_B$  values are closed to those given by the diagram of Grace & Wairegi [7]. By using the experimental results of the bubble diameter ( $d_B$ ) and the bubble rising velocity ( $U_B$ ), the calculated bubble formation frequencies ( $f_B$ ) related to the gas flow rates can be calculated. The interfacial area increases linearly with the gas flow rate. The a-area vary between 4.7 and 13.8  $\text{m}^2/\text{m}^3$  whereas the gas flow rates change between 1 and 4 L/min. Theoretically, the values are directly linked to bubble diameter, bubble rising velocity and static surface tension of liquid phases under test. The effects of physical characteristic on the bubble formation phenomenon and on the interfacial area being clearly proved, their consequences on the liquid-side mass transfer coefficient ( $k_L$ ) have to be evaluated now: this is the aim of the next section.

#### 2.5.4 Liquid-side mass transfer coefficient ( $k_L$ )

As shown in the table 2.4, the liquid-side mass transfer coefficient ( $k_L$ ) following by the gas flow rate between  $5.10 \times 10^{-4}$  and  $6.0 \times 10^{-4}$  m/s when gas flow rates varying between 1 and 4 L/min. Whatever the gas flow rates, the  $k_L$  values remain roughly constant for each diffuser. These results conform to those of Calderbank and Mooyong [8]: the authors have shown that the  $k_L$  values are constant for bubbles having diameters greater than 2–3 mm behaving usually like fluid particles with a mobile surface. Note that the bubble sizes generated in this study were controlled by tube physical characteristic and greater than 2 mm (Figure 2.10). Moreover, the lowest and highest  $k_L$  coefficients were obtained with the tube No. 3 and tube No. 16, respectively. Due to the existing  $k_L$  model [9, 10], the experimental  $k_L$  values vary between the two equations:

Higbie: 
$$k_L = 2\sqrt{\frac{D_{O_2} \cdot U_B}{\pi \cdot h}} \quad (2.13)$$



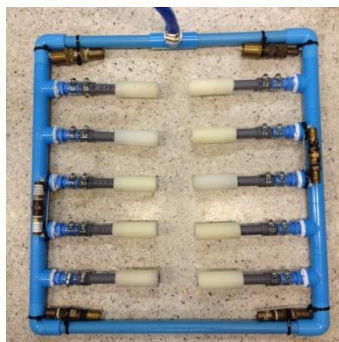
Frossling: 
$$k_L = \frac{D}{D_B} (2 + 0.6 \cdot Re^{1/2} \cdot Sc^{1/3}) \quad (2.14)$$

where  $h$  is the bubble height close to its diameter at low gas flow rates (Figure 2.10).  
 $Re$  the bubble Reynolds number ( $Re = \frac{\rho \cdot D_B \cdot U_B}{\mu}$ ) and  $Sc$  the Schmidt number ( $Sc = \frac{\nu}{D_{AB}}$ ).

Therefore, it can be concluded that the bubble hydrodynamic parameters ( $d_B$ ,  $U_B$ , and  $f_B$ ) should be related and cause the difference in values. It appears from this study, that it is not necessary to generate too much fine bubbles to increase mass transfer capacities. In fact, the increase of interfacial area obtained by the generation of fine bubbles (high power consumption) can be dropped by the great decrease of the  $k_L$  coefficient. A balancing point should be between a small bubble diameter (i.e. a high interfacial area) and a high  $k_L$  coefficient. The physical characteristic parameters (tube wall thickness, tensile strength, tube hardness and elongation) should be considered as the key factor for controlling the power consumption, operating cost, bubble hydrodynamic parameters and thus oxygen transfer efficiency of the flexible aeration diffuser tube.

### 2.5.5 Comparison to the conventional aerators

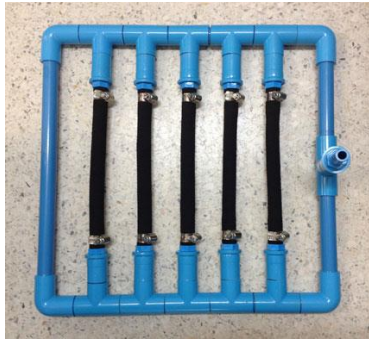
In this experiment, 4 types of diffused aerator: porous stone tube, porous stone ball, flexible rubber tube, and membrane disc, were selected by their general applications as in the wastewater treatment processes or aquaculture ponds. In order to compare the volumetric mass transfer coefficient ( $k_L a$ ) representing their oxygen transfer efficiency, the 4 types of diffuser were prepared as a set of the aerator by the same perforated area (the surface area of the diffuser the can produce bubbles)  $0.04 \text{ m}^2$  of the perforated area per  $0.33 \text{ m}^2$  of the water surface area in the aeration tank, as shown in the following figure,



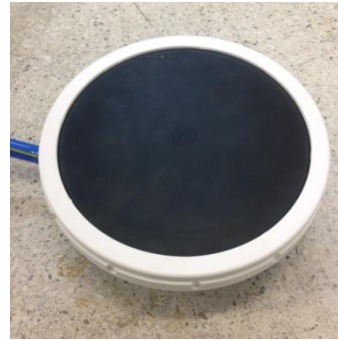
(a) Porous stone tube diffuser



(b) Porous stone ball diffuser



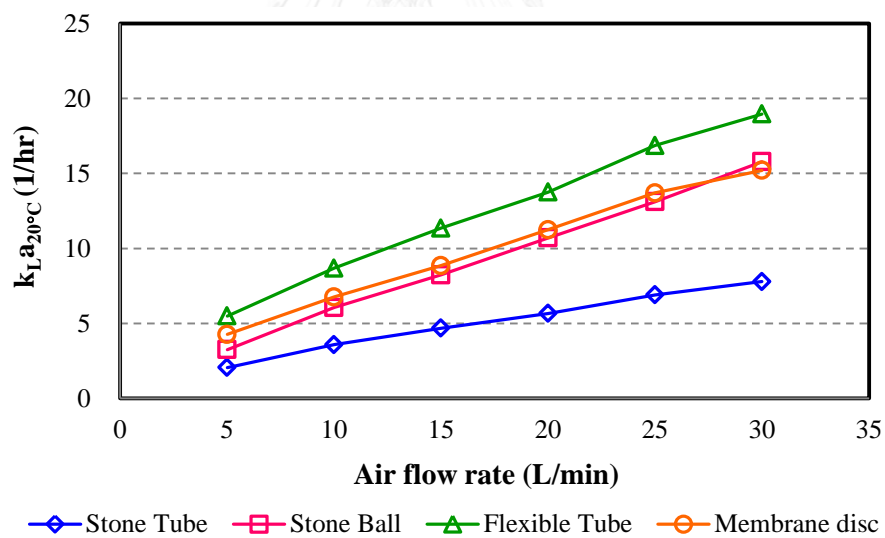
(c) Flexible rubber tube diffuser

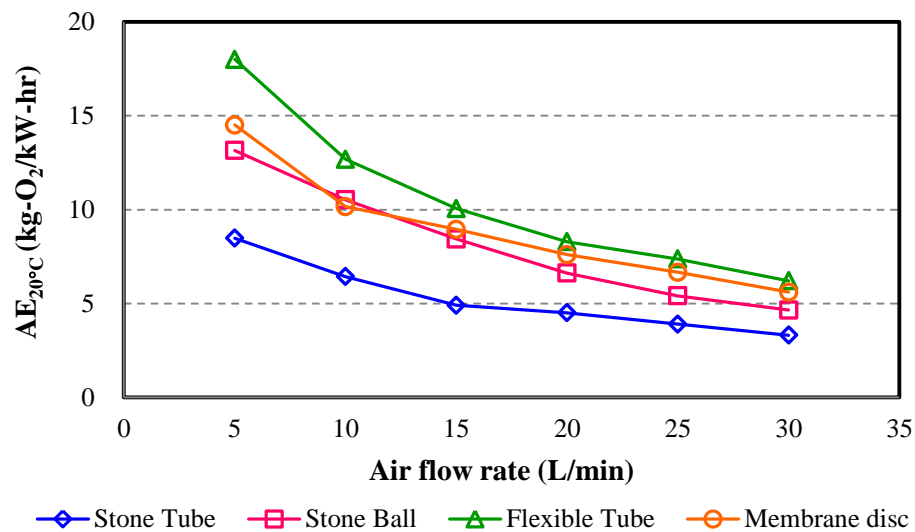


(d) Membrane disc diffuser

**Figure 2.11** The conventional diffused aerators

The experiments were carried out in 190 L of aeration tank, 0.6m x 0.6m x 0.6m. Their performance were evaluated by the  $k_L a$ , and the bubble hydrodynamic parameters were observed by the same way as the previous experiment.

(a) Volumetric mass transfer coefficient ( $k_L a$ )



(b) Aeration efficiency (AE)

**Figure 2.12** Comparison of the flexible tube to the conventional aerators in term of  $k_L a$  and AE

It was found that the highest  $k_L a$  value was obtained by the flexible tube, because of the installation and arrangement of the tube that can cover almost all area of the bottom tank. While the membrane disc seemed to be effective in uniformly bubble producing, but the bubble plume covered just only the center of the tank. So, the high  $k_L a$  value of the membrane was still lower the flexible tube.

**Table 2.5** Bubble hydrodynamic parameters of the studied diffusers: bubble diameter ( $d_B$ ), bubble rising velocity ( $U_B$ ), and specific interfacial area ( $a$ )

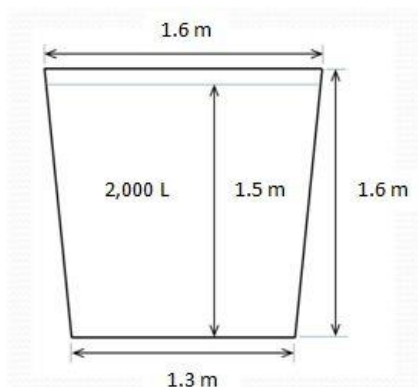
Diffuser type	$k_L a_{20^\circ C}$	$d_B$	$U_B$	$a$
	1/h	mm	m/s	$m^2/m^3$
Porous stone tube	2.0 - 7.8	4.2 - 5.8 ( $\pm 0.61$ )	0.3 - 0.5 ( $\pm 0.06$ )	1.1 - 3.2
Porous stone ball	3.2 - 15.8	4.2 - 5.2 ( $\pm 0.40$ )	0.3 - 0.4 ( $\pm 0.03$ )	1.1 - 4.1
Flexible rubber tube	5.5 - 19.0	3.9 - 4.7 ( $\pm 0.28$ )	0.3 - 0.4 ( $\pm 0.02$ )	1.2 - 5.2
Membrane disc	4.3 - 15.2	3.1 - 4.2 ( $\pm 0.45$ )	0.2 - 0.3 ( $\pm 0.05$ )	2.2 - 6.4

**Remark:** The data were shown as the mean  $\pm$ SD, from 50 bubble samples for  $d_B$ , and 20 bubble samples for  $U_B$ .

Considering to comparison of the bubble hydrodynamic parameters, the membrane disc was the best in bubble production, according to smallest bubble size ( $d_B$ ) and the slowest bubble rising ( $U_B$ ). Therefore, the highest interfacial area ( $a$ ) value was obtained by the membrane disc, but the covering of the bubble plume did not enhance the  $k_L a$ . For the flexible tube, it produced the interfacial area lower than the membrane around 33%, but the  $k_L a$  was still higher. From these results, it can be proved that the physical properties of the diffused aerators relate to their bubble producing behavior that effects on the interfacial area creation. And the aerator installation is another important factor, relating to its aeration performance.

### 2.5.6 Installation test in Pilot-scale experiment

After the flexible tube No. 12 was presented as the best tube with the optimum physical properties, the pilot-scale experiment was set up in 2,000 L of aeration tank to validate its performance and find out the best installation pattern. The 7.5 m of tube was assembled and arranged at the bottom of the tank with the same length of tube per surface area of the aeration tank as conducted in the lab-scale, as shown in figure 2.11. The best installation pattern was the pattern No. 2 which separated the tube into 16 branches that can cover overall area of the aeration tank, and the shortest tube for each branch produced the lowest operational pressure, comparing to the others pattern. The  $k_L a$  of the pattern No. 2 slightly increased from  $2.4 \times 10^{-3}$  to  $4.9 \times 10^{-3}$  1/s with the air flow rate varying between 60-100 L/min. And the operational pressure was the lowest around 3.5-5.5 psi, as shown in figure 2.12. Considering to the length of the tube per branch, the order was found that pattern 3 > pattern 1 > pattern 2, which were 7.5, 3.75, and 0.47, respectively. This result corresponds to the operational pressure that relate to the power consumption. So, the pattern No. 2 is the suitable installation in the pilot-scale by the lowest operational pressure or the highest aeration efficiency.



(a) 2,000 L of aeration tank



(b) Installation pattern No.1

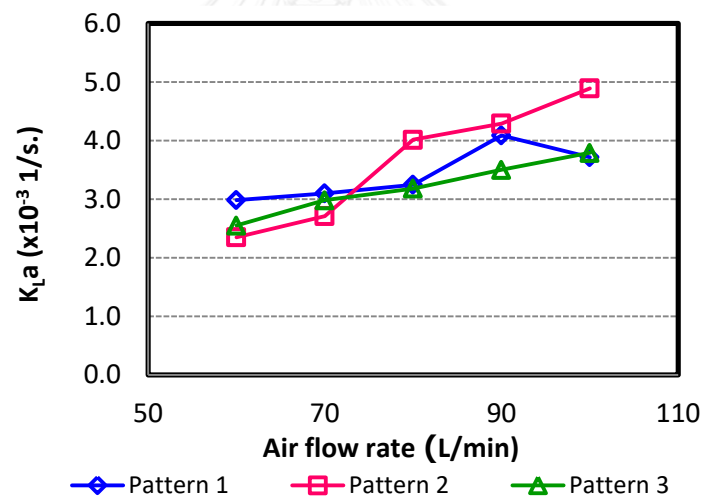


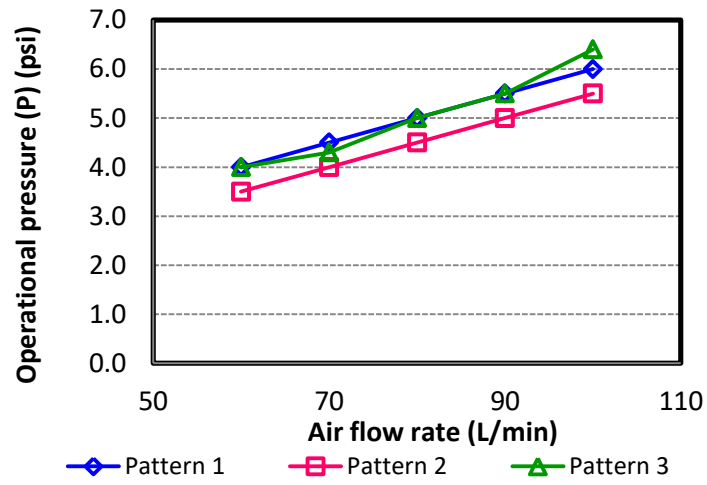
(c) Installation pattern No.2



(d) Installation pattern No.3

**Figure 2.13** Experimental set up and installation pattern in the pilot-scale

(a) Comparison of the  $k_{La}$  coefficient



(b) Comparison of the pressure

**Figure 2.14** Comparison of  $k_{La}$  coefficient and pressure of the flexible tube No. 12 in the pilot-scale

2.5.7 Residence time distribution study (RTD)

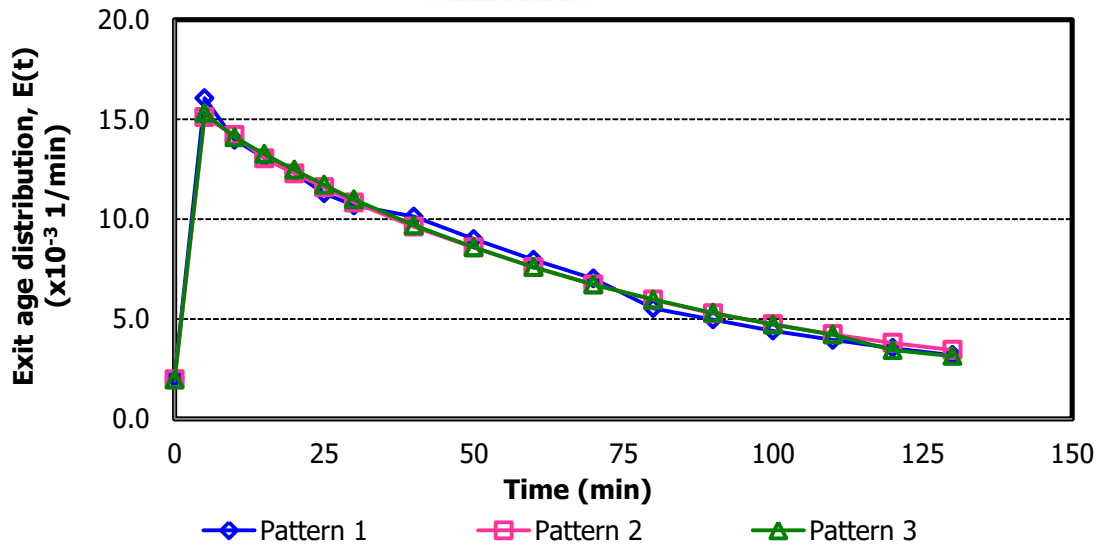


**Figure 2.15** Comparison of conductivity with time

**Table 2.6** RTD result of flexible tube No. 12 in the installation test

Pattern	$k_{La}$	P	O <sub>T</sub> E	AE	$t_{Design}$	$t_{Actual}$	Pe
	$\times 10^{-3} \text{ 1/s}$	psi	%	mg-O <sub>2</sub> /kW-s	min	min	-
1	2.3 - 3.0	4.0 - 6.0	11.4 - 15.3	772 - 1,552	56.3	49.4	1.21
2	1.8 - 3.7	3.5 - 5.0	12.2 - 15.5	1,110 - 1,430		50.3	1.22
3	1.9 - 2.8	4.0 - 6.4	11.4 - 13.1	721 - 1,325		49.8	1.22

The residence time distribution (RTD) and Peclet number (Pe) were analyzed in this aeration tank, followed to Moustiri et al., 2001 [10], to study water flow pattern or mixing level within the tank. The aeration tank was operated as a CSTR reactor together with aeration, at 45 L/min of continuous water flow, 70 L/min of the air flow rate, and used NaOH solution as a tracer pulse that was monitored in form of conductivity. It was found that all of the installation patterns had the same trend of the conductivity which increased immediately when the NaOH was dosed, after that it was slightly decreased with time, after that the result was calculated in term of the exit age ( $E(t)$ ) in the function of time as shown in figure 2.13. Then the trend of  $E(t)$  was analyzed in form of average residence time (ART) which it was around 49.4-50.5 min, comparing to 56.3 min of the designed residence time, this result represented the short circuit flow was occurred during the operation period. For the pecelet number, all of the patterns had nearly the same Pe values which more than 1, as shown in table 2.5. The result showed that all of the installation patterns can lead the completely mixed flow in the aeration tank which it was expected for the oxygen transfer and distribution during the aeration process by using the flexible tube as a diffused aerator.

#### 2.5.8 Theoretical prediction model for oxygen transfer parameters

According to Painmanakul et al. 2009 [11] who proposed the suitable theoretical prediction model for predicting the bubble hydrodynamic and mass transfer parameters by predicting the  $k_L$  coefficient and interfacial area. Then the  $k_{La}$  can be obtained as a product of the two parameters, by following equations,

$$d_B = \left[ \frac{6 \times d_{OR} \times \sigma \times g_C}{g \times \Delta p} \right]^{1/3} \quad (2.15)$$

$$U_B = \left[ \frac{2\sigma}{d_B \times \rho} + 0.5d_B \times g \right]^{0.5} \quad (2.16)$$

$$k_L - 1 = 2 \left[ \frac{D \times U_B}{\pi \times h} \right]^{0.5} \quad (2.17)$$

$$k_L - 2 = \frac{D}{d_B} \left( 2 + 0.6 \text{Re}^{1/2} \times \text{Sc}^{1/3} \right) \quad (2.18)$$

$$k_L = \frac{(k_L - 1) - (k_L - 2)}{d_{B-\text{Max}} - d_{B-\text{min}}} \times (d_B - d_{B-\text{Min}}) + (k_L - 2) \quad (2.19)$$

$$a = \frac{\text{Total surface area}}{\text{Total volume}} = \frac{f_B H_L \pi d_B^2}{U_B (A H_L + N_B V_B)} \quad (2.20)$$

$$k_L a = k_L \times a \quad (2.21)$$

After the prediction models were validated together with correction factors, it was found that the predicted results were closed to the experimental results with the error less than 30% even in the pilot-scale, as shown in figure 2.14.

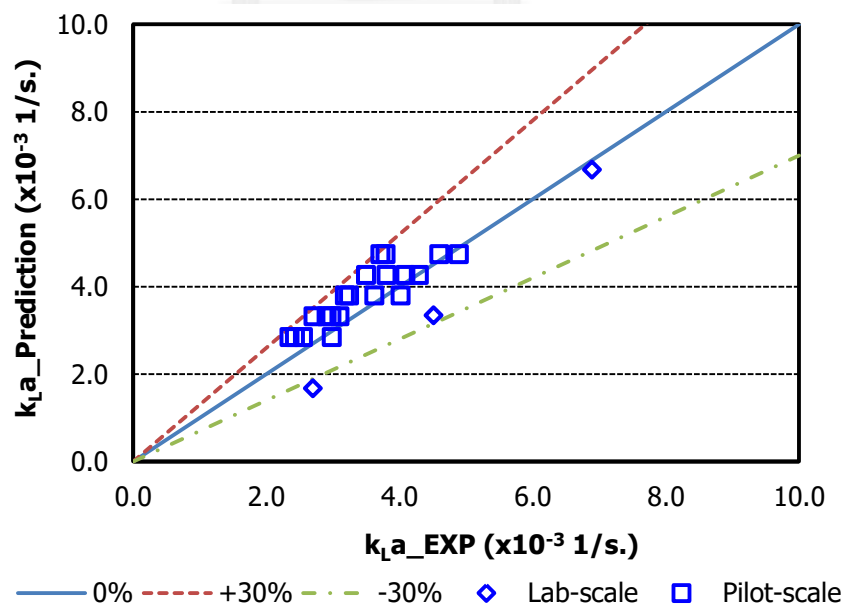


**Figure 2.16** Comparison of the experimental and predicted  $k_L a$  coefficient of flexible tube No. 12



Then, these prediction methods can be applied in order to predict the  $k_{L}a$  coefficient as a primary data for aeration process design. However, it should be studied for further in the real aerated water and large scale of the aeration tank, to improve the predictable accuracies. Moreover, the various types of aerator and operating conditions should be applied for validating the proposed  $k_{L}a$  prediction method.

## 2.6 Conclusions

This study has shown that the physical diffuser tube properties play the important role on the power consumption, operating cost, bubble hydrodynamic parameters and thus oxygen transfer efficiency. The related results have shown that:

- The volumetric mass transfer coefficient increases with the gas flow rates whatever the gas diffusers. The highest  $k_{L}a$  values can be obtained with the tube No. 16, which is 3.4 mm of thickness, 3,100 kN/m<sup>2</sup> of tensile strength, and 75% of elongation.
- The aeration efficiency (AE) should be considered in order to compare the different gas diffusers and select the suitable design and production.
- The physical diffuser properties (tube wall thickness, tensile strength, orifice size, hardness and elongation) have been proven to be the key factor that controls the oxygen transfer performance.
- The effects of physical diffuser properties (tube hardness and elongation) on the bubble formation phenomenon, orifice size and the interfacial area were clearly proved.
- It is not necessary to generate too much fine bubbles to increase the interfacial area: this relates to high power consumption and the great decrease of the  $k_{L}$  coefficient.
- Due to the values of  $k_{L}a$ , OTE,  $a$  and  $k_{L}$  obtained in this study, the physical diffuser properties associated with the tube No. 12, 3.2 mm of thickness, 1,000 kN/m<sup>2</sup> of tensile strength, and 19% of elongation, should be applied in order to produce the practical flexible aeration diffuser tube.
- Comparing to the conventional aerators, the flexible rubber tube has high aeration performance due to its fine bubble production, oxygen transfer performance presented by  $k_{L}a$  and OTE value, and energy performance presented by AE value.

**Table 2.7** The recommended operational condition for the flexible aeration diffuser tube

Parameters		Unit	Condition
Air flow rate	per surface area	$\times 10^{-3} \text{ m}^3/\text{m}^2\text{-s}$	0.4 - 1.7
	per m of tube	$\times 10^{-3} \text{ m}^3/\text{m-s}$	0.1 - 0.7
Length of tube	per surface area	$\text{m}/\text{m}^2$	2.6 - 3.6
Re of bubbles		-	527 - 648
Installation pattern		-	Pattern No.2

From the results in this chapter, the best flexible rubber tube can be obtained, which can be applied as a diffused aerator due to its high oxygen transfer performance, comparing to the other diffuser types. Therefore, this flexible tube was applied in a larger scale experiment in the next chapter, under the topic of “Improvement of oxygen transfer efficiency in term of interfacial area increase by Liquid Film Forming Apparatus (LFFA)” which focused on the possibility of the diffuser system application in a large aeration pond like aquaculture pond. And then the diffuser system performance: both term of oxygen transfer and energy performance, were compared to the conventional aeration system, called paddle wheel system. The researcher expected that high performance of the flexible tube could enhance the efficiency of the aeration system as well as saving the energy like it was in this chapter.

# CHAPTER 3

## IMPROVEMENT OF OXYGEN TRANSFER EFFICIENCY IN TERM OF INTERFACIAL AREA INCREASE BY LIQUID FILM FORMING APPARATUS (LFFA)

### 3.1 Introduction

In aeration process, oxygen is generally introduced by either diffused or mechanical aerators. Contacting between gas phase and liquid phase is the important factor for oxygen transfer, due to interface area is used as an oxygen transfer pathway. The introduced oxygen will be transferred into the liquid phase as dissolved oxygen (DO) via interfacial film between gas phase and liquid phase, after that turbulence or mixing will be needed due to distribute DO concentration uniformly [10]. The oxygen is the important factor in aerobic biological process and aquaculture system due to the vital condition for all organisms living and having an aerobic respiration in water. Therefore, the DO value is one of the parameters applied for monitoring and controlling the aeration system.

The volumetric mass transfer coefficient ( $k_L a$ ) is widely used to evaluate aeration performance, by observing the variation of DO values with time, after that the oxygen transfer efficiency and aeration efficiency (AE), which can describe oxygen transfer rate per power consumption or energy performance. Normally, the  $k_L a$  coefficient can be experimentally obtained as a combined parameter, which consists of liquid-side mass transfer coefficient ( $k_L$ ) and interfacial area ( $a$ ). The  $k_L$  coefficient relates with the properties of the water, which relate to the oxygen transfer mechanism through the interface film between the gas phase and the liquid phase [12]. Therefore, the  $k_L$  coefficient can be described as an oxygen transfer velocity through the contacting film. The  $a$ -area relates with the bubbles characteristics in term of the ratio of interface area per overall volume, which includes the gas phase volume and the liquid phase volume that can be described as an oxygen transfer pathway [11].

Generally, the mechanical surface aerators are widely used in Thailand due to their advantage for increasing DO and having the horizontal mixing of the culture pond with large-surface area. However, the low oxygen transfer efficiency (OTE) and energy performance should be considered as the main drawback of this aerator type. Then the liquid film forming apparatus (LFFA) is proposed as equipment for improving oxygen transfer performance. The objective of the LFFA is to create a large amount of interfacial area, which is a thin film of the liquid phase, in form of

bubble foam at the water surface. The oxygen can transfer both inner and outer interface of the bubble foam, then the oxygen performance can be improved. To complete this research, the aeration system design and the suitable operational condition should be studied and applied.

### 3.2 Objectives

- 3.2.1 To compare aeration efficiency of different types of diffused aerator: porous stone, punched polymeric membrane, and perforated rubber tube, when they are combined with the Liquid-Film-Forming Apparatus (LFFA) as an efficiency enhancement.
- 3.2.2 To investigate the suitable operational condition: installation pattern, amount of required diffusers, and air flow rate for the LFFA application.
- 3.2.3 To study mechanism of the oxygen transfer efficiency enhancement by the LFFA application, through the bubble hydrodynamic parameters observation.

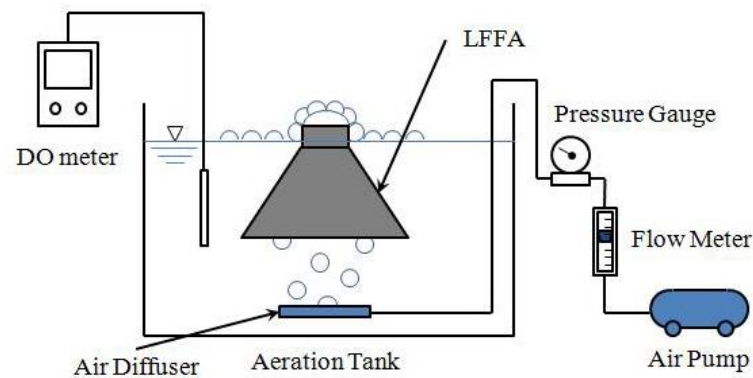
### 3.3 Literature Review

In 2007, Zhu and his research team studied about improvement of oxygen transfer for diffuser systems by Liquid-Film-Forming technique in laboratory experiment. It was found that when the diffuser was operated together with the LFFA, volumetric mass transfer coefficient ( $k_{La}$ ) at the water surface could be increased around 5.3 times, comparing to the diffuser individual due to foaming at the water surface. And total volumetric mass transfer coefficient was increased around 37%. By this research the suitable structure of the LFFA was studied and optimized, to propose the suitable shape of the LFFA for oxygen transfer improvement in aeration system [13].

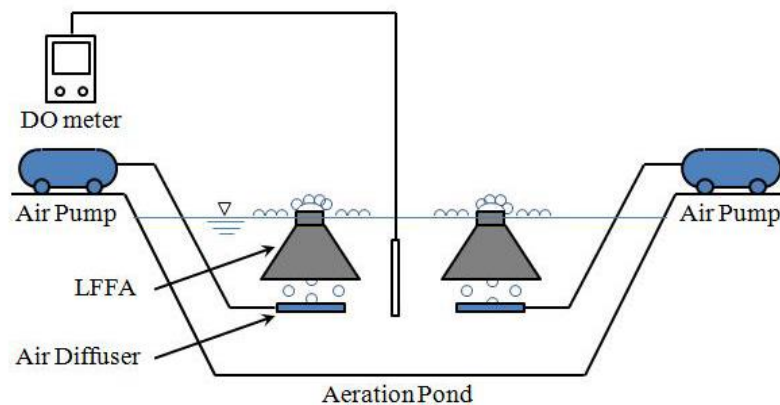
Gresch and research team studied about effect of aeration patterns on the flow field in wastewater aeration tanks, in 2010. They observed water flow and ammonium concentration profile in wastewater aeration tank that was divided into 5 sections with different diffusers, 300-420 pieces. The computational Fluid Dynamics (CFD) was used to analyze flow pattern by the different number of diffusers. It was found that the diffuser layout can lead to oscillations in the flow field and mixing that linked to aeration efficiency directly. Optimizing diffusers layout in aeration tanks is important factor that lead to the best aeration efficiency achievement. So this research considers this issue as a factor to improve aeration system by the suitable installation for diffused aerator system [14].

### 3.4 Materials and Methods

The experiment will be set up in 200 L of aeration tank in laboratory scale, 0.6 m in width, 0.6 m in length, and 0.6 m in water depth, to compare aeration efficiency of the different types of diffused aerators both systems of the diffusers individual and combined with the LFFA. Then the result will be validated in 90,000 L of an actual scale of aquaculture pond, 10 m in width, 10 m in length, and 1.5 m in water depth, as shown by following figure,

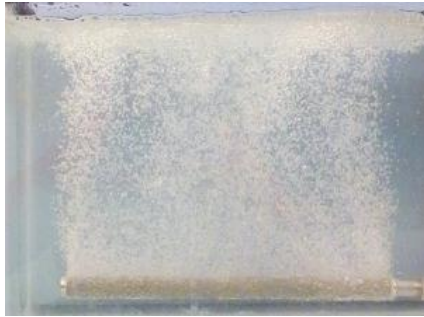


(a) Experimental set up in laboratory aeration tank

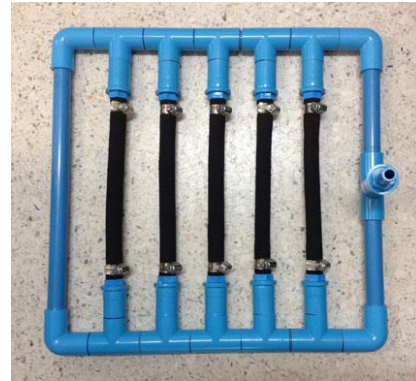


(b) Experimental set up in aquaculture pond

**Figure 3.1** Schematic diagrams of the experimental set up for the Liquid-Film-Forming Apparatus (LFFA)



(a) Porous stone tube diffuser



(b) Flexible rubber tube diffuser



(c) Mechanical surface aerator or paddle wheels

**Figure 3.2** The studied aerators in the aquaculture pond**Table 3.1** The operational conditions of the experiment

Conditions	Laboratory Aeration Tank	Aquaculture Pond
Air flow rate per diffuser (L/min)	0-100	100
Water volume (L)	200	90,000
Number of LFFA + Diffuser	1 unit	1 - 4 sets
Submerged depth of diffuser (m)	0.40	0.50
Submerged depth of DO measurement (m)		
- Surface	-	0.10
- Middle	0.30	0.75
- Bottom	-	1.50
Temperature (°C)	5 - 33	30 - 35
Pressure (atm)	1.00	1.00

In the laboratory scale experiment, the different types of the diffused aerators are chosen: porous stone, punched polymeric membrane, and perforated rubber tube, by their general application, such as wastewater treatment, aquarium, or aquaculture. The aeration system will be operated by the diffuser individually and combine with the LFFA in clean water (tap water) to study the improvement of aeration efficiency by the LFFA. Oxygen will be supplied in foam of atmospheric air and varied around 0-100 L/min of air flow rate to investigate the suitable air flow rate for this system. Volumetric mass transfer coefficient ( $k_{La}$ ) will be measured together with operational pressure to estimate the oxygen transfer efficiency and aeration efficiency as an energy performance for each diffused aerator type. Bubble hydrodynamic parameters will be observed to study oxygen transfer mechanism that will be occurred by each type of diffused aerator. Furthermore, the oxygen transfer mechanism could be classified into oxygen transfer by bubble and foaming at water surface, which can be described by as volumetric mass transfer coefficient by bubble ( $k_{LaB}$ ), and equivalent volumetric mass transfer coefficient at water surface ( $k_{LaS}$ ), respectively.

After the result from laboratory experiment is obtained, the suitable operational condition of the diffused aerator system will be validated in the 90,000 L of aquaculture pond, which located in Chanthaburi province, provided by Marine Technology Research Center, Faculty of Marine Technology, Burapha University, Chanthaburi campus. The experiment will be operated with local saline water (11% of salinity) to study feasibility of the actual application for aquaculture. This study will focus on installation pattern, number of aerators, air flow rate, oxygen transfer efficiency and aeration efficiency comparing to the conventional aeration system (mechanical surface aerators or paddle wheels). In this actual scale experiment, 4 units of the LFFA will be assembled and combined with a piece of diffused aerator as a set of the aerator, then it will be applied by floating type due convenience of its installation and operation, as shown by following figure.

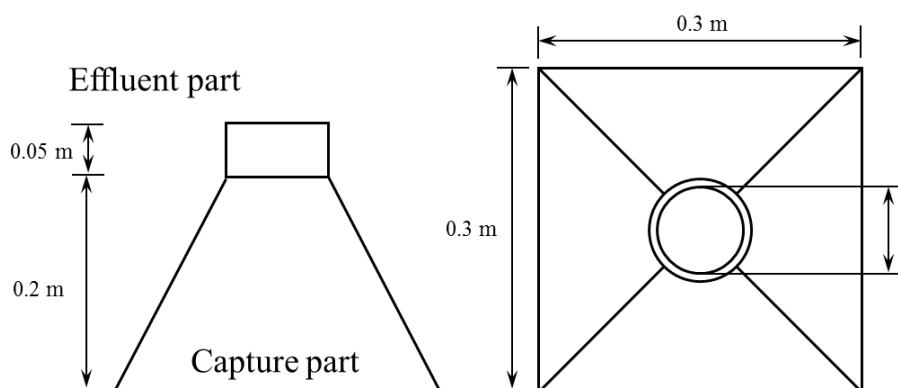


**Figure 3.3** Schematic diagram of the Liquid-Film-Forming Apparatus (LFFA)

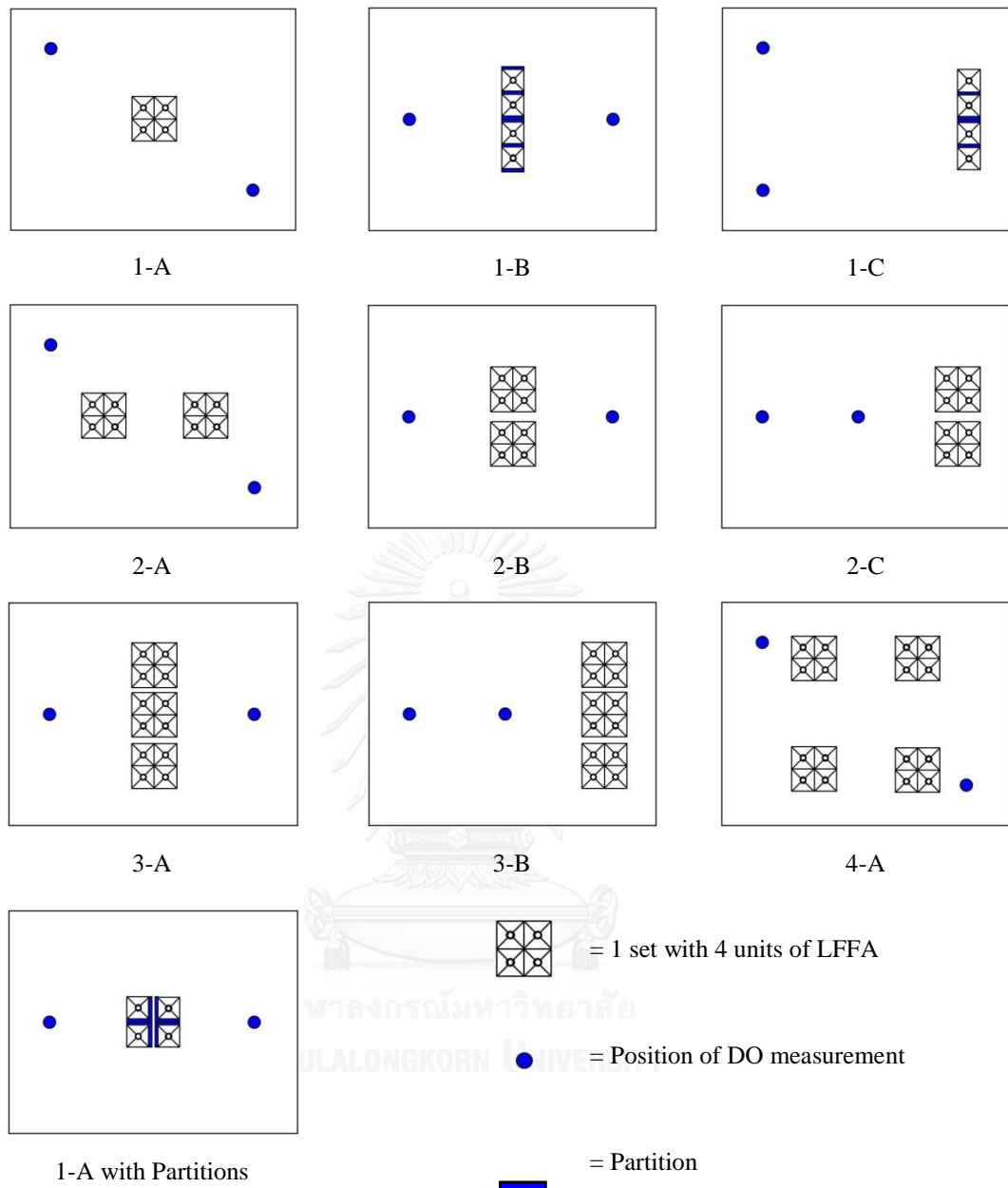


**Figure 3.4** Top view of the LFFA installation in the laboratory aeration tank



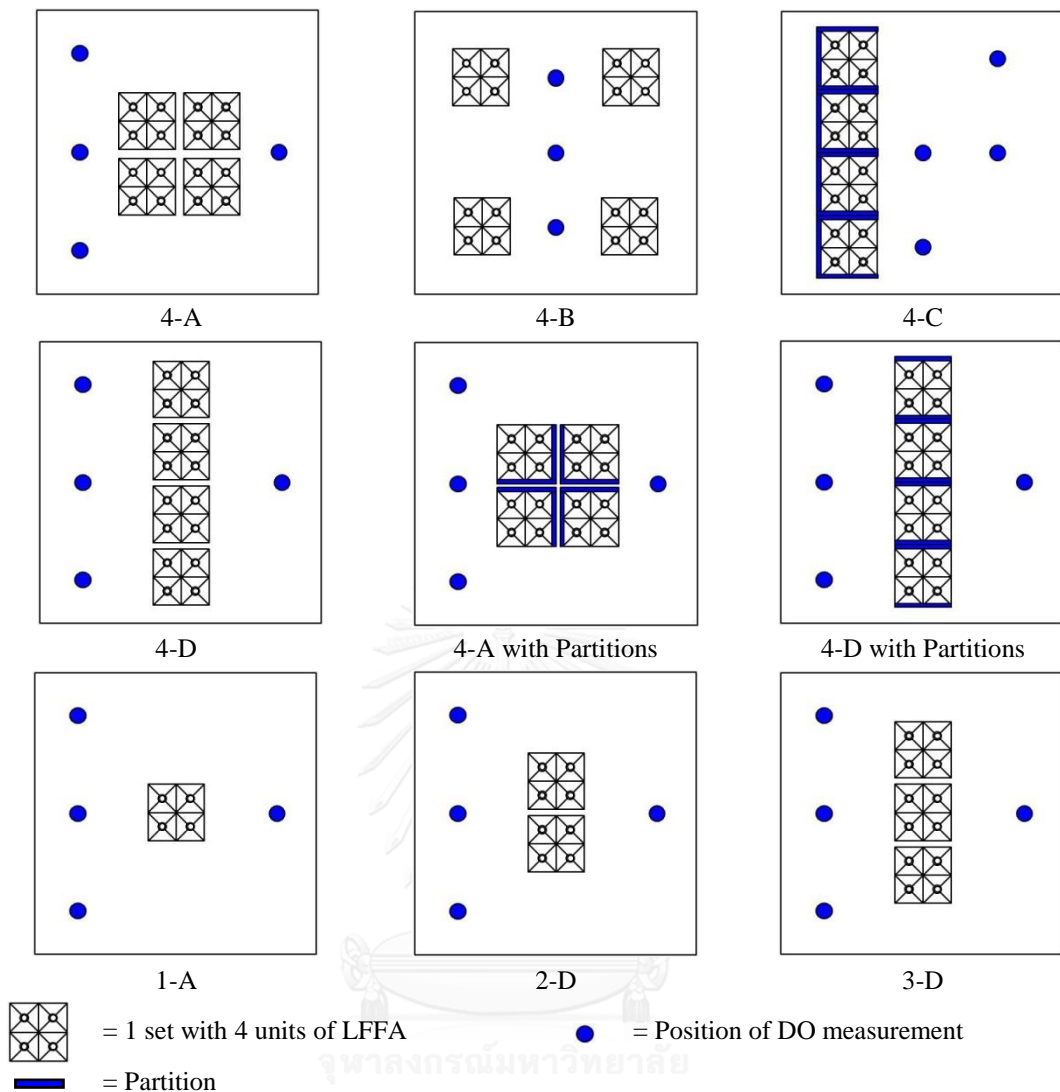


**Figure 3.5** Top view of the Liquid-Film-Forming Apparatus (LFFA) installation

This figure shows installation of the aerators that will be varied and compared in this experiment. Positions of DO measurement are located with 3 depths: 10-20 cm from water surface, middle and bottom of the pond, to measure the  $k_{L,a}$  coefficient and study oxygen distribution with water depth.

For the analytical parameters, the volumetric mass transfer coefficient ( $k_{L,a}$ ) is the main parameter for evaluating oxygen transfer performance, which can be measured by the American Society of Civil Engineers method (ASCE), and using sodium sulfite ( $\text{Na}_2\text{SO}_3$ ) for de-oxygenation, the same as previous chapter. After that  $k_{L,a}$  coefficients will be converted into the  $k_{L,a}$  at  $20^\circ\text{C}$  due to the temperature effect, by this equation.

$$k_L a_T = k_L a_{20^\circ\text{C}} \times 1.024^{T-20} \quad (3.1)$$

Where 1.024 is a constant of air-diffusers and mechanical aerators, and T (°C) is an operating temperature. Then the oxygen transfer efficiency (OTE) and aeration efficient (AE) can be estimated by the same equations as previous chapter.

From this study, the suitable operational condition is expected to be investigated for the combination aeration system between diffused aerators and the LFFA. High oxygen transfer efficiency and energy performance might be obtained as an advantage of this aeration system. Then the result could be summarized and proposed as an operation guideline for the LFFA, then it could be applied as a simple method to improve efficiency of the diffuser system for aquaculture pond.



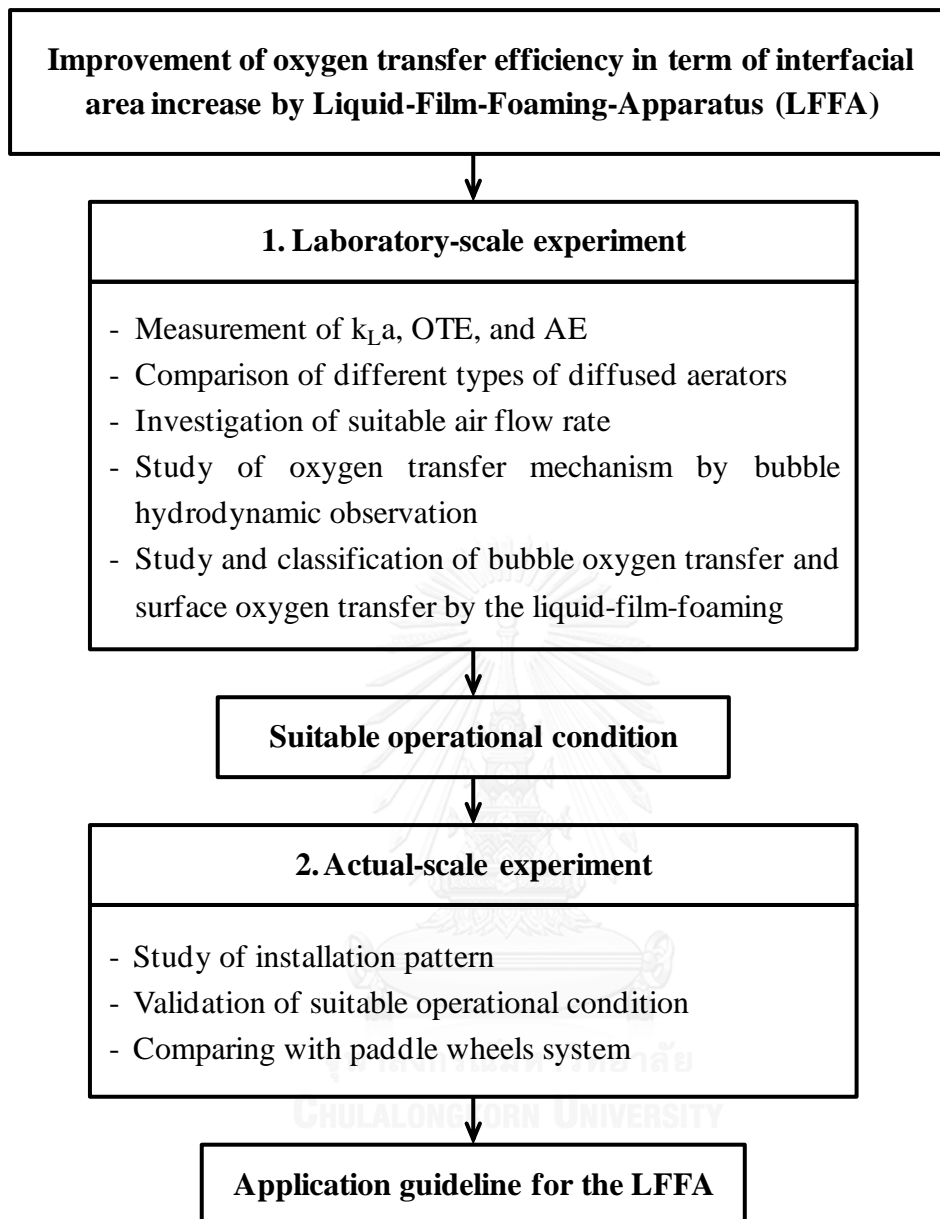


**Figure 3.6** Diagram of improvement of oxygen transfer efficiency by the LFFA

### 3.5 Results and Discussion

#### 3.5.1 Results from laboratory aeration tank

Firstly, the oxygen transfer performance of the stone tube diffuser was measured in an aeration tank, then compared with itself combined with the LFFA. The result was that the  $k_L a$  was improved by around 21% from the initial value. After that, the installation patterns were compared in the laboratory aeration tank for investigating the most

suitable installation. The  $k_{La20^{\circ}C}$  and OTE were used for evaluating the installation patterns in terms of oxygen transfer performance, as presented by table 3.2, [15].

**Table 3.2** Oxygen transfer performance of LFFA in the laboratory aeration tank

Condition	$k_{La20^{\circ}C}$	OTE	AE
	1/hr	%	kg-O <sub>2</sub> /kW-hr
Stone tube	2.0 - 6.3	1.9 - 3.8	1.8 - 7.2
Stone tube + LFFA	1.9 - 7.9	2.4 - 3.7	2.3 - 7.0
Improved (%)	21 ( $\pm 5.06$ )	23 ( $\pm 6.77$ )	23 ( $\pm 6.77$ )
<b>Installation Pattern</b>			
1-A	1.91 ( $\pm 0.09$ )	1.61 ( $\pm 0.08$ )	-
1-A + Partitions	1.77 ( $\pm 0.09$ )	1.45 ( $\pm 0.08$ )	-
1-B	1.90 ( $\pm 0.05$ )	1.55 ( $\pm 0.04$ )	-
1-C	2.02 ( $\pm 0.01$ )	1.64 ( $\pm 0.01$ )	-
2-A	3.99 ( $\pm 0.09$ )	1.68 ( $\pm 0.04$ )	-
2-B	3.21 ( $\pm 0.75$ )	1.37 ( $\pm 0.32$ )	-
2-C	3.01 ( $\pm 0.11$ )	1.29 ( $\pm 0.05$ )	-
3-A	5.15 ( $\pm 0.58$ )	1.44 ( $\pm 0.16$ )	-
3-B	5.03 ( $\pm 0.18$ )	1.43 ( $\pm 0.05$ )	-
4-A	4.55 ( $\pm 0.14$ )	0.97 ( $\pm 0.03$ )	-

Remark: The data was shown as the mean  $\pm$  SD, from 2 monitoring positions.

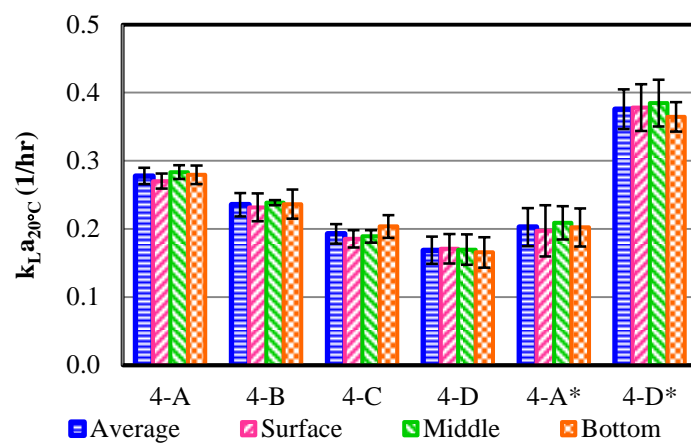
It was found that the best installation pattern was “3-A” with 5.2 1/hr of  $k_{La20^{\circ}C}$ , and 1.4% of OTE. In this pattern, 3 sets of LFFA were installed at the center of the tank, as shown in Figure 3.5. Due to water circulation around the LFFA, the oxygen could be transferred into the water throughout the overall volume, and then the  $k_{La20^{\circ}C}$  was improved.

Regarding [16], the partitions were equipped, in this work, in order to control the water flow direction and to improve the oxygen distribution. But, the partitions seemed to be unnecessary for the pattern “1-A” in this experiment: the OTE value seemed slightly drop. Moreover, it can be noted that the  $k_{La}$  and OTE increased with the number of LFFA, and then they decreased after 3 sets of the LFFA. So, the optimum number of the LFFA in this scale was 3 sets with an air flow rate per area of

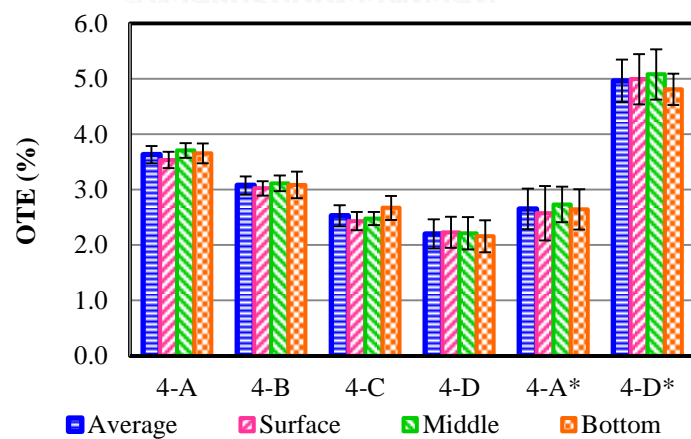
around  $3.6 \text{ m}^3/\text{m}^2\text{-h}$ , which could be applied for the scaled up experiment in the next part.

### 3.5.2 Results from aquaculture pond

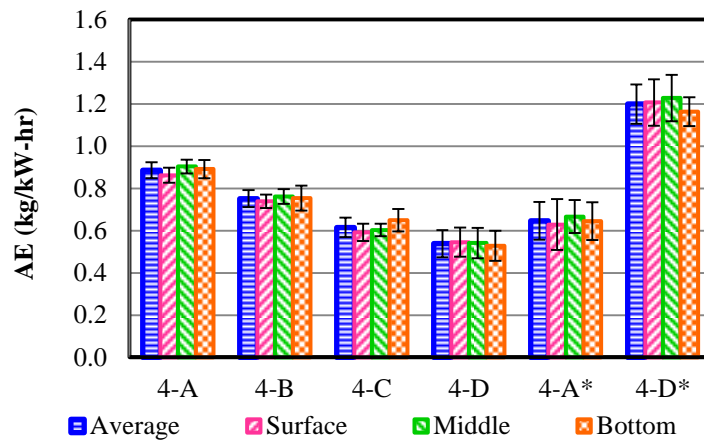
After the suitable installation pattern could be obtained in the laboratory aeration tank, it was then confirmed and applied in the aquaculture pond.  $k_{L,a_{20^\circ\text{C}}}$ , OTE, and AE were used for evaluating, as shown in Figure 3.7.



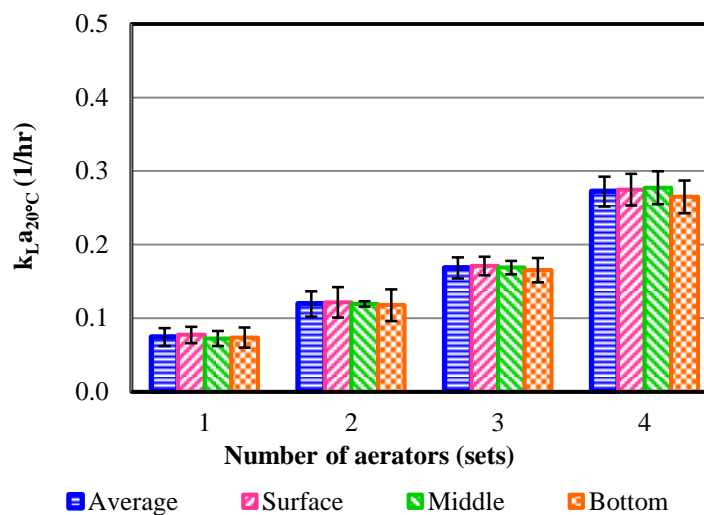
(a) The volumetric mass transfer coefficient at  $20^\circ\text{C}$  ( $k_{L,a_{20^\circ\text{C}}}$ )



(b) The oxygen transfer efficiency at  $20^\circ\text{C}$  (OTE)



(c) The aeration efficient at 20°C (AE)

(d)  $k_L a$  profile of stone tube diffuser and LFFA

**Figure 3.7** Oxygen transfer performance of LFFA in the aquaculture pond.

The data was shown as the mean  $\pm$  SD, from 12 monitoring positions.

Figure 3.7 shows that the best installation pattern was “4-D\*”: this conforms to pattern “3-A” in the laboratory experiment, and the application of partitions can enhance the overall aeration performance. The highest oxygen transfer enactment that was achieved was 0.4 1/hr of  $k_L a_{20°C}$ , 5.0% of OTE, and 1.2 kg/kW-hr of AE. The generated bubble plume from LFFA that covered the water surface was responsible

for increasing the interfacial area, especially at the surface, in a gas-liquid mass transfer mechanism. After the high oxygen transfer was caused by the liquid film forming on the water surface, the oxygen could be transferred into the deeper levels via the water circulation that was caused by the bubble plume itself. While the bubbles were rising up from the diffusers, they pushed some water to go up with them, and the surrounding water came to replace that water from the bottom side of the diffusers. The water circulation in the vertical direction can be created by this phenomenon, and could be used for the oxygen transfer under the water, together with the transferring by the bubbles. Note that the distribution of bubble plume relates to the installation pattern (diffuser number, gas flow velocity and installed position) [17]. In addition, oxygen transfer performance was improved by 35% of the OTE by adding the partitions in the pattern “4-D\*”. The liquid flow can occur from the both sides of LFFA: this phenomenon can improve the bubble redistribution in the liquid phase, and thus the aeration performance.

In order to observe the mixing condition in the horizontal direction, the distribution of the  $k_{La}$  coefficient was analyzed for 4 monitoring positions and 3 different depths. Then the  $k_{La}$  results were compared by the same water depth between 4 monitoring positions, while varying the number of diffuser sets [14]. The 4-D, 4-D\*, 3-D, 2-D, and 1-A installation patterns were selected for comparison. From the results, it was found that the  $k_{La}$  values become more uniform when increasing the number of the diffusers (1 to 4 sets). Improvement of mixing conditions was represented by a decrement of the different  $k_{La}$  values, which was 44% with 1 set of the LFFA, then it was decreased up to 5% with the use of 4 sets of the LFFA with the “4-D\*” installation pattern. Thus the horizontal mixing might be the key factor for the oxygen distribution in an entire large volume of aquaculture pond according to the uniform  $k_{La}$  values or oxygen transfer. As the lowest of the different  $k_{La}$  values, the influence of liquid flow and bubble redistribution phenomena can be proven and concluded. Therefore, the suitable installation pattern should be considered both in terms of oxygen transfer performance and mixing performance [18].

### 3.5.3 Comparison of standing and floating types

According to the suitable installation pattern, LFFA were applied as a floating unit due to convenience of installation and operation. Then the oxygen transfer performance was compared between the original type (Standing type) and the Floating type by the same criteria: installation pattern and operational condition. It was found that both of them were the same tendency with 0.1 1/hr of the  $k_{La20^{\circ}C}$  as well as the OTE and AE were 2.4-2.6%, and 0.6 kg/kW-hr, respectively. Therefore, the LFFA could be applied as a floating unit with the same efficiency.

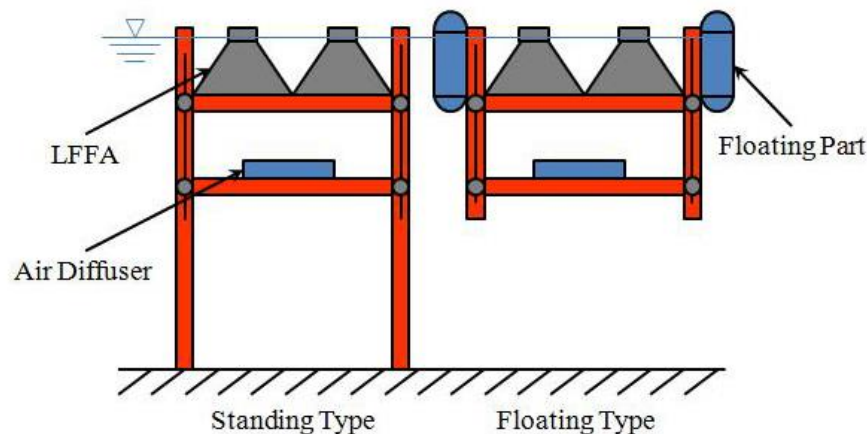


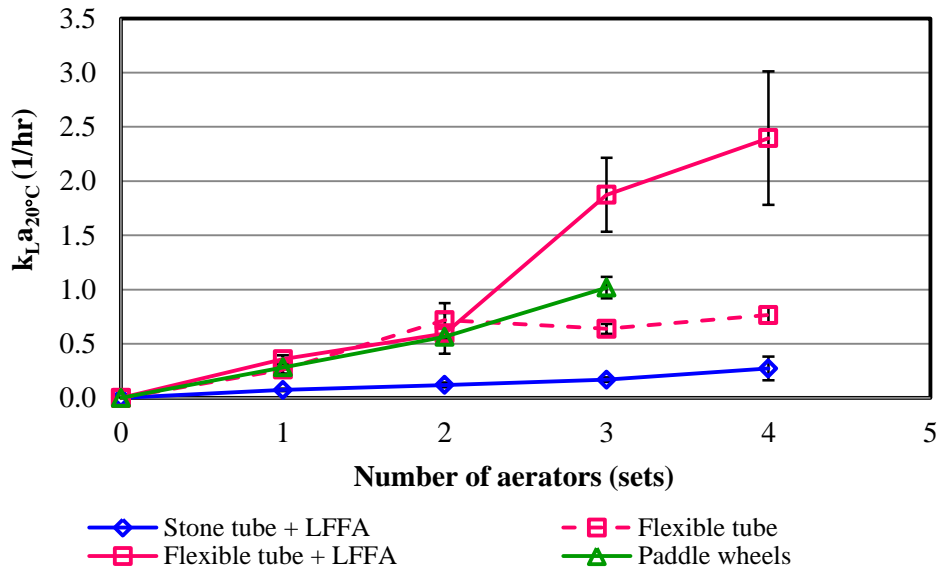
**Figure 3.8** Application of the LFFA

Moreover, not only the lighter weight which was the benefit of the floating type, but also flexible for the variable water level which can maintain the submerged depth of the diffusers. For the submerged depth of the diffusers was an important factor for the oxygen transfer due to the contacting time between bubbles and water. Longer contacting periods occur in greater submerged depth, but the operational pressure of the air pump was a limitation. The air pump might not generate any bubbles if the installation is too deep, and the required pressure was over its capacity. The energy consumption related to the operational pressure and the submerged depth in the same way, therefore the diffusers (both of stone tube and flexible tube) in this experiment were installed with 0.5 m of submerged depth, considering AE as in the previous experiment [19].

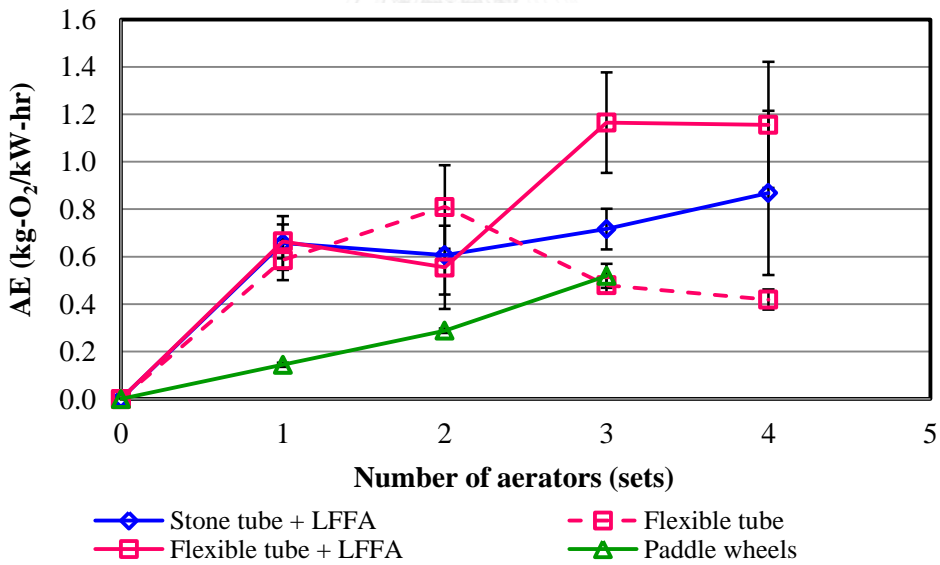
#### 3.5.4 Comparison of LFFA and mechanical surface aerator in real operating condition

In this part, the various LFFA systems were analyzed and applied into the aquaculture pond, as well as compared with the existing mechanical surface aerator (paddle wheel aerator). Note that the recommended patterns with different LFFA numbers (4-D, 4-D\*, 3-D, 2-D, and 1-A) were selected in order to relate with the paddle wheel numbers, as well as to provide a better understanding of the proposed design criteria and operating conditions. Considering the effect of bubble hydrodynamic parameters (bubble size and rising velocity), the fine bubble diffuser (flexible rubber tube) has been chosen in this research. For flexible tube installation, it was arranged by the recommended pattern as the stone tube previously concluded. The  $k_{LA20^{\circ}\text{C}}$  and AE were used for comparing and evaluating the oxygen transfer performance, as shown in the Figure 3.8.





(a) The volumetric mass transfer coefficient at 20°C (k<sub>L</sub>a<sub>20°C</sub>)



(b) The aeration efficiency at 20°C (AE)

**Figure 3.9** Comparison of the oxygen transfer performance. The data was shown as the mean ± SD, from 12 monitoring positions.

As shown in Figure 3.8-a, it was found that the values of  $k_{La20^{\circ}C}$  obtained with the mechanical surface aerator (around 0.3-1.0 1/hr) were greater than those obtained with the LFFA system with stone tube diffuser by about 2 or 3 times (around 0.1-0.3 1/hr). The bubble size and related rising velocity were 3-5 mm and 21-28 cm/s, respectively [2]. According to the results from flexible tube diffuser, it can be noted that similar trend with paddle wheel aerator was observed (0.3-0.8 1/hr). However, when the flexible tube was combined with the LFFA, the  $k_{La}$  increased around 100%, which means it was more effective at high air flow rate or high number of diffuser sets, and almost twice as effective as paddle wheels with 3-4 of the diffuser sets. The influence of bubble hydrodynamic parameters: bubble size of 2-3 mm and bubble rising velocity of 19-25 cm/s obtained with fine bubble diffuser has been proven: these results can show the high interfacial area for oxygen transfer rate and overall performance. Considering the bubble collection within the LFFA, many bubbles floated through the effluent part easily at the low air flow rate due to the low turbulence, but it seemed to be more effective with increased air flow rate causing high turbulence. Under the high turbulence conditions, bubbles floated and hit with the LFFA wall, which can create a bubble pack inside and produce a large contacting area during the collection. The bubble pack within the LFFA can enlarge the contacting period by obstructing the other bubbles, resulting in more interfacial area. When comparing the small bubble size from the flexible tube to the coarse bubbles from the stone tube, the bubble collection phenomenon seemed to be more effective than the coarse bubbles. Because small bubbles can create a tighter bubble pack than coarse bubbles, they can produce a large interfacial area, while the coarse bubbles had a greater chance of coalescing together and losing their interfacial area. When increasing the number of diffuser and LFFA up to 3-4 sets, the generated liquid film on the water surface seemed to cover the entire area, which also accelerates oxygen transfer rate. Due to those reasons, the oxygen transfer efficiency of the flexible tube and LFFA was greater than the stone tube. The LFFA was also effective at high rates of air flow that create turbulence and liquid film on water surface sufficiently, with the final result of an increase in efficiency of the flexible tube compared to paddle wheels by up to 2-3 times.

The aeration efficiency (AE), as shown in Figure 3.8-b, had higher values of AE obtained with diffused aerators (stone tube and flexible tube) than those obtained with paddle wheels by about 2 times. These results can be explained by the fact that high oxygen transfer efficiency (OTE) 5.0% for the stone tube and 16.8% for the flexible tube compared to the diffuser in other application [20-22], as well as low operational pressure for bubble generation. The elasticity of the flexible tube could increase resistance for orifice enlargement during the aeration, the supplied air passing through

the tube wall [5]. Therefore, the AE values from flexible tube seem to be lower than from the stone tube, especially at high rates of air flow.

Considering the installation cost, the diffused aerator system was around \$700, including 4 air pumps, 4 sets of diffusers (stone or flexible rubber tube), 4 sets of the LFFA and floating part. The Paddle wheel system, on the other hand, costs around \$900, including a 3Hp motor, a branch of paddle set, and floating part. So, the diffused aerator system was about 20% cheaper, but it needs more careful maintenance because of the fouling problem. However, the new pieces of the diffusers can be replaced quite easily, and are less expensive than paddle parts. For the operation costs, which are related to the electrical power consumption or AE as mentioned above, the diffused aerator system consumed 0.06-0.24 kW, while the paddle consumed around 1.5 kW. This means that the diffused aerator is clearly more energy efficient.

As previously mentioned, the LFFA system with fine bubble diffuser should be applied, in practice, in the aquaculture pond due to advantages in terms of oxygen transfer rate and energy performance. The diffuser and LFFA aeration systems should be studied further in terms of life expectancy and maintenance, as well as for their applications in other processes, such as separation, disinfection, or other advance processes [23].

### 3.6 Conclusions

The results clearly show that the LFFA has the potential to be a superior aerator system for aquaculture ponds due to its high AE. The “4-D\*” (with partitions) is preferable as the suitable installation pattern for this experiment, with 100% of the maximum oxygen transfer improvement:  $k_{La_{20^{\circ}C}}$ , OTE, and AE for the flexible rubber tube diffuser, due to liquid film forming on water surface which increases the contacting area. For convenient installation, the LFFA can be applied as a floating type with the same oxygen transfer efficiency.

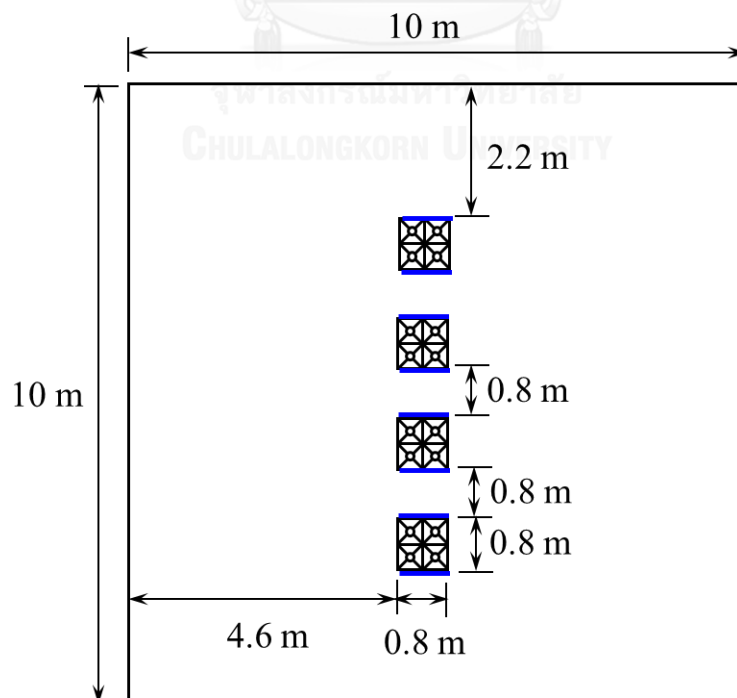
**Table 3.3** The operation conditions of the experiment

Conditions	Laboratory Aeration Tank	Aquaculture Pond
Air flow rate per diffuser (L/min)	24 - 96	100 - 400
Water volume (L)	330	62,000
LFFA + Diffuser sets	1 - 4	1 - 4

Submerged depth of diffuser (m)	0.4	0.5
Submerged depth of DO measurement (m)		
- Surface	-	0.1
- Middle	0.2	0.7
- Bottom	-	1.4
Temperature (°C)	5 - 33	30 - 35
Pressure (atm)	1.0	1.0

**Table 3.4** The recommended operation condition for the LFFA

Parameters		Unit	Condition
Air flow rate	per surface area	m/hr	0.24
	per unit of LFFA	m <sup>3</sup> /hr-unit	1.5
	per set of LFFA	m <sup>3</sup> /hr-set	6
Number of LFFA	per surface area	unit/m <sup>2</sup>	0.16
		set/m <sup>2</sup>	0.04
Submerged depth		m	0.5



Installation pattern: 4-D with Partition

## **CHAPTER 4**

### **STUDY OF COMBINATION AERATION SYSTEM IN TERM OF OXYGEN TRANSFER EFFICIENCY AND ENERGY PERFORMANCE IN PILOT-SCALE EXPERIMENT**

#### **4.1 Introduction**

According to the aeration in a large surface area of aeration pond like an aquaculture pond, the mechanical surface aerators called “paddle wheel” are always used due to their convenient installation and operation, with ability to supply oxygen together with making water flow as their advantage. However, the low oxygen transfer efficiency and energy performance should be considered as the main drawback of this aerator type, because they can make contacting area between air (oxygen) and water at water surface only with low contacting time. And the actual operation in the aquaculture ponds, there was no pattern to solve the problem when the oxygen was not enough, the operators always add more paddles set into the aeration system, which it was wasting of energy. On the other hand, diffused aerators have high oxygen transfer efficiency and energy performance, due to a large contacting area by bubbling underneath the water with longer contacting time. However, for a large aeration pond as aquaculture pond mixing function is another important factor for oxygen distribution. So, vertical mixing by diffused aerator only might not be enough for this case if diffused aerators are applied individually. Then it is necessary to apply another equipment to perform water flow or horizontal water mixing, such as axial propellers, water pump, or paddle wheels. To fulfill this gap, diffused aerators could be applied for aeration or oxygen transfer mechanism, and mixing devices for oxygen distribution and aeration system improvement. Then advantage can be obtained as a combination of them: the diffusers for aeration while the paddle wheels for mixing or oxygen distribution. Furthermore, bubble diameter will be reduced by shear force from the water cross-flow that can improve the oxygen transfer rate by increase of the a-area. The objective of this research is to study the oxygen transfer mechanism and bubble hydrodynamic parameters, which can be occurred by the combination of different aerators (diffusers and paddle wheels), due to improve the aeration system both term of oxygen transfer efficiency and energy performance. Then the optimum operating condition, which can achieve the best oxygen transfer efficiency while consume the lowest of energy, will be investigated. After that the results are expected to be proposed as a design criteria and operation guideline for this alternative aeration system.

## 4.2 Objectives

- 4.2.1 To study and improve aeration efficiency of aeration systems by applying horizontal water flow together with aeration through combination of mechanical surface aerators and diffused aerators.
- 4.2.2 To investigate the suitable operational condition: installation pattern, air flow rate, and horizontal water flow velocity for the combination aeration system.
- 4.2.3 To propose the suitable theoretical prediction model for predicting bubble hydrodynamic and oxygen transfer parameters that can be used for aeration process design and operational guideline.

## 4.3 Literature Review

In 2004, Loubiere and research team studied about bubble formation at a flexible orifice with liquid cross-flow. It was found that the bubble formation under liquid cross-flow condition made smaller bubble size comparing to normal condition. And the detached bubbles tend to be swept away from the orifices that reduce likelihood of bubble coalescence. By these results, water cross-flow is important factor for aeration system improvement in term of bubble size, bubble formation frequency, interfacial area, and oxygen transfer [18].

In 2010, Kumar and research team studied about performance evaluation of propeller-aspirator-pump aerator to investigate the suitable installation of the propeller-aspirator-pump aerator. From the result, it was found that the best aeration efficiency of the system can be achieved by optimum installation of the aerator: positional angle, rotation speed, and submergence depth. This result just confirms that the aeration efficiency can be improved by optimum water flow as a mixing function together with aeration [14].

Gillot and research team proposed their prediction models for predicting transfer number ( $N_T$ ), which described as oxygen transfer efficiency from their research: Prediction oxygen transfer of fine bubble diffused aeration systems-model issued from dimensional analysis, in 2005,S

$$N_T = \frac{k_L a_{20}}{U_G} \left( \frac{v^2}{g} \right)^{1/3} = 7.77 \times 10^{-5} \left( \frac{S_P}{S} \right)^{0.24} \left( \frac{S_P}{S_a} \right)^{-0.15} \left( \frac{D}{h} \right)^{0.13} \quad (4.1)$$

$$k_L a_{20} = 1.69 Q_G S^{-1.18} S_P^{0.10} S_a^{0.15} h^{-0.13} \quad (4.2)$$

$$SSOTE = 5.27 S^{-0.18} S_P^{0.10} S_a^{0.15} \quad (4.3)$$

When  $U_G$  is superficial velocity,  $\nu$  is kinetic viscosity of water.  $S_P$ ,  $S$ , and  $S_a$  are total surface area of perforated membrane diffusers, surface area of aeration tank, and total surface of the zones occupied by the diffusers, respectively.  $D$  is tank diameter,  $h$  is diffuser submergence, and  $Q_G$  is air flow rate. This result is shown that accuracy of the prediction model can be improved by dimensional factor as a correction factor [24]. However, the prediction for oxygen transfer is still inaccurate, until now. And these equations were taken from aeration tank in wastewater treatment plant, but for a large aeration pond as aquaculture pond, the correction factor should be studied in the actual pond for further.

Pittoors and research team showed another way to improve accuracy of prediction model for oxygen transfer coefficient ( $k_L a$ ) by dimensional factor and dimensionless number: Reynolds number ( $Re$ ) and Froude number ( $Fr$ ), as following equation,

$$\frac{D_t^2 k_L a_{CW}}{D} = 0.030 Re^{1.718} Fr^{-0.709} \left(\frac{d_b}{h_d}\right)^{-0.291} \left(\frac{H_t}{D_t}\right)^{-0.554} \left(\frac{A_d}{A_t}\right)^{0.135} \left(\frac{D_t}{h_d}\right)^{0.321} \left(\frac{H_t}{h_d}\right)^{0.086} \left(\frac{V_t}{A_d^{1.5}}\right)^{-0.017} \quad (4.4)$$

$$\frac{D_t^2 k_L a_{AS}}{D} = 0.060 Re^{1.906} Fr^{-0.631} \left(\frac{d_b}{h_d}\right)^{-0.23} \left(\frac{H_t}{D_t}\right)^{-0.120} \left(\frac{A_d}{A_t}\right)^{0.326} \left(\frac{D_t}{h_d}\right)^{0.164} \left(\frac{H_t}{h_d}\right)^{0.173} \left(\frac{V_t}{A_d^{1.5}}\right)^{-0.01} \quad (4.5)$$

$$Re = \frac{vL}{\nu} = \frac{Q_a \rho}{D \eta} \quad (4.6)$$

$$Fr = -\frac{v}{\sqrt{Lg}} = \frac{Q_a}{\sqrt{D_t^5 g}} \quad (4.7)$$

Where  $d_b$  is bubble diameter,  $h_d$  is diffusers submergence,  $H_t$  and  $D_t$  are height and diameter of aeration tank, respectively.  $A_d$  is total coverage area of diffusers,  $A_t$  is total area of aeration tank.  $V_T$  is working volume of the aeration tank,  $\nu$  is kinetic

viscosity,  $L$  is length of aeration tank, and  $Q_a$  is air flow rate. From this research, dimensional factors were obtained by experiment in 3-9 L of cylindrical aeration tank that have small surface area. In case of aquaculture pond that has a large surface area, and always filled with local water, which is sea water or saline water, then the dimensional factor is still needed to be investigated for further [25].

#### 4.4 Materials and Methods

##### 4.4.1 Materials

This experiment was conducted in a 680L aeration tank, the flexible rubber tube was assembled to be a frame of diffused aerator. A frame of diffuser was designed follow to the same ratio as the previous experiment in an actual aquaculture pond (around 4 m of the tube per 1 m<sup>2</sup> of surface area of the tank). Then the number of diffuser was increased up to 4 frames which represent the condition in a wastewater treatment plant that the aerators were installed cover overall of the area of the tank. The water pumps were selected to create the horizontal water circulation for the combination aeration system, and varied the pump size for varying the water velocity, therefore the optimum velocity can be investigated.



**Figure 4.1** Flexible rubber tube diffuser



Pump model	Power (W)	Units	Water velocity (mm/s)
SONIC AP1000	5.5	1	39
		2	57
SONIC AP1200	8	1	42
SONIC AP1600	20	1	87
SONIC AP2500	30	1	113
SONIC AP5000	60	1	183
		2	249

**Figure 4.2** Water pump





#### 4.4.2 Experimental set up

The experimental was set up in a 680L aeration tank, 1.08 m in width, 2.30 m in length, and 0.3 m in water depth. The aeration was classified into 3 systems: Diffuser system, Paddle wheels system, and combination aeration system.

- 1.) Diffuser system: the diffuser number was varied 1-4 frames, and the 10 L/min of air flow was supplied for each diffuser frame, so that the flow rate was varied from 10 L/min to 40 L/min.
- 2.) Paddle wheels system: the system was conducted by 2 water pumps with the largest size (60W) to create the horizontal water velocity around 0.25 m/s, closed to the actual condition of the paddle wheels (0.2 m/s).
- 3.) Combination aeration system: at first, the optimum water velocity was investigated by operating 1 diffuser frame together with 1 water pump. The water pump size was varied due to vary the water velocity. The 10 L/min of air flow was supplied for each diffuser frame. After that the combination aeration system was compared to other systems by combing 2 diffuser frames and 2 water pumps (the suitable size and water velocity).

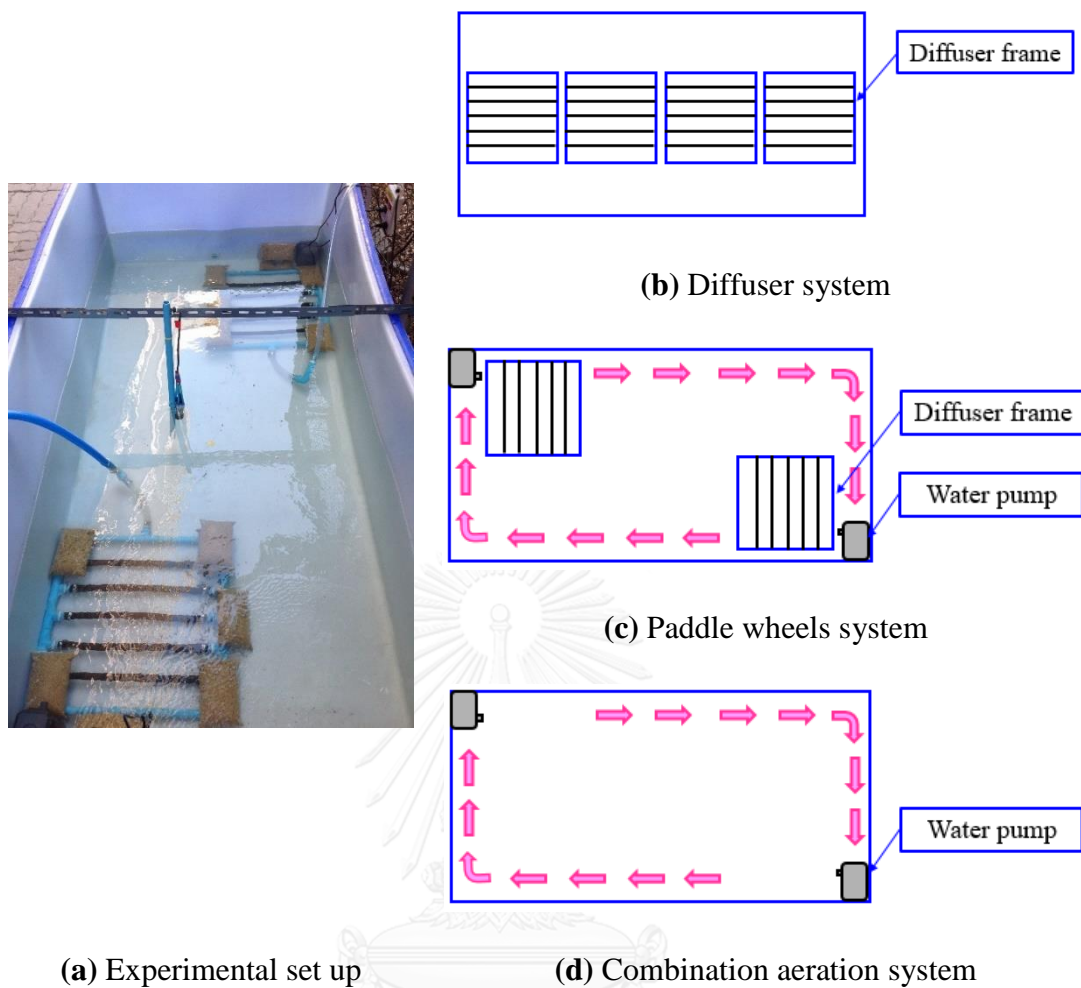


**Figure 4.3** Schematic diagrams of the Experimental set up

For the volumetric mass transfer coefficient ( $k_L a$ ) analysis, the gas flow rate ( $Q_g$ ), operational pressure ( $P$ ) and dissolved oxygen (DO) were monitored by a gas flow meter, pressure gauge and DO-meter (EUTECH DO110), respectively. The  $d_B$  and  $U_B$  were observed by a camera with the caption rate 30 frames/s. Tap water is used as the liquid phase ( $\sigma_L = 71.8 \text{ mN/m}$ ,  $\mu_L = 1.003 \times 10^{-3} \text{ Pa.s}$ , and  $\rho_L = 997 \text{ kg/m}^3$ ). The operating conditions were summarized as follows:  $Q_g = 10 \text{ L/min}$  for each diffuser frame, liquid volume = 680 L, liquid height = 0.3 m and temperature = 25-30°C. Sodium sulphite was used to desorb the initial oxygen in the water before starting the experiment.

#### 4.4.3 Bubble hydrodynamic parameters

According to the opaque wall of the aeration tank, the bubble movement cannot be observed during the experiment directly. Therefore, the bubble hydrodynamic parameters measurement was conducted in another laboratory aeration tank. The flexible tube was installed in the 200L of aeration tank, 0.6m x 0.6m x 0.6m of the dimension, by the same ratio as the pilot-scale. And the other operating conditions, such as air flow rate, water depth, and the horizontal water velocity were simulated by the same way also. The bubble movement was observed by the video camera with a 30 frames/s of caption rate, and then the bubble diameter ( $d_B$ ) and bubble rising velocity ( $U_B$ ) were calculated by the same way as the previous experiment.

#### 4.4.4 Theoretical prediction model for oxygen transfer parameters

After the results are obtained from the both scales of experiment, oxygen transfer parameters and bubble hydrodynamic parameters from every operational condition will be studied to find out their relation. By the existing correlations and prediction models, bubble hydrodynamic parameters: bubble diameter ( $d_B$ ) and bubble rising velocity ( $U_B$ ), which are the main parameters for calculating interfacial area ( $a$ ), can be determined.

**Table 4.1** Existing correlations for predicting bubble diameter ( $d_B$ ) [11]

Eq.	Correlations	Conditions	References
$d_{B-1}$	$d_B = \left( \frac{6d_{OR}\sigma g_c}{g\Delta\rho} \right)^{1/3}$	$Q_{go} < \left[ \frac{20(\sigma d_0 g_c)^5}{(g\Delta\rho)^2 \rho_L^3} \right]^{1/6}$	Van Krevelen [26]
$d_{B-2}$	$d_B = 0.0287d_{OR}^{1/2} Re^{1/3}$	$Re < 2,100$	Leibson [18]
$d_{B-3}$	$d_B = \left( \frac{72\rho_L}{\pi^2 g\Delta\rho} \right)^{1/5} Q_{q0}^{0.4}$		Van Krevelen [26]
$d_{B-4}$	$d_B = 1.7 \times 10^{-4} \Delta P^{0.328}$	$\Delta P$ in Pa	Hebrard [27]
$d_{B-5}$	$d_B = 15.73 \times 10^{-3} D_c^{0.32} \left( \frac{Q_g}{A_{BC}} \right)^{0.16}$		Hebrard [27]

d <sub>B</sub> -6	$d_B = 1.56 \text{Re}^{0.058} \left( \frac{d_{OR}^2 \sigma}{\Delta \rho g} \right)^{1/4}$ $d_B = 0.32 \text{Re}^{0.425} \left( \frac{d_{OR}^2 \sigma}{\Delta \rho g} \right)^{1/4}$	$1 < \text{Re} < 10$ $10 < \text{Re} < 21,000$	Kumar et al. [28]
d <sub>B</sub> -7	$\frac{g \rho_L d_B^2}{\sigma} = 8.8 \left( \frac{u_G \mu_L}{\sigma} \right)^{-0.04} \left( \frac{\sigma^3 \rho_L}{g \mu_L^4} \right)^{-0.12} \left( \frac{\rho_L}{\rho_G} \right)^{0.22}$		Wilkinson et al. [29]

**Table 4.2** Existing correlations for predicting bubble rising velocity ( $U_B$ ) [11]

Eq.	Correlations	Conditions	References
U <sub>B</sub> -1	$U_B = \frac{g \Delta \rho d_B^2}{12 \mu_L}$	$\text{Re} < 250, \frac{\mu_G}{\mu_L} = 0$	Hadamard et Rybczynski [30]
U <sub>B</sub> -2	$U_B = \frac{g \Delta \rho d_B^2}{18 \mu_L}$	$\text{Re} < 250, \frac{\mu_G}{\mu_L} \rightarrow \infty$	Frumkin et Levich [31]
U <sub>B</sub> -3	$U_B = \frac{\mu_L}{\rho_L d_B} (J - 0.857) M_o^{-0.149}$ $J = 0.94 H^{0.757} \quad (2 < H \leq 59.3)$ $J = 0.32 H^{0.441} \quad (H > 59.3)$ $H = \frac{4}{3} E_o M_o^{-0.149} \left( \frac{\mu_L}{0.0009} \right)^{-0.14}$	$250 < \text{Re} < 6,000$	Grace et al. [32]
U <sub>B</sub> -4	$U_B = \left( \frac{2\sigma}{d_B \rho} + 0.5 d_B g \right)^{0.5}$	$0.2 \leq d_B \leq 8 \text{cm}$	Mendelson [33]
U <sub>B</sub> -5	Experimental curve for the bubble rising velocity		Grace & Wairegi [7]

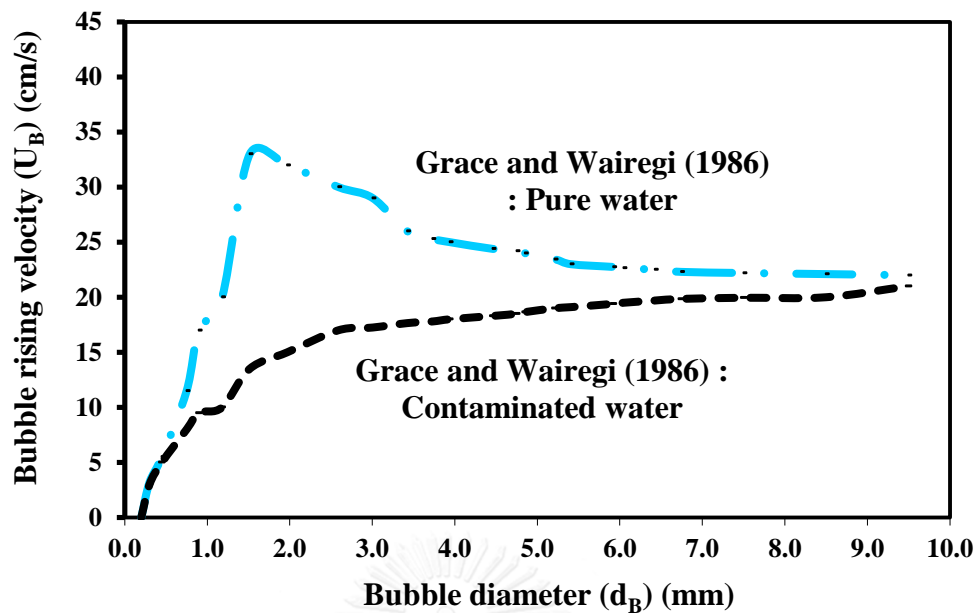


**Figure 4.4** Relation of generated bubble diameter ( $d_B$ ) and bubble rising velocity ( $U_B$ ) (Grace and Wairegi [7])

After bubble diameter ( $d_B$ ), and their rising velocity ( $U_B$ ) can be calculated, then interfacial area ( $a$ ) can be estimated by this following equation,

$$a = \frac{\text{Total surface area}}{\text{Total volume}} = \frac{f_B H_L \pi d_B^2}{U_B (A H_L + N_B V_B)} \quad (4.1)$$

Where  $N_B$  is the generated bubble number,  $f_B$  is the bubble formation frequency,  $H_L$  is the liquid height,  $V_B$  is the bubble volume and  $S_B$  is the bubble surface area and  $A$  is cross-sectional area of the aeration tank [5]. For liquid-side mass transfer coefficient ( $k_L$ ), it can be estimated by Higbie's equation or Frossling's equation as follow [34],

$$k_L = 2 \sqrt{\frac{D U_B}{\pi h}} \quad (4.2)$$

$$k_L = \frac{D}{d_B} (2 + 0.6 \text{Re}^{1/2} \text{Sc}^{1/3}) \quad (4.3)$$

Where  $h$  is the bubble height.  $\text{Re}$  is the bubble Reynolds number and  $\text{Sc}$  is the Schmidt number, respectively. Normally, the Higbie's theory is valid for mobile spherical bubbles ( $d_B > 2.5$  mm) having short contact times with the liquid, whereas

the Frossling's equation deals with spherical bubbles having rigid interface ( $0.1 \text{ mm} < d_B < 2 \text{ mm}$ ). Finally, volumetric mass transfer coefficient ( $k_L a$ ) can be predicted by a simple relation as follow,

$$k_L a = k_L \times a \quad (4.4)$$

According to these existing correlations and models were taken from small-scale experiment, which they have some conditions and might not be fitted with the actual-scale of aeration system. Therefore, this study aims to develop accuracy of the prediction models by applying correction factor and fitting the parameters that can be obtained from the experiment to their correlations. Then the suitable prediction model is expected to be proposed, and used as criteria for aeration system design.

#### Notation

a	interfacial area ( $\text{m}^{-1}$ )	P	Pressure (Pa)
A	cross-sectional area of aeration tank ( $\text{m}^2$ )	$Q_g$	gas flow rate ( $\text{m}^3/\text{s}$ )
$A_{OR}$	cross-section area of orifice ( $\text{m}^2$ )	$Q_{go}$	gas flow rate through orifice ( $\text{m}^3/\text{s}$ )
$C_{NaCl}$	sodium chloride concentration (mole/L)	Re	Reynolds number
D	oxygen diffusion coefficient in aerated water	$S_B$	bubble surface ( $\text{m}^2$ )
$D_{Water}$	oxygen diffusion coefficient in clean water	Sc	Schmidt number
$d_B$	bubble diameter (m)	$t_{Frame}$	time of bubble spatial displacement (s)
$d_{OR}$	orifice diameter (m)	$U_B$	bubble rising velocity (m/s)
$f_B$	bubble formation frequency (1/s)	$U_G$	gas velocity through orifice (m/s)
$h_B$	bubble height (m)	$V_B$	bubble volume ( $\text{m}^3$ )
$H_L$	liquid height (m)	$V_{OR}$	orifice volume ( $\text{m}^3$ )
$H_{OR}$	orifice height (m)	$W_D$	weight of flexible tube (g)
$k_L$	liquid-side mass transfer coefficient (m/s)	$\phi_D$	factor of void volume per weight of flexible tube ( $\text{m}^3/\text{g}$ )
$k_L a$	volumetric mass transfer coefficient (1/s)	$\Delta D$	bubble spatial displacement (m)
$l_B$	bubble length (m)	$\mu_L$	liquid viscosity (Pa.s)
$N_B$	generated bubble number	$\rho_L$	liquid density ( $\text{kg}/\text{m}^3$ )
$N_{OR}$	orifice number	$\sigma_L$	liquid surface tension (N/m)

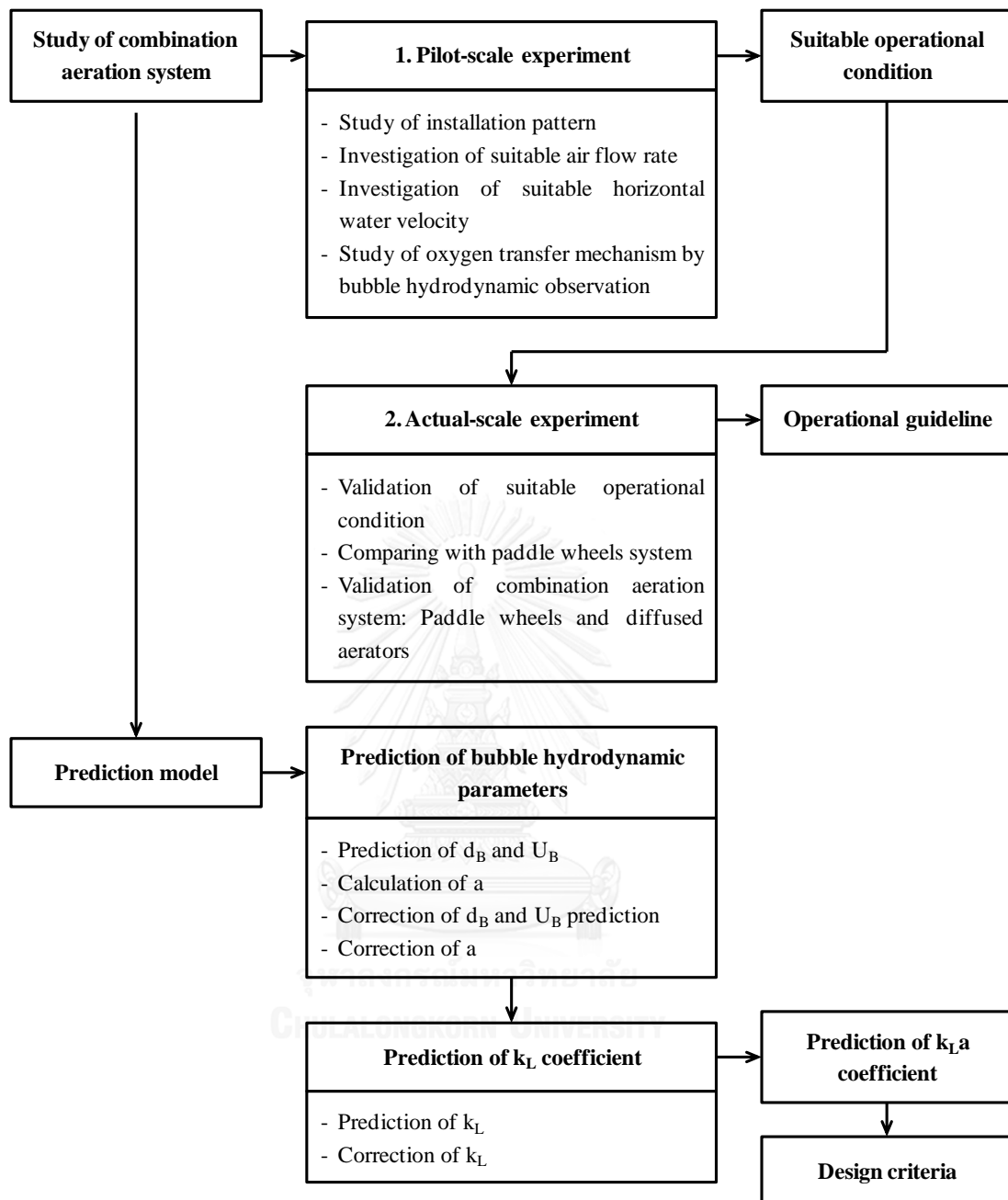


**Figure 4.5** Diagram of Combination aeration system study

## 4.5 Results and Discussion

### 4.5.1 The horizontal water velocity for the combination aeration system

In this part, the suitable horizontal water velocity was investigated in the 680L of pilot-scale aeration tank by varying the water pumps, and combining with the diffusers. The provided horizontal water velocity related to the pump sizes. One pump



was combined with a frame of the flexible tube diffuser which consisted of 1.5m of the tube length. The tube length within a frame was designed by the same ratio as the LFFA experiment in the previous chapter (around 3.6m of tube length per frame, 4 frames per 100m<sup>2</sup> of surface area of the pond) then the required tube length was scaled down from 90,000L of the aquaculture pond into this 680L of the aeration tank, therefore 1.5m was selected to be a frame of diffuser. The aeration tank was filled up with 680L of tap water by 0.3m of the depth, simulating a shallow aeration tank as same as the aquaculture pond, by the same ratio 0.3m of the depth per 2m of the length and 1.5m of the depth per 2m of the length, respectively. And 10 L/min of the air flow rate was also supplied to a frame of diffuser by the same ratio. In order to evaluate the combination aeration system by the  $k_{La}$  coefficient, DO values were monitored by 3 positions: center, and 2 opposite sides closed to the tank wall. Then the  $k_{La}$  values of the combination aeration system were compared to the  $k_{La}$  of the diffuser system (1-4 frames of diffuser).

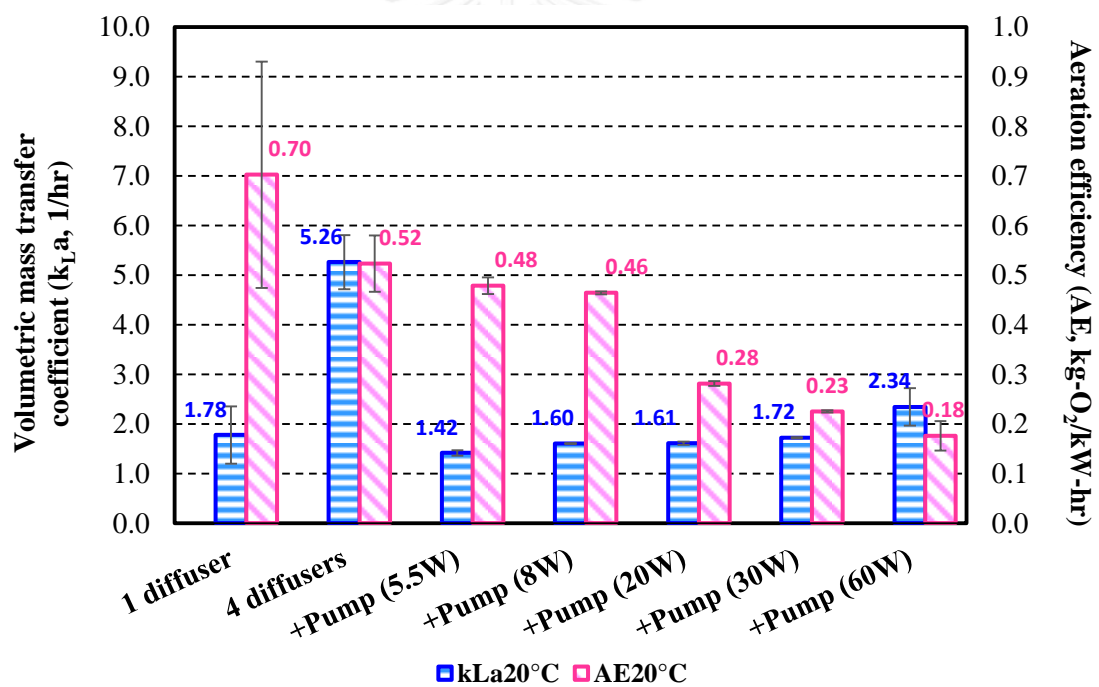


**Figure 4.6** Effects of the horizontal water velocity ( $v_H$ ) on the oxygen transfer performance

It was found that the average  $k_{La}$  of the combination system trend to be increased (1.42- 2.34 1/h) when increased the pump size or the horizontal water velocity ( $v_H$ ) (39-183 mm/s), because of the increasing of the  $v_H$  gave a higher mixing potential that can be obviously observed by the water flow within the tank. Not only the  $k_{La}$  was increased by the  $v_H$ , but it also become more uniform when applying the  $v_H$ ,

represented by the narrow standard deviation bar within the graph. In the contrast, AE was dropped from 0.48 to 0.18 kg-O<sub>2</sub>/kW-hr when combining the pump with the diffuser, because the applied pump consumed more electric power than the diffuser individually. From the LFFA experiment, it was shown that only high AE value of the diffuser system was not enough to maintain the aerobic condition during the shrimp cultivation, the required diffuser number was double into 8 frames. So, it was proved that the mixing was another important mechanism for the aeration. Therefore, the 5.5W of water should be combined with the flexible tube to be the combination aeration system, due to enhancement of the mixing performance.

#### 4.5.2 Comparison of aeration systems both term of oxygen transfer and energy performance

After the suitable water pump (5.5W) can be obtained by the previous section, it was combined with the flexible tube to be the combination aeration system. This combination consisted of 2 units of the pump and 2 frames of the tube in order to create a stable horizontal water velocity, after that its performance was compared to the other systems: diffuser system and paddle wheel system (only water circulation by 2 units of the water pumps). The  $k_L a$  and AE values were shown by the following graph,

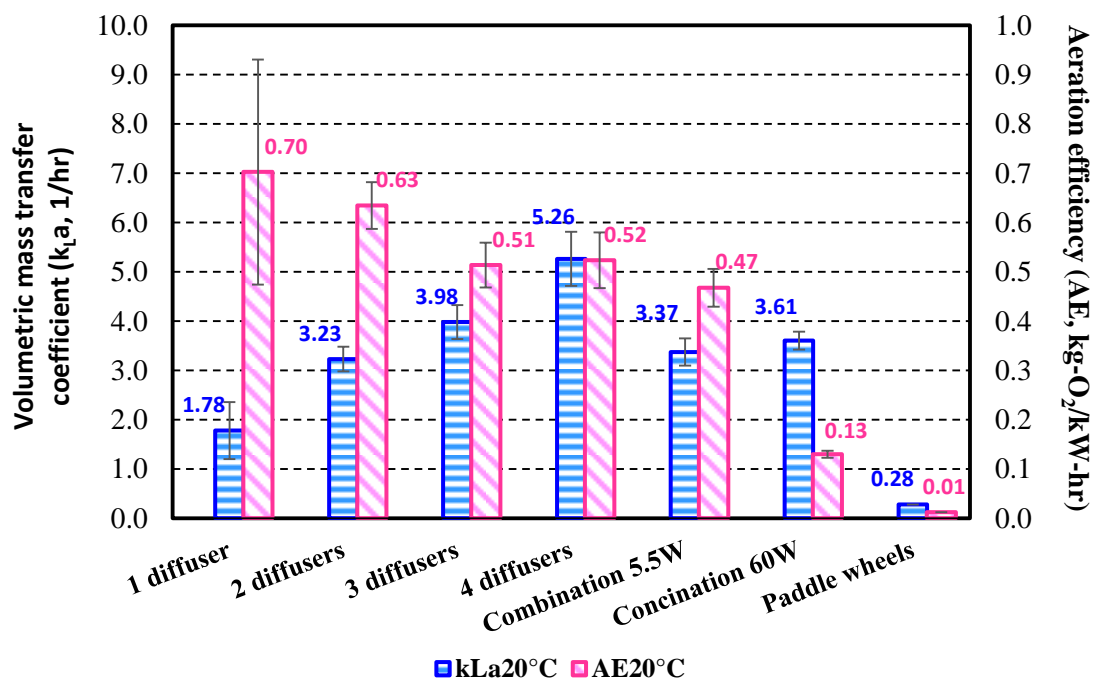
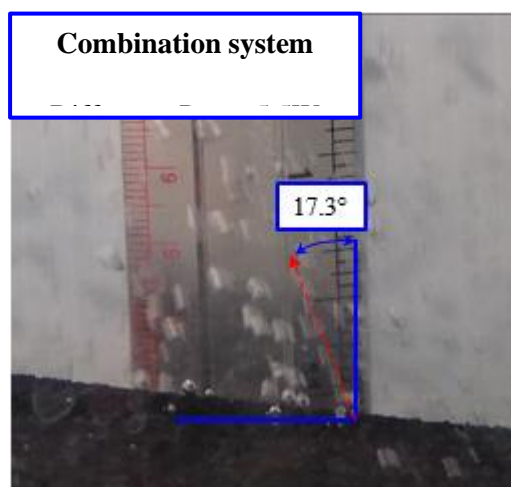


**Figure 4.7** Comparison of the aeration systems in term of the oxygen transfer performance

From the result, the diffuser system gave the highest performance both of  $k_{La}$  and AE values as expected, while the paddle wheel system was the lowest performance. Because the flexible tube can produce the fine bubbles with a large interfacial area that can transfer the oxygen effectively, while interfacial area from the water circulation in the paddle system was limited only on water surface. However, the  $k_{La}$  values from 3 monitoring positions of the paddle wheel system were equal due to its mixing by the water circulation. For the combination system, its  $k_{La}$  and AE values (3.37 1/hr and 0.47 kg-O<sub>2</sub>/kW-hr) was almost equal those values from 3 frames of the diffusers (3.98 1/hr and 0.51 kg-O<sub>2</sub>/kW-hr, respectively) that could be considered as an effective system. And the performance was improved more than 100%, comparing to the paddle system (conventional system). From the result, it can be concluded that the combination aeration system (diffusers and water pumps as a mixing device) can be applied to the large aeration tank/pond as same as aquaculture pond, and it can save the energy 100% (indicated by AE) more than the paddle wheel system (the conventional system) by following to this operational condition. Because a high oxygen transfer comes from the diffusers and a sufficient mixing performance comes from the mixing device.

#### 4.5.3 Bubble hydrodynamic parameters in the combination aeration system

In order to understand the oxygen transfer mechanism in the combination system, the bubble hydrodynamic parameters were observed in a 180L aeration tank. The horizontal water velocity was simulated by the same values from the same pumps. At first, the bubble rising was changed from the vertical by the  $v_H$ , and the degree of changing was increased (17.3°-66.1°) when  $v_H$  increasing (39-183 mm/s).



System	$v_H$	Changing
	mm/s	Degree
+Pump (5.5W)	39	17.3
+Pump (8W)	42	33.2
+Pump (20W)	87	52.7
+Pump (30W)	113	59.0
+Pump (60W)	183	66.1

**Figure 4.8** Changing of bubble rising direction by the horizontal water velocity ( $v_H$ )

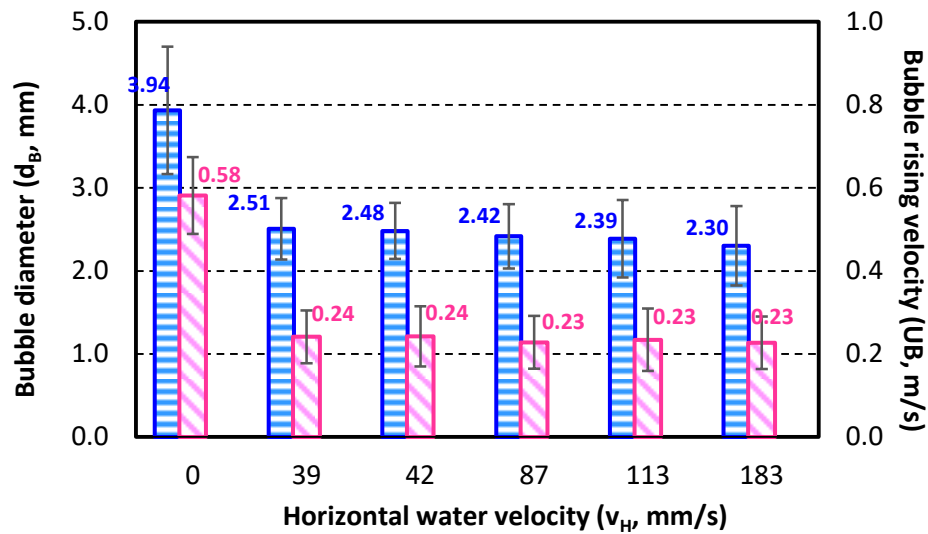


**Figure 4.9** Effects of the horizontal water velocity ( $v_H$ ) on the bubble hydrodynamic parameter ( $d_B$  and  $U_B$ )

As a result of the  $v_H$  applying, the bubble size trended to be decreased (2.51-2.30 mm) due to the shear force from the water cross flow cutting the bubbles and releasing them faster than usual. The bubble rising velocity which related to the bubble size was also decreased (0.24-0.23 m/s). The smaller bubble size brought the lower different density between bubbles and water that decreased the bubble rising velocity, according to the Buoyant force concept. So, the slower bubble rising, keeping the bubbles stay longer in the water and giving the oxygen transfer.

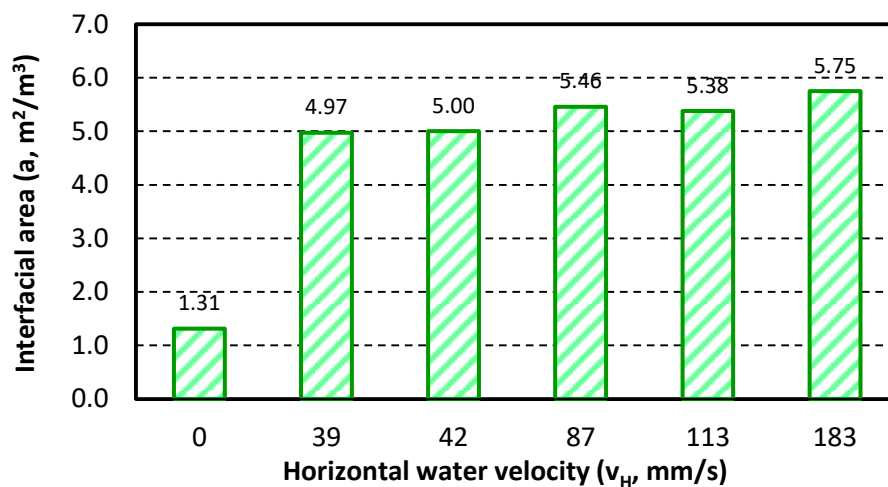


**Figure 4.10** Effects of the horizontal water velocity ( $v_H$ ) on the Interfacial area ( $a$ )

According to the smaller bubbles and slower bubble rising, the system provided more interfacial area ( $4.97\text{-}5.75\text{ m}^2/\text{m}^3$ ) around 300%, comparing to the normal condition of the diffuser system. For the recommended  $v_H$  (57 mm/s), the  $d_B$  was reduced into 2.51 mm, and  $v_H$  was decreased to 0.24 m/s that were sufficient to produce more interfacial area with the lowest energy consumption from the smallest water pump (5.5W). So, the combination aeration system was improved the oxygen transfer performance in term of increasing of the interfacial area by this phenomenon, while it can save the energy by the highest AE coming from the water pump (5.5W) as a mixing device.

#### 4.5.4 Residence time distribution study in the combination aeration system

Considering to the mixing performance, it was measured by the tracer study which operated during the aeration, the 680L aeration tank was modified to be a continuous reactor with the influent and effluent water flow. Sodium chloride was selected to be a pulse tracer, which dissolved and dosed in the solution form. The conductivity after dosing the sodium chloride solution was designed to be around 1,100  $\mu\text{s}/\text{cm}$  that was higher than tap water 3 times, so that the conductivity can be observed obviously. The 3 aeration systems: paddle wheel (2 units of 60W water pump), diffuser (4 frames), and combination system (2 sets of diffuser and 2 units of 5.5W water pump) were compared their mixing performance. The obtained conductivity by time for each system was analyzed into the exit age distribution ( $E(t)$ ), called residence time distribution (RTD), in order to estimate the actual residence time of the water flow within the tank. After that the effective volume or dead volume can be estimated. The mixing performance can be represented by the equivalent number of tanks-in-series ( $N$ ), and pecelet number ( $Pe$ ) by these following equation [35, 36],

$$E(t) = \frac{C}{\sum C\Delta t} \quad (4.5)$$

$$\bar{t} = \sum_i t_i E_i(t) \Delta t_i \quad (4.6)$$

$$\sigma_t^2 = \sum_i t_i^2 E_i(t) \Delta t_i - \bar{t}^2 \quad (4.7)$$

$$\frac{\sigma^2}{\bar{t}^2} = \frac{2}{Pe} - \left(\frac{2}{Pe}\right)(1 - e^{-Pe}) \quad (4.8)$$

$$E_{\theta-\max} = \frac{N(N-1)^{(N-1)}}{(N-1)!} e^{-(N-1)} \quad (4.9)$$

Where  $E(t)$  is an exit age distribution function,  $C$  is the tracer concentration or the conductivity for this case, and  $\Delta t$  is differential monitoring time.  $\bar{t}$  is an actual residence time,  $\sigma_t^2$  is variance based on the time, and  $Pe$  is pecelet number.  $E_{\Theta-\max}$  is normalized exit age distribution function,  $N$  is number of the reactor or tank in serie.

**Table 4.3** Residence time distribution study (RTD) results

Aeration systems	$\tau$	$\bar{t}$	Dead volume		Number of tank in serie	$Pe$
	min	min	L	%	Tanks	-
Paddle Wheel	68	62	58	8.51	2	1.22
Diffuser	68	62	62	9.12	2	1.21
Combination	68	63	47	6.91	2	1.23

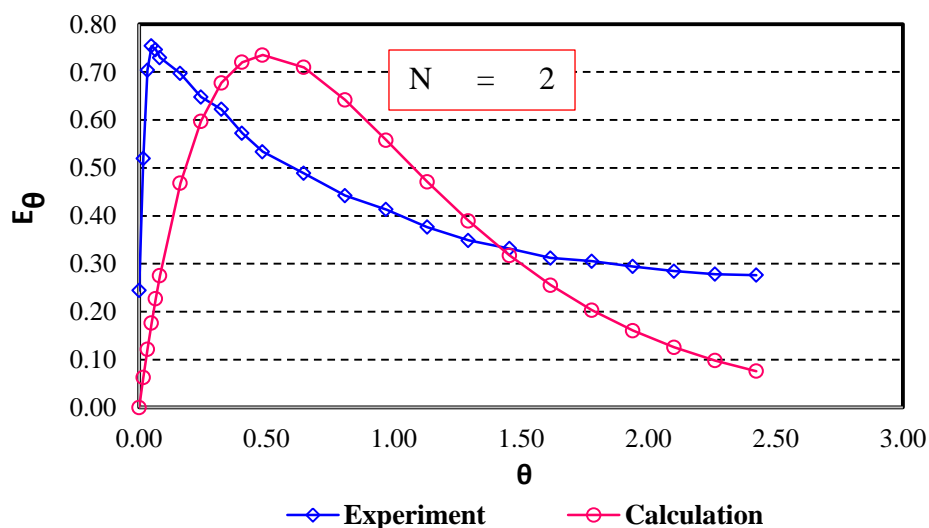


**Figure 4.11** The effluent residence time distribution curve and the tanks-in-series model

According to the paddle wheel is the conventional system for the aquaculture with a high mixing performance, so its mixing can be considered as a sufficient level for the aeration. From the result it was found that the simulated paddle wheel system had 62 min of the actual residence time, because the water circulation might brought the short circuit on water surface, resulting in a 9% of the tank volume loss. However, the water flow pattern can be classified as a completely mixed when the number of tank is below 6 tanks, and it becomes more completely mixed when the number is closed to 1 tank, according to the non-ideal flow model. Therefore, the result of paddle wheel was

around 2 tanks-in-series, and 1.22 of Pe that can be classified as the completely mixed flow with the tank as well as its Peclet number that was more than 1 [21].

For the diffuser system, it had to increase the number of diffuser up to 4 frames, in order to achieve the sufficient mixing level. Even the diffuser has a high energy performance, but the 4 frames of it will cover overall area of the tank, then the turbulence and flow pattern from their bubble rising might be the same as the aeration in the activated sludge process that will not be suitable for the aquaculture.

While the combination aeration system which consisted of 2 frames of diffuser and 2 units of pump can achieve the sufficient mixing level also, and it created the water flow in the proper direction as same as the conventional system (paddle wheel system). Therefore, the combination system has a feasibility to apply in the aquaculture due to its oxygen transfer and mixing performance.

#### 4.5.5 Theoretical prediction model for oxygen transfer parameters

According to the aeration systems, their performance is related to several factors: aeration tank dimension, aerator type and its properties, aerator installation and arrangement, aerated water properties, and operating condition. So, it can be considered as a specific performance for each system that has to measure the  $k_La$  in the actual operation, in order to know its real performance. For the  $k_La$  measurement, it is quite difficult to do in a large scale of the aeration tank, which will consume a lot of chemical to desorb the initial dissolved oxygen before starting the experiment. From this reason, the  $k_La$  prediction comes up to solve this gap, and to get the primary information for the aeration system design.

For this study, the presented prediction models were selected to estimate bubble hydrodynamic parameters, and then predicting the  $k_La$  for the combination aeration system.

**Table 4.4** Correlations for bubble diameter ( $d_B$ ) prediction

Eq.	Correlation	Condition	Reference
$d_{B-1}$	$d_B = \left( \frac{6 \cdot d_{OR} \cdot \sigma \cdot g_c}{g \cdot \Delta \rho} \right)^{1/5}$	$Q_{go} < \left( \frac{20(\sigma \cdot d_o \cdot g_c)^5}{(g \cdot \Delta \rho)^2 \cdot \rho_L^3} \right)^{1/6}$	Krevelen et al. (1959)
$d_{B-2}$	$d_B = 0.0287 d_{OR}^{1/2} \cdot Re^{1/3}$	$Re < 2100$	Leibson et al. (1956)
$d_{B-3}$	$d_B = \left( \frac{72 \rho_L}{\pi^2 \cdot g \cdot \Delta \rho} \right)^{1/5} \cdot Q_{go}^{0.4}$		Krevelen et al. (1959)
$d_{B-4}$	$d_B = 7.1 \times 10^{-4} \cdot \Delta P^{0.328}$		Hebrard (1995)
$d_{B-5}$	$d_B = 15.73 \times 10^{-3} \cdot D_C^{0.32} \left( \frac{Q_g}{D_{OR}} \right)^{0.16}$		Hebrard (1995)
$d_{B-6}$	$d_B = 1.56 Re^{0.058} \left( \frac{d_{OR}^2 \cdot \sigma}{\Delta \rho g} \right)^{1/4}$ $d_B = 0.32 Re^{0.425} \left( \frac{d_{OR}^2 \cdot \sigma}{\Delta \rho g} \right)^{1/4}$	$1 < Re < 10$  $10 < Re < 21000$	Kumar et al. (1976)
$d_{B-7}$	$\frac{g \cdot \rho_L \cdot d_B^2}{\sigma} = 8.8 \left( \frac{u_G \cdot \mu_L}{\sigma} \right)^{-0.04} \left( \frac{\sigma^3 \cdot \rho_L}{g \cdot \mu_L} \right)^{-0.12} \left( \frac{\rho_L}{\rho_G} \right)^{0.22}$		Wilkinson et al. (1994)

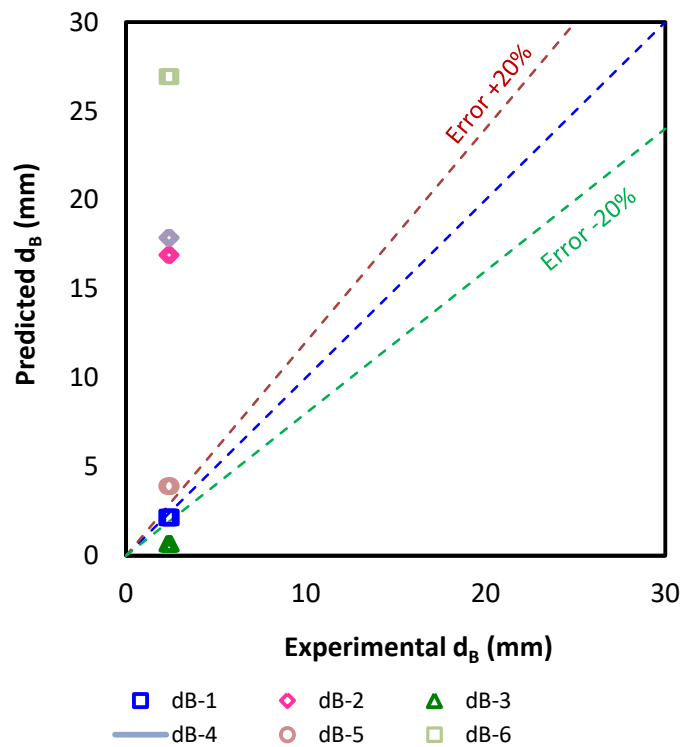
**Table 4.5** Correlations for bubble rising velocity ( $U_B$ ) prediction

Eq.	Correlation	Condition	Reference
$U_{B-1}$	$U_B = \frac{g \cdot \Delta \rho \cdot d_B^2}{12 \cdot \mu}$	$Re < 250$ , $\frac{\mu_G}{\mu_L} = 0$	Hadamard and Ryazantsev (1911)
$U_{B-2}$	$U_B = \frac{g \cdot \Delta \rho \cdot d_B^2}{18 \cdot \mu}$	$Re < 250$ , $\frac{\mu_G}{\mu_L} = \infty$	Frumkin and Levich (1947)
$U_{B-3}$	$U_B = \frac{\mu_L (J - 0.875) M_o^{-0.149}}{\rho_L \cdot d_B}$ $J = 0.94H^{0.757} ; 2 < H \leq 59.3$ $J = 0.32H^{0.441} ; H > 59.3$ $H = \frac{4}{3} E_o \cdot M_o^{-0.149} \left( \frac{\mu_L}{0.0009} \right)^{-0.14}$	$250 < Re < 6000$	Grace et al. (1976)
$U_{B-4}$	$U_B = \left( \frac{2\sigma}{d_B \cdot \rho} + 0.5d_B \cdot g \right)^{0.5}$	$0.2 \leq d_B \leq 8 \text{ cm.}$	Mendelson (1967)
$U_{B-5}$	Experimental curve for the bubble rising velocity		Grace and Wairegi (1986)



**Table 4.6** Correlations for liquid-side mass transfer coefficient ( $k_L$ ) prediction

Eq.	Correlation	Reference
$k_{L-1}$	$k_L = 2 \left( \frac{D_{O_2} \cdot U_B}{\pi \cdot h} \right)^{0.5}$	Higbie's equation (Roustan, 2003)
$k_{L-2}$	$k_L = \frac{D}{d_B} (2 + 0.6Re^{(1/2)} \cdot Sc^{(1/3)})$	Frossling's equation (Roustan, 2003)

**Figure 4.12** Predicted results of bubble diameter ( $d_B$ ) for the combination aeration system

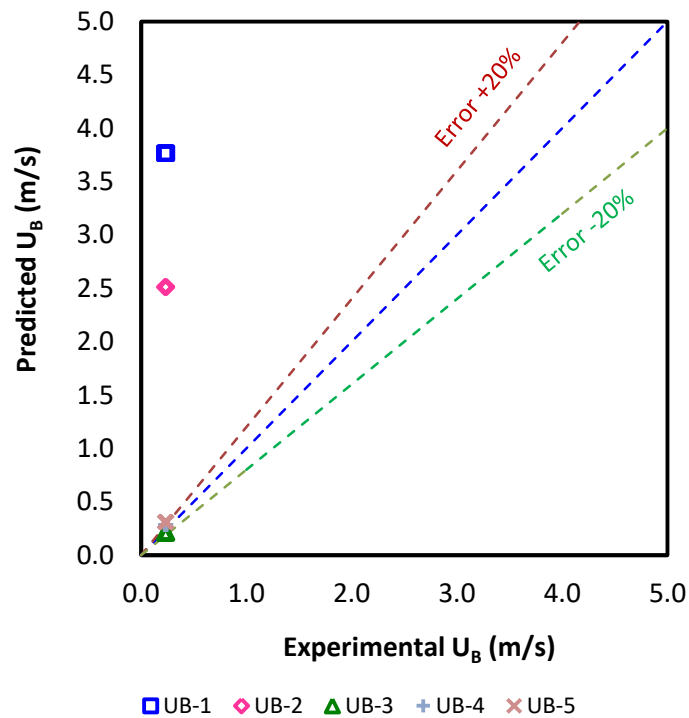


**Figure 4.13** Predicted results of bubble rising velocity ( $U_B$ ) for the combination aeration system

From the result, it was found that some prediction models gave an error over than 20% for the  $d_B$  and  $U_B$  prediction, while some of them gave a constant value even the air flow rate was increase or the other conditions were changed. According to the result, only the present prediction models were not suitable for the combination system, due to their accuracy and specific application. Therefore, another correction factor was needed to improve the accuracy, and modifying the model for the widely application.

This section aims to propose the suitable prediction model for the  $k_L a$  by selecting the presented prediction models from the previous works, and trying to improve the prediction accuracy in order to predict and design an aeration system before measuring the actual  $k_L a$  value. The prediction started from the bubble size ( $d_B$ ) and its rising velocity ( $U_B$ ) that were the primary parameters to estimate the interfacial area ( $a$ ). After that the liquid side mass transfer coefficient ( $k_L$ ) was predicted by another equation that relate with some parameters such as air flow rate ( $Q_g$ ), water characteristics,  $d_B$  and  $U_B$  also. Finally, the volumetric mass transfer coefficient ( $k_L a$ ) can be obtained by the multiplying result between  $k_L$  and  $a$ -area. The predicted results

were compared the experimental results from several aeration tanks: 10L, 180L, 2,000L, and 680L, including the combination system test also.

$$d_B = 15.73 \times 10^{-3} D_C^{0.32} \left( \frac{Q_G}{d_{OR}} \right)^{0.16} \quad (4.10)$$

At first, the Hebrard's equation (1995) was selected as a base equation to predict bubble diameter, due to its accuracy in the previous work. Where  $D_C$  is aeration column diameter,  $Q_G$  is supplied air flow rate, and  $d_{OR}$  is orifice diameter. From the equation, the dimension of the aeration tank, air flow rate, diffuser properties related to the bubble size, those parameters were applied and modified in the new equation for the accuracy improvement as following equation [24, 25],

$$d_B = 4.71 D_{Submerged}^{1.1} + 0.78 \left( \frac{WL}{A_{OR}} \right)^{0.03} + 0.77 \left( \frac{Q_G}{d_{OR}} \right)^{0.46} - 0.92 v_H^{0.25} \quad (4.11)$$

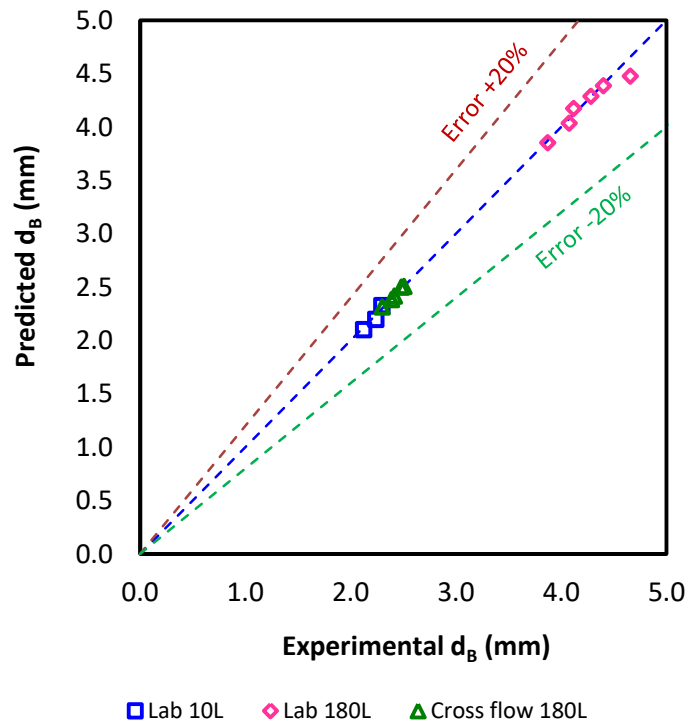


**Figure 4.14** Comparison of predicted bubble diameter to the experimental result

Where  $D_{\text{Submerged}}$  is submerged of the diffuser,  $W$  and  $L$  are the aeration tank width and length respectively,  $A_{\text{OR}}$  is total orifice area. It was found that  $d_B$  can be predicted with an error lower than 5% for all experiment in the lab scale, even applying the water cross flow for the combination system.

For the bubble rising velocity prediction, there was no accurate equation to predict it from the previous work, therefore  $d_B$  and other water characteristics were applied into the new equation, as shown by following equation,

$$U_B = 1.262\rho_L^{2.115}\mu_L^{2.211}g^{0.562}d_B^{0.26}Q_G^{0.057} - 0.079v_H^{0.087} \quad (4.12)$$

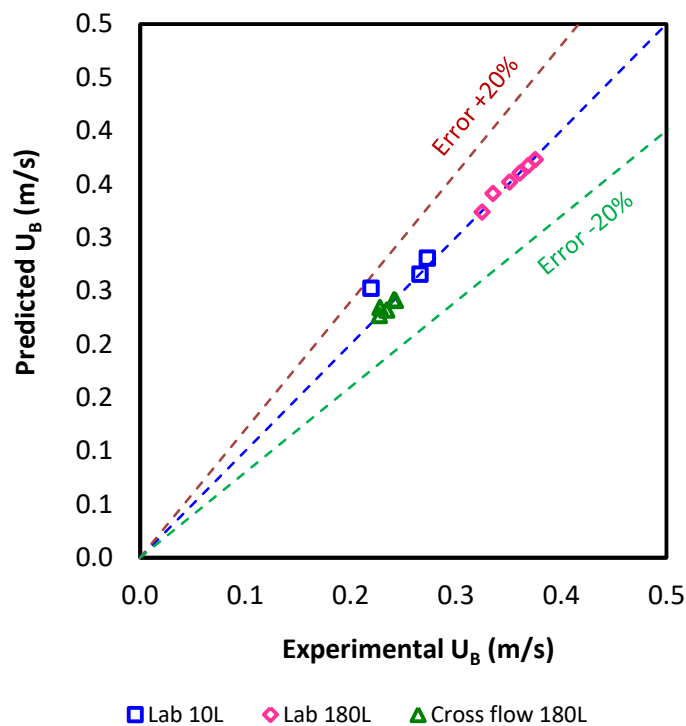


**Figure 4.15** Comparison of predicted bubble rising velocity to the experimental result

Where  $\rho_L$  and  $\mu_L$  are liquid density and liquid viscosity respectively, and  $g$  is acceleration due to gravity. From the result,  $U_B$  can be predicted with the maximum error around 12% because of this parameter was more difficult than the bubble size, resulting in some error occurred in some experiment condition.

After the  $d_B$  and  $U_B$  can be predicted by the Painmanakul's equation (2005) the same way as the previous chapters. Then the Higbie's equation was selected to be a based

equation for the  $k_L$  coefficient prediction. The tank dimension,  $d_B$ ,  $U_B$ , and  $Q_G$  were applied to improve the prediction accuracy.

$$k_L = 0.767 \frac{(WL)^{0.207} d_B^{1.496} U_B^{0.654}}{D_{\text{Submerged}}^{0.234} Q_G^{0.307}} - 4.11 \times 10^{-5} \ln(v_H) + 2.10 \times 10^{-5} \quad (4.13)$$

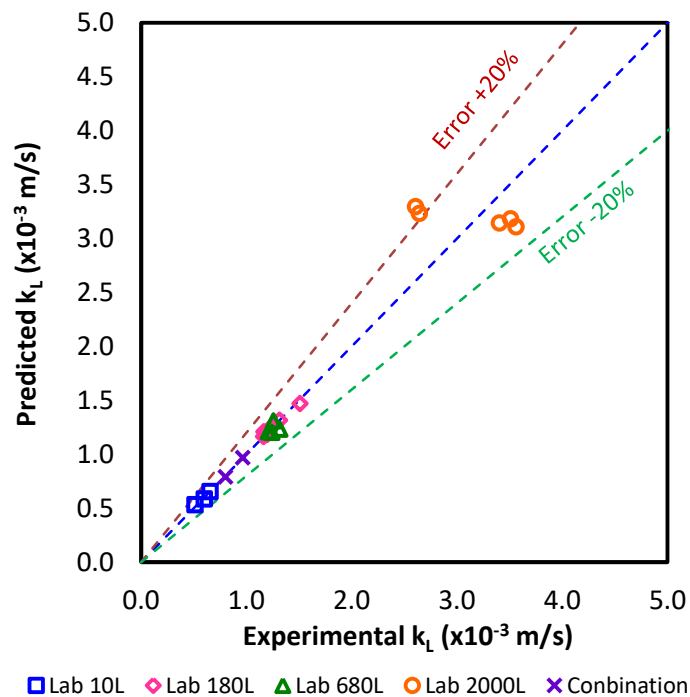


**Figure 4.16** Comparison of predicted liquid side mass transfer coefficient to the experimental result

According to the  $k_L$  cannot be measure directly, the obtained values also came from the dividing result between the experimental  $k_L a$  and  $a$ -area, therefore the equation was verified by the pilot-scale experiment. It was found that the  $k_L$  can be predicted with an error lower than 6% for the 10L, 180L and 680L of aeration tank including the combination system, because of their dimension were nearly the same, while the 2000L of aeration tank with the column shape got more error up to 26%. Therefore, the  $k_L$  prediction should be studied for further by correcting more experimental data or conducting the experiment for the  $k_L$  measurement directly.

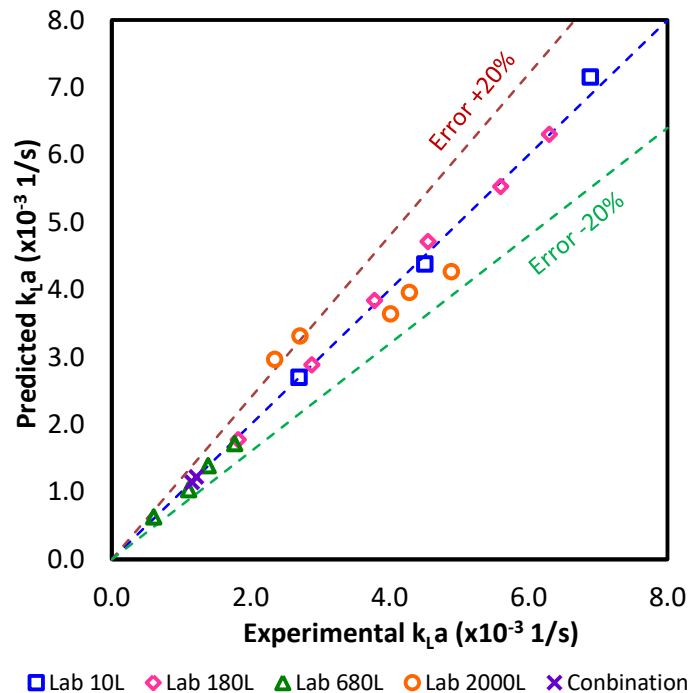


**Figure 4.17** Comparison of predicted volumetric mass transfer coefficient to the experimental result

Finally, the  $k_{L,a}$  coefficient can be predicted as a product between  $k_L$  coefficient and  $a$ -area. It was found that the  $k_{L,a}$  from 10L, 180L, 680L of the aeration including the combination system can be predicted accurately with an error 6%, while the 2000L got an error around 26% coming the error of the  $k_L$  prediction. Therefore, these prediction models can be applied to predict the bubble hydrodynamic parameters and the oxygen transfer parameters accurately that can be used as a criterion for the aeration system design. However, the  $k_L$  prediction should be studied for further to improve the predicting accuracy and widely application of the prediction model.

#### 4.6 Conclusions

This study has proved that the applying horizontal water flow during the aeration is the effective way to improve the oxygen transfer and energy performance. Moreover, the bubble hydrodynamic parameters and the oxygen transfer parameters can be predicted and used as a criterion for the aeration system design in the future. The results can be concluded by following issues:

- The 57 mm/s of the horizontal water velocity is suitable for the combination aeration system due to improving both term of the oxygen transfer and energy performance.
- The aeration efficiency presenting the energy performance can be improved more than 100% by the combination aeration system, comparing to the conventional aeration system in the aquaculture.
- The horizontal water velocity can improve the oxygen transfer mechanism by producing more interfacial area 300% comparing to the diffuser system individually.
- The combination aeration system can distribute the dissolved oxygen uniformly by its mixing performance which is the same level as the conventional aeration system in the aquaculture.
- Both of oxygen transfer parameters and bubble hydrodynamic parameters can be predicted accurately by the presented prediction models with an error lower than 10% for the combination aeration system.

**Table 4.7** The recommended installation and operational condition for the combination aeration system

**Installation pattern**

Parameters	Conditions	Unit
Flexible rubber tube	0.4	m <sup>2</sup> -surface area per m-tube
Air flow rate	9 - 10	L/min per m <sup>2</sup> -surface area
Horizontal water velocity	60 - 70	mm/s
Re for bubbles	520 - 602	-
Re for Liquid	20,000 - 28,000	-


**Table 4.8** The recommended prediction model for the volumetric mass transfer coefficient


$d_B = 4.71 D_{\text{Submerged}}^{1.1} + 0.78 \left( \frac{WL}{A_{\text{OR}}} \right)^{0.03} + 0.77 \left( \frac{Q_G}{d_{\text{OR}}} \right)^{0.46} - 0.92 v_H^{0.25}$
$U_B = 1.262 \rho_L^{2.115} \mu_L^{2.211} g^{0.562} d_B^{0.26} Q_G^{0.057} - 0.079 v_H^{0.087}$
$k_L = 0.767 \frac{(WL)^{0.207} d_B^{1.496} U_B^{0.654}}{D_{\text{Submerged}}^{0.234} Q_G^{0.307}} - 4.11 \times 10^{-5} \ln(v_H) + 2.10 \times 10^{-5}$
$a = \frac{\text{Total surface area}}{\text{Total volume}} = \frac{f_B H_L \pi d_B^2}{U_B (A H_L + N_B V_B)}$
$k_L a = k_L \times a$





### The system design step

1. Calculating the required length of the flexible tube by  

$$0.03 \frac{\text{m}^2\text{-surface area}}{\text{m-tube}}$$

2. Arranging the tube as a frame of diffuser around  

$$0.3 \frac{\text{m-tube}}{\text{set}}$$

3. Calculating the required air flow rate by  

$$9.1 \frac{\text{L}}{\text{min-m}^2}$$

4. Installing the diffuser and mixing devices at the opposite side to circulate the water by  

$$57 \frac{\text{mm}}{\text{s}}$$
 of the horizontal water velocity  

5. Recheck the system performance by the recommended prediction model

**Figure 4.18** The guideline for the combination aeration system design

## CHAPTER 5

### CONCLUSIONS AND RECOMMENDATIONS

According to the research scope, the 3 simple ways, to improve aeration systems both terms of oxygen transfer efficiency and energy performance, were studied. The results were presented that the 3 improvement ways are effective, and can be applied in the actual applications of the aeration, which can be described by following issues,

#### **5.1 Effects of physical properties of diffused aerator on oxygen transfer efficiency and bubble hydrodynamic parameters**

The result has shown that the physical diffuser tube properties play the important role on bubble hydrodynamic parameters, oxygen transfer efficiency, power consumption, and thus the operating cost, which can be summarized as following:

- The volumetric mass transfer coefficient increases with the gas flow rates whatever the gas diffusers. The highest  $k_L a$  values can be obtained with the tube No. 16, which is 3.4 mm of thickness, 3,100 kN/m<sup>2</sup> of tensile strength, and 75% of elongation, which can produce the smallest bubbles. However, the tube No. 16 requires the highest operating pressure, resulting in the lowest aeration efficiency. So, it is not suitable for the aeration.
- The aeration efficiency (AE) should be considered in order to compare the different gas diffusers and select the suitable design and production;
- The physical diffuser properties (tube wall thickness, tensile strength, orifice size, hardness and elongation) have been proven to be the key factor that controls the oxygen transfer performance;
- The effects of physical diffuser properties (tube hardness and elongation) on the bubble formation phenomenon, orifice size and the interfacial area were clearly proved;
- It is not necessary to generate too much fine bubbles to increase the interfacial area: this relates to high power consumption and the great decrease of the  $k_L$  coefficient.
- Due to the values of  $k_L a$ , OTE,  $a$  and  $k_L$  obtained in this study, the physical diffuser properties associated with the tube No. 12: 3.2 mm of thickness, 1,000

$\text{kN/m}^2$  of tensile strength, and 19% of elongation, should be applied in order to produce the practical flexible aeration diffuser tube.

- Comparing to the conventional aerators, the flexible rubber tube has high aeration performance due to its fine bubble production, oxygen transfer performance presented by  $k_La$  and OTE value, and energy performance presented by AE value.

From the results, the best flexible rubber tube can be obtained, then it can be applied as a diffused aerator in the next part. The operating condition: air flow rate, the tube length per surface area of the aeration tank were applied into the next experiment by the same range, so that the suitable operating condition can be investigated and summarized as a design criterion.

## **5.2 Improvement of oxygen transfer efficiency in term of interfacial area increase by Liquid Film Forming Apparatus (LFFA)**

The results clearly show that the LFFA has the potential to be a superior aerator system for aquaculture ponds due to its high aeration efficiency. The “4-D\*” (with partitions), which consists of 4 sets of diffusers combined with the 4 sets LFFA, including the partitions to control the water flow, is preferable as the suitable installation pattern for this experiment, with 100% of the maximum oxygen transfer improvement:  $k_{La_{20^\circ\text{C}}}$ , OTE, and AE for the flexible rubber tube diffuser, due to liquid film forming on water surface which increases the contacting area. For convenient installation and flexible for the variable water level, the LFFA can be applied as a floating type with the same oxygen transfer efficiency. Therefore, the diffusers can be applied in a large aeration pond like aquaculture ponds. Their performance can be improved by the LFFA to create a large interfacial area by capturing bubbles to stay in the water, and creating some foam on the water surface for a while, which is an effective improvement method without more energy requirement. However, the mixing performance during the aeration is another important factor that should be considered in the aeration system, so that the combination system is set up and studied in the next part.

## **5.3 Study of combination aeration system in term of oxygen transfer efficiency and energy performance in pilot-scale experiment**

The result has shown that the applying horizontal water flow during the aeration is the effective way to improve the oxygen transfer and energy performance. Moreover, the

bubble hydrodynamic parameters and the oxygen transfer parameters can be predicted and used as a criterion for the aeration system design in the future.

- The 40-60 mm/s of the horizontal water velocity is suitable range for the combination aeration system due to improving both term of the oxygen transfer and energy performance.
- The aeration efficiency presenting the energy performance can be improved more than 100% by the combination aeration system, comparing to the conventional aeration system in the aquaculture.
- The horizontal water velocity can improve the oxygen transfer mechanism by producing more interfacial area 300% comparing to the diffuser system individually.
- The combination aeration system can distribute the dissolved oxygen uniformly by its mixing performance which is the same level as the conventional aeration system in the aquaculture.
- Both of oxygen transfer parameters and bubble hydrodynamic parameters can be predicted accurately by the presented prediction models with an error lower than 10% for the combination aeration system.

From the result, the combination aeration system, which combining between diffused aerators and mixing devices, can be presented as an alternative aeration system for a large aeration pond like aquaculture ponds. Which is an effective aeration system in oxygen transfer, oxygen distribution, and energy performance. Moreover, the parameters related to the oxygen transfer and bubble hydrodynamic parameters can be predicted accurately by the presented models, which can be used for the aeration system design in the future.

#### **5.4 Recommendations for the future**

Even the results have shown the significant improvement by the experiment, but there are some details are still needed to be studied for further in the actual application, so the researcher would like to recommend the following topics for the future work,

- The suitable operating condition for the combination aeration system should be validated in an actual aquaculture pond, and compared to the conventional aeration system (paddle wheels system).

- The diffused aerators within the combination aeration system could be combined with the LFFA for more oxygen transfer improvement, together with the mixing performance consideration.
- The combination aeration system should be studied and applied for the wastewater treatment processes, which require high oxygen supply rate while the highly mixing in the same time.
- There many parameters are still needed to be investigated for the accuracy improvement, which can make the prediction model become more widely application.

The researcher hopes that this research would provide ideas in order to enhance efficiency of the aeration. The ideas will illustrate aeration mechanism, equipment installation, setting up system, operation, and efficiency improvement.

The aerators selection is the first priority to consider. Then, the understanding in their mechanism will lead to the effective installation and operation. The LFFA is a good technique for the aeration system improvement, as well as the applying water cross flow during the aeration in the combination aeration system. However, it should be studied for further according to the above recommendations, in order to fulfill the gap of the aeration applications in the present and future situation.



## REFERENCES

1. Rosso, D., J.A. Libra, W. Wiehe, and M.K. Stenstrom. 2008. Membrane properties change in fine-pore aeration diffusers: Full-scale variations of transfer efficiency and headloss. *WATER RESEARCH* 42: 2640-2648.
2. Hongprasith, N. 2010. Analysis of Flexible Aeration Diffuser Tube From Rubber Waste in Aeration Process. Master Degree of Engineering Program in Environmental Engineering, Department of Environmental Engineering, Faculty of Engineering, Chulalongkorn University.
3. Metcalf & Eddy, I. 2004. *Wastewater Engineering Treatment and Reuse*. Fourth Edition. International Edition. Singapore : McGraw-Hill.
4. Hasanen, A., P. Orivuori, and J. Aittamaa. 2006. Measurements of local bubble size distributions from various flexible membrane diffusers. *Chemical Engineering and Processing* 45: 291-302.
5. Painmanakul, P., K. Loubiere, G. Hebrard, and P. Buffiere. 2004. Study of different membrane spargers used in waste water treatment: characterisation and performance. *Chemical Engineering and Processing* 43: 1347–1359.
6. Loubiere, K. and G. Hebrard. 2003. Bubble formation from a flexible hole submerged in an inviscid liquid. *Chemical Engineering Science* 58: 135-148.
7. Grace, J.R. and T. Wairegi. 1986. Properties and Characteristics of Drops and Bubbles. *Encyclopedia of Fluid Mechanics*. Huston: Gulf Publishing
8. Calderbank, P.H. and M.B. Moo-Young. 1961. The continuous phase heat and mass-transfer properties of dispersions. *Chemical Engineering Science* 16: 39-54.
9. Painmanakul, P., K. Loubière, G. Hébrard, M. Mietton-Peuchot, and M. Roustan. 2005. Effect of surfactants on liquid-side mass transfer coefficients. *Chemical Engineering Science* 60: 6480-6491.
10. Moustiri, S., G. Hebrard, S.S. Thakre, and M. Roustan. 2001. A unified correlation for predicting liquid axial dispersion coefficient in bubble columns. *Chemical Engineering Science* 56: 1041-1047.
11. Painmanakul, P., J. Wachirasak, M. Jamnongwong, and G. Hebrard. 2009. Theoretical Prediction of Volumetric Mass Transfer Coefficient (kLa) for Designing an Aeration Tank. *Engineering Journal* 13: 13-28.
12. Jamnongwong, M., K. Loubiere, N. Dietrich, and G. Hebrard. 2010. Experimental study of oxygen diffusion coefficients in clean water containing salt, glucose or surfactant: Consequences on the liquid-side mass transfer coefficients. *Chemical Engineering Journal* 165: 758-768.

13. Zhu, H., T. Imai, K. Tani, M. Ukita, M. Sekine, T. Higuchi, and Z. Zhang. 2007. Improvement of oxygen transfer efficiency in aerated ponds using liquid-film-assisted approach. *Water Science and Technology* 55: 183-191.
14. Kumar, A., S. Moulick, and B.C. Mal. 2010. Performance evaluation of propeller-aspirator-pump aerator. *Aquacultural Engineering* 42: 70-74.
15. Charoenpittaya, T. 2013. Analysis of diffused aeration system using Liquid-Film-Forming Apparatus (LFFA). Master's thesis Department of Environmental Engineering, Faculty of Engineering, Chulalongkorn University, Thailand
16. Yum, K., S.H. Kim, and H. Park. 2008. Effects of plum spacing and flowrate on destratification efficiency of air diffusers. *WATER RESEARCH* 42: 3249-3262.
17. Schumpe, A. and W. Deckwer. 1982. Gas holdups, specific interfacial areas, and mass transfer coefficients of aerated carboxymethyl cellulose solutions in a bubble column. *Industrial & Engineering Chemistry Process Design and Development* 21: 706-711.
18. Loubiere, K., V. Castaignede, G. Hebrard, and R. M. 2004. Bubble formation at a flexible orifice with liquid cross-flow. *Chemical Engineering and Processing* 43: 717-725.
19. Zhu, H., K. Tani, M. Ukita, M. Sekine, T. Higuchi, and Z.J. Zhang. 2007. Enhancement of oxygen transfer efficiency in diffused aeration systems using Liquid-Film-Forming Apparatus. *Environmental Technology* 28: 511-519.
20. Ashley, K.I., D.S. Mavinic, and K.J. Hall. 1992. Bench-scale study of oxygen transfer in coarse bubble diffused aeration. *WATER RESEARCH* 26: 1289-1295.
21. Zhou, X., Y. Wu, H. Shi, and Y. Song. 2013. Evaluation of oxygen transfer parameters of fine-bubble aeration system in plug flow aeration of wastewater treatment plant. *Journal of environmental sciences (China)* 25: 295-301.
22. Ashley, K.I., K.J. Hall, and D.S. Mavinic. 1991. Factors influencing oxygen transfer in fine pore diffused aeration. *WATER RESEARCH* 25: 1479-1486.
23. Khan, A.A., R.Z. Gaur, B. Lew, I. Mehrotra, and A.A. Kazmi. 2011. Effect of Aeration on the Quality of Effluent from UASB Reactor Treating Sewage. *Journal of Environmental Engineering* 137: 464-471.
24. Gillot, S., S. Capela-Marsal, M. Roustan, and A. Heduit. 2005. Prediction oxygen transfer of fine bubble diffused aeration systems-model issued from dimensional analysis. *Water Research* 39: 1379-1387.

25. Pittoors, E., Y. Gou, and S.W.H. Van Hulle. 2014. Oxygen transfer model development based on activated sludge and clean water in diffused aerated cylindrical tanks. *Chemical Engineering Journal* 243: 51-59.
26. Krevelen, W.V. and M.J. Jackson. 1956. *Industrial Engineering Chemical Program* 46: 29.
27. Hébrard, G. 1995. Etude de l'influence du distributeur de gaz sur l'hydrodynamique et le transfert de matière gaz-liquide des colonnes à bulles. INSA Toulouse.
28. Kumar, A., T.E. Delgaleesan, G.S. Laddha, and H.E. Hoelscher. 2009. Bubble swarm characteristics in bubble columns. *The Canadian Journal of Chemical Engineering* 54: 503-508.
29. Wilkinson, P.M., H. Haringa, and L.L.V. Dierendonck. 1994. Mass transfer and bubble size in a bubble column under pressure. *Chemical Engineering Science Journal* 49: 1417-1427.
30. Hadamard, J.S. and Ryazantsev. 1911. Mouvement permanent lent d'une sphere liquide et visqueuse dans un liquid visqueux. *Comptes rendus de l'Académie des sciences* 152: 1735-1738.
31. Frumkin, A. and V.G. Levich. 1947. On surfactants an interfacial motion. *Zh. Fiz. Khim* 21: 1183-1204.
32. Grace, J.R., T. Wairegi, and T.H. Nguyen. 1976. Shapes and velocities of single drops and bubbles moving freely through immiscible liquids. *Chemical Engineering Research and Design* 54: 167-173.
33. Mendelson, H.D. 1967. The prediction of bubble terminal velocities from wave theory. *American Institute of Chemical Engineers Journal* 13: 250-253.
34. Roustan, M. 1987. Coefficient de transfert et modèle de transferts. Transferts gaz-liquide dans les procédés de traitement des eaux et des effluents gazeux. Paris: Lavoisier
35. Levenspiel, O. 1999. *Chemical Reaction Engineering*. Third Edition. John Wiley & Sons. New York.
36. Levenspiel, O. 2012. *Tracer Technology: Modeling the Flow of Fluids*. Springer New York Dordrecht Heidelberg London.



**APPENDIX**



จุฬาลงกรณ์มหาวิทยาลัย  
CHULALONGKORN UNIVERSITY

**Appendix A** The oxygen transfer performance of the flexible tube diffuser

**Table A-1** The volumetric mass transfer coefficient ( $k_{La}$ ) and the operating pressure (P) of the 18 Flexible tube samples

Tube No.	$\times 10^{-3} k_{La}$ (1/s)			P (psi)		
	$Q_G$ (L/min)			$Q_G$ (L/min)		
	1	2	4	1	2	4
1	1.22	2.33	5.37	3.0	6.0	12.0
2	1.28	2.33	3.19	1.0	1.0	1.0
3	1.12	2.08	2.66	0.8	1.0	1.2
4	1.32	-	-	14.0	-	-
5	1.18	1.92	3.03	1.0	1.4	3.0
6	1.07	2.14	3.00	0.8	1.0	1.2
7	1.27	2.23	-	8.0	17.5	-
8	1.06	2.34	3.73	0.8	1.2	1.8
9	1.05	2.05	3.78	1.0	1.2	2.0
10	1.24	2.77	4.70	3.2	6.8	14.0
11	1.37	2.19	3.38	1.8	3.0	6.0
12	1.37	2.43	3.93	0.8	0.9	1.1
13	1.21	2.41	3.62	1.8	4.0	13.0
14	1.20	2.20	3.72	0.8	1.0	1.2
15	1.31	2.11	3.27	0.8	1.0	1.2
16	1.28	2.51	1.22	4.0	11.0	31.0
17	1.13	2.35	3.71	1.0	1.4	2.8
18	1.25	2.23	3.26	0.8	1.0	1.2

**Table A-2** Oxygen transfer efficiency (OTE) and Aeration efficiency (AE) of the 18 Flexible tube sample

Tube No.	OTE (%)			AE (kq-O <sub>2</sub> /kW-hr)		
	Q <sub>G</sub> (L/min)			Q <sub>G</sub> (L/min)		
	1	2	4	1	2	4
1.1	2.16	2.07	2.38	287	137	79
1.2	2.27	2.07	1.41	904	686	402
1.3	1.99	1.84	1.18	989	735	391
2.1	2.34	-	-	67	-	-
2.2	2.09	1.70	1.34	833	484	178
2.3	1.90	1.90	1.33	945	756	441
3.1	2.25	1.98	-	112	45	-
3.2	1.88	2.08	1.65	936	689	366
3.3	1.86	1.82	1.68	742	603	334
6.1	2.20	2.46	2.08	274	144	59
6.2	2.43	1.94	1.50	538	258	99
6.3	2.43	2.16	1.74	1,210	954	631
7.1	2.15	2.14	1.61	475	213	49
7.2	2.13	1.95	1.65	1,059	777	547
7.3	2.32	1.87	1.45	1,157	745	481
8.1	2.27	2.23	5.41	226	81	69
8.2	2.00	2.08	1.65	798	593	234
8.3	2.22	1.98	1.45	1,104	788	480

**Table A-3** Oxygen transfer performance of the stone tube diffuser:  $k_{La}$ , OTE, and AE in 180L aeration tank

Air flow rate	$k_{La_{20^{\circ}C}}$				$AE_{20^{\circ}C}$			
	1/hr				kg-O <sub>2</sub> /kW-hr			
L/min	1	2	3	Avg.	1	2	3	Avg.
5	1.82	2.43	1.90	<b>2.05</b>	7.64	9.90	7.90	<b>8.48</b>
10	3.25	4.30	3.18	<b>3.58</b>	5.88	7.65	5.77	<b>6.43</b>
15	4.43	5.37	4.25	<b>4.68</b>	4.68	5.57	4.48	<b>4.91</b>
20	5.40	6.56	5.02	<b>5.66</b>	4.28	5.19	4.05	<b>4.51</b>
25	6.74	7.87	6.08	<b>6.90</b>	3.80	4.43	3.49	<b>3.91</b>
30	7.55	9.02	6.78	<b>7.78</b>	3.22	3.81	2.92	<b>3.32</b>

**Table A-4** Oxygen transfer performance of the stone ball diffuser:  $k_{La}$ , OTE, and AE in 180L aeration tank

Air flow rate	$k_{La_{20^{\circ}C}}$				$AE_{20^{\circ}C}$			
	1/hr				kg-O <sub>2</sub> /kW-hr			
L/min	Center	Wall	Corner	Avg.	Center	Wall	Corner	Avg.
5	2.52	3.48	3.75	<b>3.25</b>	10.00	14.43	15.02	<b>13.15</b>
10	4.83	5.89	7.45	<b>6.05</b>	8.22	10.47	12.89	<b>10.53</b>
15	6.70	8.29	9.72	<b>8.24</b>	6.83	8.61	9.87	<b>8.44</b>
20	8.49	10.99	12.63	<b>10.70</b>	5.19	6.96	7.72	<b>6.63</b>
25	10.54	12.93	15.87	<b>13.11</b>	4.30	5.46	6.47	<b>5.41</b>
30	12.42	15.61	19.33	<b>15.79</b>	3.62	4.71	5.63	<b>4.65</b>

**Table A-5** Oxygen transfer performance of the flexible tube diffuser:  $k_La$ , OTE, and AE in 180L aeration tank

Air flow rate	$k_La_{20^\circ\text{C}}$				$AE_{20^\circ\text{C}}$			
	1/hr				kg-O <sub>2</sub> /kW-hr			
L/min	Center	Wall	Corner	Avg.	Center	Wall	Corner	Avg.
5	4.96	7.65	3.86	<b>5.49</b>	17.98	26.50	9.52	<b>18.00</b>
10	7.62	11.42	7.02	<b>8.69</b>	12.07	17.30	8.67	<b>12.68</b>
15	9.37	14.98	9.71	<b>11.35</b>	8.79	13.45	7.92	<b>10.05</b>
20	11.62	18.13	11.53	<b>13.76</b>	7.36	10.99	6.52	<b>8.29</b>
25	13.15	22.54	14.89	<b>16.86</b>	6.06	9.94	6.12	<b>7.37</b>
30	15.14	24.22	17.54	<b>18.97</b>	5.33	8.16	5.15	<b>6.21</b>

**Table A-6** Oxygen transfer performance of the membrane disc diffuser:  $k_La$ , OTE, and AE in 180L aeration tank

Air flow rate	$k_La_{20^\circ\text{C}}$				$AE_{20^\circ\text{C}}$			
	1/hr				kg-O <sub>2</sub> /kW-hr			
L/min	Center	Wall	Corner	Avg.	Center	Wall	Corner	Avg.
5	2.90	5.18	4.71	<b>4.26</b>	9.96	17.77	15.77	<b>14.50</b>
10	5.18	8.32	6.80	<b>6.77</b>	7.77	12.49	10.22	<b>10.16</b>
15	7.71	10.15	8.70	<b>8.85</b>	7.79	10.35	8.71	<b>8.95</b>
20	10.69	12.48	10.59	<b>11.25</b>	7.27	8.48	7.07	<b>7.60</b>
25	13.45	15.37	12.30	<b>13.70</b>	6.52	7.52	5.97	<b>6.67</b>
30	16.19	16.26	13.18	<b>15.21</b>	5.95	6.03	4.84	<b>5.61</b>

**Table A-7** The volumetric mass transfer coefficient ( $k_{La}$ ) of the tube No.12 in the 2,000L of pilot-scale experiment

Installation pattern	$\times 10^{-3} k_{La_{20^{\circ}C}} (1/s)$				
	$Q_G (L/min)$				
	60	70	80	90	100
1	2.25	2.30	2.44	3.04	2.79
2	1.81	2.09	3.02	3.23	3.68
3	1.92	2.24	2.39	2.57	2.78
4	1.83	2.19	2.73	2.86	3.46

**Table A-8** The volumetric mass transfer coefficient ( $k_{La}$ ) of the tube No.12 in the 2,000L of pilot-scale experiment

Installation pattern	$OTE_{20^{\circ}C} (1/s)$					Pressure (ปอนด์/ตร.นิ้ว)				
	$Q_G (L/min)$					$Q_G (L/min)$				
	60	70	80	90	100	60	70	80	90	100
1	15.33	13.48	12.50	13.83	11.45	4.00	4.50	5.00	5.50	6.00
2	12.36	12.22	15.47	14.69	15.08	3.50	4.00	4.50	5.00	5.50
3	13.10	13.12	12.25	11.70	11.41	4.00	4.30	5.00	5.50	6.40
4	12.48	12.79	13.97	13.03	14.18	3.50	3.90	4.60	5.00	5.80

**Table A-9** The volumetric mass transfer coefficient ( $k_{La}$ ) of the tube No.12 in the 2,000L of pilot-scale experiment

Installation pattern	$AE_{20^{\circ}C} \text{ kg-O}_2/\text{kW-hr}$				
	$Q_G (L/min)$				
	60	70	80	90	100
1	1,552	1,212	1,012	1,018	772
2	1,430	1,236	1,391	1,189	1,110
3	1,325	1,235	992	861	721
4	1,444	1,327	1,229	1,055	989

**Table A-10** The monitored conductivity in the RTD study in 2,000L aeration tank

<u>Pattern 1</u>				<u>Pattern 2</u>			
<b>Time</b>	<b>Conductivity</b>	<b>Time</b>	<b>Conductivity</b>	<b>Time</b>	<b>Conductivity</b>	<b>Time</b>	<b>Conductivity</b>
<b>min</b>	<b>μS</b>	<b>min</b>	<b>μS</b>	<b>min</b>	<b>μS</b>	<b>min</b>	<b>μS</b>
0	264	60	1,026	0	262	60	1,005
5	2,070	70	905	5	2,000	70	890
10	1,801	80	713	10	1,880	80	789
15	1,684	90	640	15	1,725	90	698
20	1,586	100	568	20	1,626	100	627
25	1,455	110	509	25	1,534	110	560
30	1,377	120	456	30	1,433	120	503
40	1,305	130	411	40	1,273	130	456
50	1,160	-	-	50	1,135	-	-
<u>Pattern 3</u>				<u>Pattern 4</u>			
<b>Time</b>	<b>Conductivity</b>	<b>Time</b>	<b>Conductivity</b>	<b>Time</b>	<b>Conductivity</b>	<b>Time</b>	<b>Conductivity</b>
<b>min</b>	<b>μS</b>	<b>min</b>	<b>μS</b>	<b>min</b>	<b>μS</b>	<b>min</b>	<b>μS</b>
0	258	60	998	0	272	40	1,263
5	2,010	70	882	3	1,926	50	1,122
10	1,851	80	784	6	1,927	60	995
15	1,741	90	696	9	1,836	70	887
20	1,637	100	620	12	1,781	80	788
25	1,538	110	553	15	1,726	100	700
30	1,442	120	451	20	1,609	110	622
40	1,272	130	412	30	1,426	120	559
50	1,127	-	-	-	-	-	-

## Appendix B Liquid Film Forming Apparatus (LFFA) in the aquaculture pond

**Table B-1** Oxygen transfer performance of the stone tube diffuser combining with LFFA in the aquaculture pond

Pattern	$k_L a_{20^\circ C}$ (1/hr)				AE (kg/kW-hr)			
	Avg.	Surface	Middle	Bottom	Avg.	Surface	Middle	Bottom
4-A	0.28	0.27	0.28	0.28	0.89	0.86	0.90	0.89
4-B	0.24	0.23	0.24	0.24	0.75	0.74	0.76	0.75
4-C	0.19	0.19	0.19	0.20	0.61	0.59	0.60	0.65
4-D	0.17	0.17	0.17	0.17	0.54	0.55	0.54	0.53
4-A*	0.20	0.20	0.21	0.20	0.65	0.63	0.67	0.64
4-D*	0.38	0.38	0.38	0.36	1.20	1.21	1.23	1.16

**Table B-2** Comparison of the flexible tube diffuser to the paddle wheel system

Unit	Flexible tube			Flexible tube + LFFA		
	$k_L a$	OTE	AE	$k_L a$	OTE	AE
	1/hr	%	kg/kWatt-hr	1/hr	%	kg/kWatt-hr
0	0	0	0	0	0	0
1	0.04	1.23	0.08	0.04	1.04	0.07
2	0.16	2.56	0.18	0.19	2.55	0.18
3	0.05	0.51	0.03	0.34	3.07	0.21
4	0.08	0.62	0.04	0.61	3.87	0.27

Unit	Paddle wheels		
	$k_L a$	OTE	AE
	1/hr	%	kg/kWatt-hr
0	0.00	-	0.00
1	0.02	-	0.01
2	0.02	-	0.01
3	0.10	-	0.05
4		-	



**Appendix C** The combination aeration system performance in 680L of pilot-scale experiment

**Table C-1** Results of the horizontal water velocity ( $v_H$ ) on the oxygen transfer performance when combined with the flexible tube diffuser

Number	$k_L a_{20^\circ C}$				$AE_{20^\circ C}$			
	1/hr				kg-O <sub>2</sub> /kW-hr			
sets	A	B	C	Avg.	A	B	C	Avg.
1 diffuser	1.67	2.40	1.26	<b>1.78</b>	0.66	0.95	0.50	<b>0.70</b>
2 diffusers	3.52	3.11	3.06	<b>3.23</b>	0.69	0.61	0.60	<b>0.63</b>
3 diffusers	3.86	4.37	3.71	<b>3.98</b>	0.50	0.57	0.48	<b>0.51</b>
4 diffusers	4.80	5.87	5.12	<b>5.26</b>	0.47	0.58	0.51	<b>0.52</b>

**Table C-2** Comparison of the aeration systems in term of the oxygen transfer performance

Diffuser + Pump	$k_L a_{20^\circ C}$				$AE_{20^\circ C}$			
	1/hr				kg-O <sub>2</sub> /kW-hr			
sets	A	B	C	Avg.	A	B	C	Avg.
+Pump (5.5W)	1.42	1.47	1.36	<b>1.42</b>	0.48	0.50	0.46	<b>0.48</b>
+Pump (8W)	1.60	1.60	1.61	<b>1.60</b>	0.46	0.46	0.47	<b>0.46</b>
+Pump (20W)	1.60	1.65	1.59	<b>1.61</b>	0.28	0.29	0.28	<b>0.28</b>
+Pump (30W)	1.71	1.73	1.73	<b>1.72</b>	0.22	0.23	0.23	<b>0.23</b>
+Pump (60W)	2.57	2.55	1.90	<b>2.34</b>	0.19	0.19	0.14	<b>0.18</b>
Combination 5.5W	3.66	3.34	3.11	<b>3.37</b>	0.51	0.46	0.43	<b>0.47</b>
Combination 60W	3.53	3.47	3.81	<b>3.61</b>	0.13	0.12	0.14	<b>0.13</b>
Paddle wheels	0.28	0.28	0.28	<b>0.28</b>	0.01	0.01	0.01	<b>0.01</b>

**Table C-3** Measure of the horizontal water velocity ( $v_H$ )

Pump (W)	Side	$t_1$	$t_2$	$t_3$	$t_4$	$t_5$	Avg.	Avg. $v_{HL}$
		s	s	s	s	s	s	m/s
1x60W	A	5.97	5.60	4.52	4.86	5.41	<b>5.27</b>	<b>0.18 (<math>\pm 1.5</math>)</b>
	B	8.21	8.60	8.61	6.80	7.04	<b>7.85</b>	
2x60W	-	4.56	4.88	4.91	4.57	5.17	<b>4.82</b>	<b>0.25 (<math>\pm 0.3</math>)</b>
1x30W	A	10.16	7.26	9.42	12.07	11.85	<b>10.15</b>	<b>0.11 (<math>\pm 2.0</math>)</b>
	B	14.31	9.24	12.16	9.43	10.62	<b>11.15</b>	
1x20W	A	11.70	10.83	13.71	11.39	11.87	<b>11.90</b>	<b>0.09 (<math>\pm 2.3</math>)</b>
	B	16.59	14.14	14.47	17.38	15.38	<b>15.59</b>	
1x8W	A	26.68	24.71	21.92	24.23	28.30	<b>25.17</b>	<b>0.04 (<math>\pm 4.8</math>)</b>
	B	35.30	30.88	26.40	34.08	35.26	<b>32.38</b>	
1x5.5W	A	33.76	31.90	27.97	27.84	27.24	<b>29.74</b>	<b>0.04 (<math>\pm 3.1</math>)</b>
	B	29.47	29.21	28.57	31.54	36.83	<b>31.12</b>	
2x5.5W	-	22.80	19.55	19.38	22.00	22.42	<b>21.23</b>	<b>0.06 (<math>\pm 1.6</math>)</b>

**Table C-4** Effects of the horizontal water velocity ( $v_H$ ) on the bubble hydrodynamic parameters

Diffuser + Pump	$d_B$	$U_B$	$f_B$	$N_B$	$a$
sets	mm	m/s	1/s	-	$m^2/m^3$
1	<b>3.94 (<math>\pm 0.8</math>)</b>	<b>0.58 (<math>\pm 0.1</math>)</b>	5,223	4,865	<b>1.31</b>
1 + 1 (5.5W)	<b>2.51 (<math>\pm 0.4</math>)</b>	<b>0.24 (<math>\pm 0.1</math>)</b>	20,197	45,345	<b>4.97</b>
1 + 1 (8W)	<b>2.48 (<math>\pm 0.3</math>)</b>	<b>0.24 (<math>\pm 0.1</math>)</b>	20,808	46,497	<b>5.00</b>
1 + 1 (20W)	<b>2.42 (<math>\pm 0.4</math>)</b>	<b>0.23 (<math>\pm 0.1</math>)</b>	22,539	53,542	<b>5.46</b>
1 + 1 (30W)	<b>2.39 (<math>\pm 0.5</math>)</b>	<b>0.23 (<math>\pm 0.1</math>)</b>	23,362	54,029	<b>5.38</b>
1 + 1 (60W)	<b>2.30 (<math>\pm 0.5</math>)</b>	<b>0.23 (<math>\pm 0.1</math>)</b>	26,074	62,175	<b>5.75</b>

**Table C-5** The residence time distribution study (RTD) results of the diffuser system (4 frames)

Time	$\theta$	Conductivity	E(t)	$E\theta = \frac{t}{x} \times E(t)$
min.	-	mS	1/min.	-
0	0.00	352	0.0044	0.2796
1	0.02	706	0.0088	0.5608
2	0.03	792	0.0099	0.6291
3	0.05	856	0.0107	0.6799
4	0.06	875	0.0110	0.6950
5	0.08	883	0.0111	0.7013
10	0.16	864	0.0108	0.6863
15	0.24	814	0.0102	0.6465
20	0.32	767	0.0096	0.6092
25	0.39	728	0.0091	0.5782
30	0.47	696	0.0087	0.5528
40	0.63	619	0.0078	0.4917
50	0.79	563	0.0071	0.4472
60	0.95	518	0.0065	0.4114
70	1.10	485	0.0061	0.3852
80	1.26	458	0.0057	0.3638
90	1.42	442	0.0055	0.3511
100	1.58	420	0.0053	0.3336
110	1.74	409	0.0051	0.3249
120	1.89	395	0.0049	0.3137
130	2.05	385	0.0048	0.3058
140	2.21	384	0.0048	0.3050
150	2.37	377	0.0047	0.2994

**Table C-6** The residence time distribution study (RTD) results of the paddle system

Time	$\theta$	Conductivity	E(t)	$E\theta^{-1} \times E(t)$
min.	-	mS	1/min.	-
0	0.00	356	0.0041	0.2571
1	0.02	1,050	0.0122	0.7584
2	0.03	1,035	0.0120	0.7476
3	0.05	1,017	0.0118	0.7346
4	0.06	996	0.0115	0.7194
5	0.08	980	0.0114	0.7079
10	0.16	914	0.0106	0.6602
15	0.24	896	0.0104	0.6472
20	0.32	830	0.0096	0.5995
25	0.40	781	0.0091	0.5641
30	0.48	741	0.0086	0.5352
40	0.64	679	0.0079	0.4904
50	0.80	629	0.0073	0.4543
60	0.96	559	0.0065	0.4038
70	1.12	523	0.0061	0.3778
80	1.28	505	0.0059	0.3648
90	1.44	468	0.0054	0.3380
100	1.61	441	0.0051	0.3185
110	1.77	429	0.0050	0.3099
120	1.93	411	0.0048	0.2969
130	2.09	404	0.0047	0.2918
140	2.25	395	0.0046	0.2853
150	2.41	387	0.0045	0.2795

**Table C-7** The residence time distribution study (RTD) results of the combination aeration system (5.5W of water pump)

Time	$\theta$	Conductivity	E(t)	$E\theta = \int_0^t E(t) \times E(t)$
min.	-	mS	1/min.	-
0	0.00	353	0.0039	0.2443
1	0.02	751	0.0084	0.5198
2	0.03	1,017	0.0114	0.7040
3	0.05	1,090	0.0122	0.7545
4	0.06	1,079	0.0121	0.7469
5	0.08	1,055	0.0118	0.7303
10	0.16	1,007	0.0113	0.6970
15	0.24	936	0.0105	0.6479
20	0.32	899	0.0101	0.6223
25	0.40	827	0.0093	0.5724
30	0.48	771	0.0086	0.5337
40	0.65	706	0.0079	0.4887
50	0.81	639	0.0071	0.4423
60	0.97	597	0.0067	0.4132
70	1.13	544	0.0061	0.3766
80	1.29	504	0.0056	0.3489
90	1.45	479	0.0054	0.3316
100	1.62	451	0.0050	0.3122
110	1.78	441	0.0049	0.3053
120	1.94	425	0.0048	0.2942
130	2.10	411	0.0046	0.2845
140	2.26	402	0.0045	0.2783
150	2.42	399	0.0045	0.2762

**Table C-8** The predicted results for bubble diameter

10L of aeration tank

<b>Qg</b>	<b>d<sub>B</sub>-Predicted</b>	<b>U<sub>B</sub>-Predicted</b>	<b>a-Predicted</b>	<b>k<sub>L</sub>-Predicted</b>	<b>k<sub>L</sub>a-Predicted</b>	<b>k<sub>L</sub>a-EXP</b>	<b>Error</b>
L/min	mm	m/s	m <sup>2</sup> /m <sup>3</sup>	x10 <sup>-4</sup> m/s	x10 <sup>-3</sup> 1/s	x10 <sup>-3</sup> 1/s	%
1	2.10	0.25	4.12	6.6	2.70	2.70	0
2	2.20	0.27	7.49	5.8	4.38	4.51	3
4	2.33	0.28	13.39	5.3	7.15	6.89	4

180L of aeration tank

<b>Qg</b>	<b>d<sub>B</sub>-Predicted</b>	<b>U<sub>B</sub>-Predicted</b>	<b>a-Predicted</b>	<b>k<sub>L</sub>-Predicted</b>	<b>k<sub>L</sub>a-Predicted</b>	<b>k<sub>L</sub>a-EXP</b>	<b>Error</b>
L/min	mm	m/s	m <sup>2</sup> /m <sup>3</sup>	x10 <sup>-4</sup> m/s	x10 <sup>-3</sup> 1/s	x10 <sup>-3</sup> 1/s	%
5	3.85	0.32	1.21	14.7	1.77	1.82	3
10	4.04	0.34	2.19	13.2	2.88	2.88	0
15	4.17	0.35	3.07	12.5	3.84	3.78	2
20	4.29	0.36	3.90	12.1	4.71	4.55	4
25	4.39	0.37	4.67	11.8	5.53	5.60	1
30	4.48	0.37	5.41	11.6	6.30	6.30	0

2,000L of aeration tank

<b>Qg</b>	<b>d<sub>B</sub>- Predicted</b>	<b>U<sub>B</sub>- Predicted</b>	<b>a- Predicted</b>	<b>k<sub>L</sub>- Predicted</b>	<b>k<sub>L</sub>a- Predicted</b>	<b>k<sub>L</sub>a-EXP</b>	<b>Error</b>
L/min	mm	m/s	m <sup>2</sup> /m <sup>3</sup>	x10 <sup>-4</sup> m/s	x10 <sup>-3</sup> 1/s	x10 <sup>-3</sup> 1/s	%
60	8.90	0.46	0.90	33.0	2.97	2.35	26
70	9.02	0.47	1.02	32.3	3.31	2.71	22
80	9.13	0.47	1.14	31.8	3.64	4.02	9
90	9.24	0.48	1.26	31.4	3.96	4.29	8
100	9.34	0.48	1.37	31.1	4.27	4.89	13

680L of aeration tank

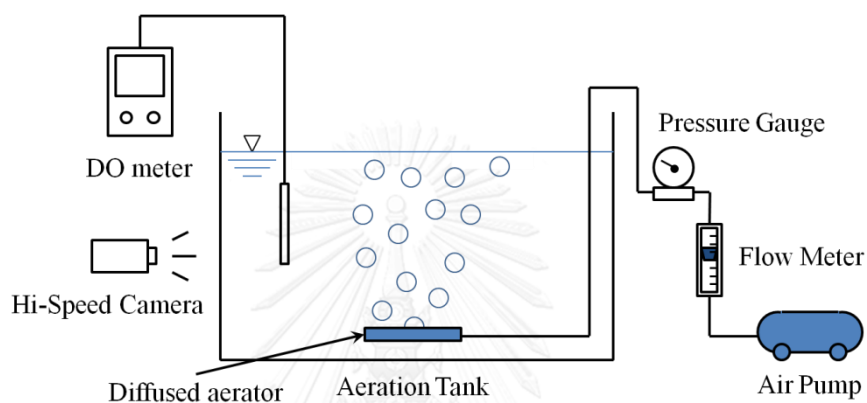
<b>Qg</b>	<b>d<sub>B</sub>- Predicted</b>	<b>U<sub>B</sub>- Predicted</b>	<b>a. Predicted</b>	<b>k<sub>L</sub>- Predicted</b>	<b>k<sub>La</sub>- Predicted</b>	<b>k<sub>La</sub>-EXP</b>	<b>Error</b>
L/min	mm	m/s	m <sup>2</sup> /m <sup>3</sup>	$\times 10^{-4}$ m/s	$\times 10^{-3}$ 1/s	$\times 10^{-3}$ 1/s	%
10	2.93	0.31	0.48	13.1	0.63	0.6.0	4
20	3.16	0.33	0.84	12.3	1.03	1.11	6
30	3.33	0.35	1.15	12.1	1.39	1.39	0
40	3.48	0.36	1.43	12.1	1.72	1.77	3



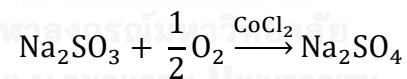
**Appendix D** The oxygen transfer parameters and bubble hydrodynamic parameters calculation

### D-1 Volumetric mass transfer coefficient ( $k_L a$ ) measurement and calculation

According to the standard for the measurement of oxygen transfer in clean water by the American Society of Civil Engineers (ASCE), New York (1992), an experiment can be set up in an aeration tank, which is filled by clean water or tap water, as following,



The initial dissolved oxygen (DO) can be eliminated by dosing a sodium sulfite ( $\text{Na}_2\text{SO}_3$ ) solution, or desorbed by nitrogen gas. The required  $\text{Na}_2\text{SO}_3$  can be estimated by this simple reaction,



And some cobalt chloride ( $\text{CoCl}_2$ ) can be added for further as a catalyst by 0.1-1% of the  $\text{Na}_2\text{SO}_3$  by mass. If the initial DO in a 10L of aeration tank is 6 mg/L, then the required  $\text{Na}_2\text{SO}_3$  will be,

$$\frac{1}{2} \text{ mole of O}_2 \quad \text{will require} \quad 1 \text{ mole of Na}_2\text{SO}_3$$

$$\text{if } \frac{6 \left(\frac{\text{mg}}{\text{L}}\right) \times 10 \text{ L}}{32 \left(\frac{\text{mg}}{\text{mmole}}\right)} \text{ mole of O}_2 \text{ will require } \frac{1}{1/2} \times \frac{60}{32} \text{ mmole of Na}_2\text{SO}_3$$

$$\text{The required Na}_2\text{SO}_3 = 3.75 \text{ mmole} \times \frac{126 \text{ mg}}{\text{mmole}} = \mathbf{472.5 \text{ mg}}$$

$$\text{The required CoCl}_2 = \frac{0.1}{100} \times 472.5 \text{ mg} = \mathbf{0.47 \text{ mg}}$$



The DO should be observed with the aeration time at the middle water depth. The measurement should be run until the DO achieve 80-90% of the saturated level. For the  $k_L a$  estimation, when an experiment for the  $k_L a$  measurement in the 180L of aeration tank, by installing a frame of flexible tube diffuser, operated by supplying 5 L/min of the air under the room temperature (26 °C). After the initial DO is removed by dosing the  $\text{Na}_2\text{SO}_3$  solution, the measurement is started with 0 mg/L of the DO, and the increasing of DO with time was monitored as following,

Operating time	DO	Operating time	DO
sec	mg/L	sec	mg/L
0	0.20	600	5.10
30	0.54	660	5.38
60	0.88	720	5.62
90	1.22	780	5.85
120	1.56	840	6.05
150	1.85	900	6.23
180	2.15	960	6.40
240	2.67	1,020	6.53
300	3.18	1,080	6.66
360	3.64	1,140	6.80
420	3.98	1,200	6.90
480	4.44	1,260	6.98
540	4.80	1,320	7.11

According to the 26 °C of operating condition then the saturated DO is 8.09 mg/L

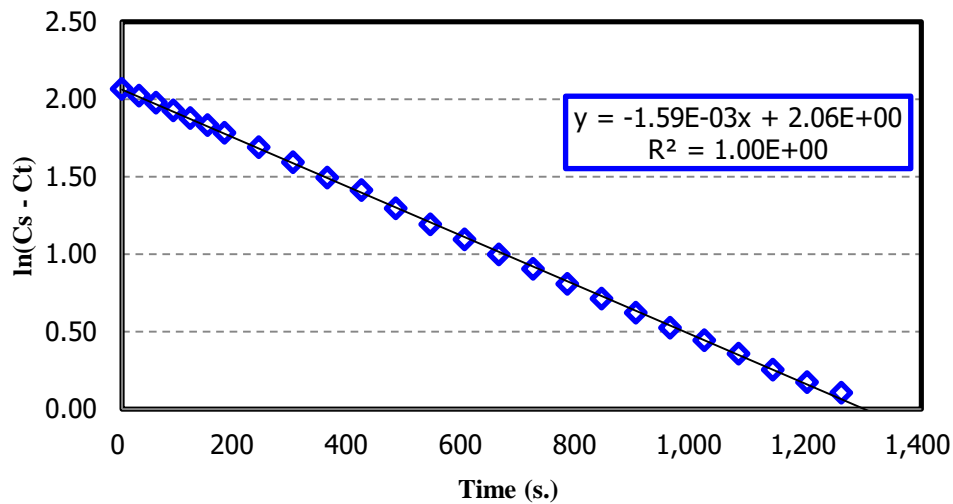
$$\text{At operating time} = 0 \text{ s} \quad C_S - C_t = 8.09 - 0.2 = 7.89$$

$$\ln(C_S - C_t) = 2.07$$

After that the values of  $\ln(C_S - C_t)$  can be obtained then the table of those can be presented as following,

Operating time	$\ln(C_s - C_t)$	Operating time	$\ln(C_s - C_t)$
sec	-	sec	-
0	2.07	600	1.10
30	2.02	660	1.00
60	1.98	720	0.90
90	1.93	780	0.81
120	1.88	840	0.71
150	1.83	900	0.62
180	1.78	960	0.52
240	1.69	1,020	0.44
300	1.59	1,080	0.36
360	1.49	1,140	0.25
420	1.41	1,200	0.17
480	1.29	1,260	0.10
540	1.19	1,320	-0.02

$\ln(C_s - C_t)$  vs. time



From the graph, the relation between  $\ln(C_s - C_t)$  and the operating time will be obtained as a linear trend, then the  $k_{L\alpha}$  value can be obtained by the slope of this linear. This  $k_{L\alpha}$  value will be considered as an actual  $k_{L\alpha}$  or  $k_{L\alpha T}$ . In order to compare to the other condition, this  $k_{L\alpha T}$  has to be converted into standard  $k_{L\alpha}$  at 20 °C or  $k_{L\alpha 20^\circ\text{C}}$ ,

$$k_{L\alpha 20^\circ\text{C}} = \frac{k_{L\alpha T}}{1.024^{(T-20)}}$$

$$k_L a_{20^\circ\text{C}} = \frac{1.59 \times 10^{-3}}{1.024^{(26-20)}} = 1.38 \times 10^{-3} \frac{1}{\text{s}}$$

$$k_L a_{20^\circ\text{C}} = 1.38 \times 10^{-3} \frac{1}{\text{s}} = 1.38 \times 10^{-3} \frac{1}{\text{s}} \times \frac{60 \text{ s}}{\text{min}} \times \frac{60 \text{ min}}{\text{hr}} = \mathbf{4.96 \frac{1}{\text{hr}}}$$

## D-2 Oxygen transfer efficiency (OTE) and Aeration efficiency (AE) calculation

After the  $k_L a_{20^\circ\text{C}}$  can be obtained the OTE can be estimated which can be considered as a standard oxygen transfer efficiency as following,

$$\text{OTE}_{20^\circ\text{C}} = \frac{\text{Oxygen}_{\text{Transferred}}}{\text{Oxygen}_{\text{Introduced}}} = \frac{k_L a \times C_S \times V}{\rho_G \times Q_G \times W_{O_2}}$$

$$\text{OTE}_{20^\circ\text{C}} = \frac{1.38 \times 10^{-3} \left(\frac{1}{\text{s}}\right) \times 8.09 \left(\frac{\text{g}}{\text{m}^3}\right) \times 0.18 \text{ (m}^3\text{)}}{1.201 \left(\frac{\text{kg}}{\text{m}^3}\right) \times 5 \left(\frac{\text{L}}{\text{min}}\right) \times \left(\frac{\text{m}^3}{1000 \text{ L}}\right) \times \left(\frac{\text{min}}{60 \text{ s}}\right) \times 0.21} = \mathbf{9.56\%}$$

When the air density ( $\rho_G$ ) is equal to  $1.201 \text{ kg/m}^3$  at  $20^\circ\text{C}$  and the oxygen contained in the air is around 21% by mass. For the operating pressure in this condition is around 0.7 psi, then the energy consumption can be estimated by

$$\text{Power} = 5 \left(\frac{\text{L}}{\text{min}}\right) \times \left(\frac{\text{m}^3}{1000 \text{ L}}\right) \times \left(\frac{\text{min}}{60 \text{ s}}\right) \times 0.7 \text{ (psi)} \times 6.895 \left(\frac{\text{kN/m}^2}{\text{psi}}\right)$$

$$\text{Power} = \mathbf{4.022 \times 10^{-4} \text{ kW}}$$

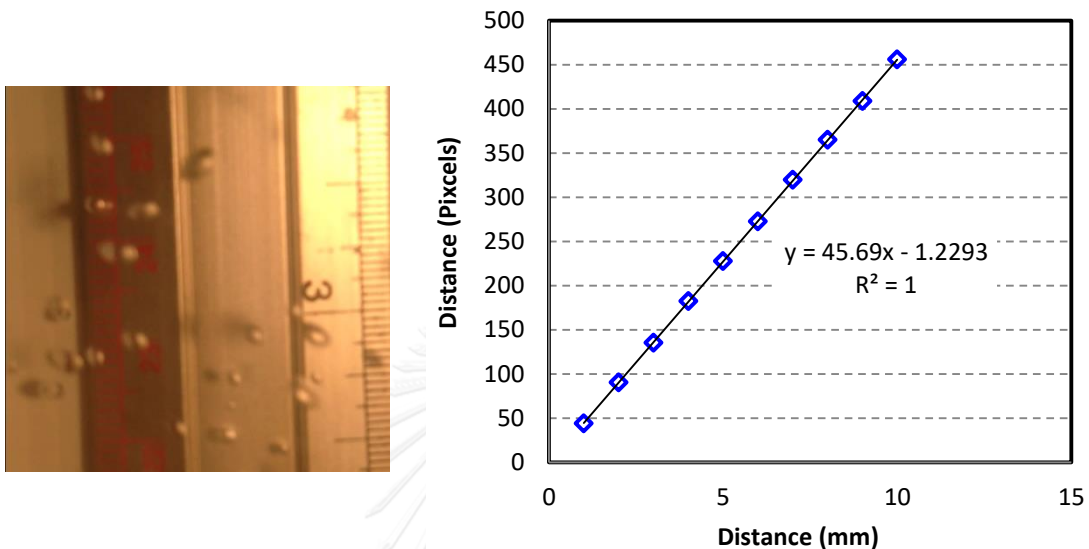
$$\text{AE} = \frac{k_L a \times C_S \times V}{\text{Power}} = \frac{1.38 \times 10^{-3} \left(\frac{1}{\text{s}}\right) \times 8.09 \left(\frac{\text{g}}{\text{m}^3}\right) \times 0.18 \text{ (m}^3\text{)}}{4.022 \times 10^{-4} \text{ kW}}$$

$$\text{AE} = \mathbf{17.98 \frac{\text{kg}_{O_2}}{\text{kW} - \text{hr}}}$$

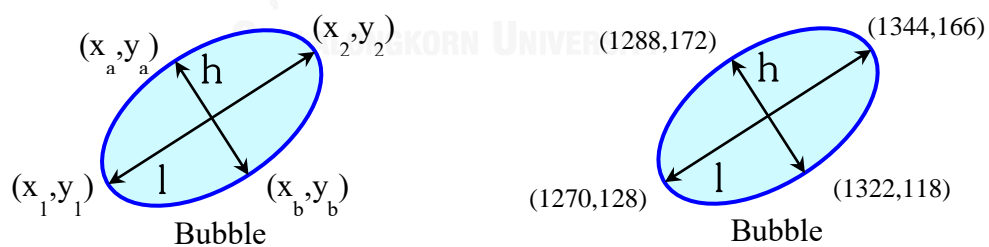
Finally, the aeration efficiency can be estimated by the above equation, which can be considered as the energy performance.

### D-3 Bubble diameter ( $d_B$ ), bubble rising velocity ( $U_B$ ), and interfacial area (a) calculation

At first, the scaling should be done by capturing the bubbles movement together with the scale,



According to the ImageJ software for the image analysis, the relation between the distance on the computer screen (pixels) and the actual size in the bubble capturing has to be investigated. From the above graph, it is found that 1 mm is equal to 45.69 pixels, when zooming 50%.



In the ImageJ software, the location on the computer screen will be shown as a coordination, then the bubble length ( $l$ ) and height ( $h$ ) can be estimated by

$$l = \sqrt{|1270 - 1344|^2 + |128 - 166|^2} = 83.19 \text{ pixels}$$

$$l = 83.19 \text{ pixels} \times \frac{\text{mm}}{45.69 \text{ pixels}} \times \frac{100}{50} \text{ zooming} = \mathbf{3.64 \text{ mm}}$$

$$h = \sqrt{|1288 - 1322|^2 + |172 - 118|^2} = 63.81 \text{ pixels}$$

$$h = 63.81 \text{ pixels} \times \frac{\text{mm}}{45.69 \text{ pixels}} \times \frac{100}{50} \text{ zooming} = \mathbf{2.79 \text{ mm}}$$

$$d_B = (l^2 \times h)^{1/3} = (3.64^2 \times 2.79)^{1/3} = \mathbf{3.33 \text{ mm}}$$

For the  $U_B$  estimation, if a bubble rises 822 pixels by the 17 frames of the capturing, and the capturing rate of this camera is around 350 frames/s. Then the its  $U_B$  can be estimated by,

$$U_B = \frac{\Delta D}{t} = \frac{822 \text{ pixels} \times \frac{\text{mm}}{45.69 \text{ pixels}} \times \frac{100}{50} \text{ zooming} \times \frac{\text{m}}{1000 \text{ mm}}}{17 \text{ frames} \times \frac{1}{350} \frac{\text{s}}{\text{frames}}}$$

$$U_B = \mathbf{0.74 \text{ m/s}}$$

After  $d_B$  and  $U_B$  can be obtained the interfacial area can be estimated as following,

$$a = \frac{N_B \times S_B}{V_{\text{Total}}} = f_B \times \frac{H_L}{U_B} \times \frac{\pi \times d_B^2}{(A \times H_L + N_B \times V_B)}$$

$$f_B = \frac{Q_G}{V_B} = \frac{5 \left( \frac{\text{L}}{\text{min}} \right) \times \left( \frac{\text{m}^3}{1000 \text{ L}} \right) \times \left( \frac{\text{min}}{60 \text{ s}} \right)}{\frac{\pi}{6} \times \left( \frac{3.33}{1000} \right)^3} = 4,310 \frac{1}{\text{s}}$$

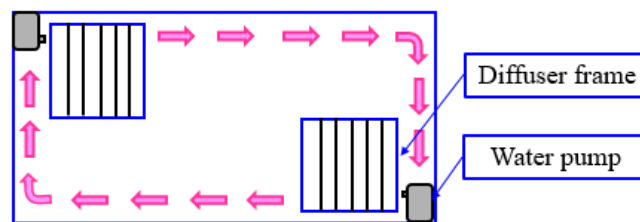
$$N_B = \frac{f_B \times H_L}{U_B} = \frac{4310 \left( \frac{1}{\text{s}} \right) \times 0.542 \text{ m}}{0.74 \left( \frac{\text{m}}{\text{s}} \right)} = 3,157 \text{ bubbles}$$

When the aeration tank is 0.563 m in width, 0.59 m in length, and 0.542 m in water depth.

$$a = 4310 \left( \frac{1}{\text{s}} \right) \times \frac{0.542 \text{ m}}{0.74 \left( \frac{\text{m}}{\text{s}} \right)} \times \frac{\frac{22}{7} \times \left( \frac{3.33}{1000} \right)^2 (\text{m}^2)}{0.18 \text{ m}^3} = \mathbf{0.61 \frac{\text{m}^2}{\text{m}^3}}$$

### D-1 Volumetric mass transfer coefficient ( $k_L a$ ) prediction

For the combination aeration system in the 680L of the tank, which is 1 m in width, 2.2 m in length, and 0.3 m in water depth. The characteristics of the flexible tube are 0.0038 mL/g-tube of total void volume, 350.52 g of the tube weight per 2.7 m of tube length, 0.23 mm of orifice size on the tube wall, a frame of the flexible tube consists of 2.7 m of tube length, tube thickness is around 2.7 mm.



If this combination system consists of 2 frames of the flexible tube, then supply 10 L/min of air flow rate for each frame (total air flow rate will be 20 L/min), the 57 mm/s of horizontal water velocity is applied by 2 water pumps. In this case, the  $k_L a$  value can be predicted by the following models,

$$A_{OR} = \frac{\text{Void volume} \times W_{\text{tube}}}{\text{Thickness}} = \frac{0.0038 \left(\frac{\text{mL}}{\text{g}}\right) \times 350.52 \text{ g}}{2.7 \text{ mm} \times \left(\frac{\text{m}}{1000 \text{ mm}}\right)} = 4.93 \times 10^{-4} \text{ m}^2$$

$$d_B = 4.71 D_{\text{Submerged}}^{1.1} + 0.78 \left(\frac{WL}{A_{OR}}\right)^{0.03} + 0.77 \left(\frac{Q_G}{d_{OR}}\right)^{0.46} - 0.92 v_H^{0.25}$$

$$d_B = 4.71(0.3)^{1.1} + 0.78 \left(\frac{1 \times 2.2}{4.93 \times 10^{-4}}\right)^{0.03} + 0.77 \left(\frac{\left(\frac{20}{1000 \times 60}\right)}{\left(\frac{0.23}{1000}\right)}\right)^{0.46} - 0.92 \left(\left(\frac{0.57}{1000}\right)\right)^{0.25}$$

$$d_B = 2.71 \text{ mm}$$

$$U_B = 1.262 \rho_L^{2.115} \mu_L^{2.211} g^{0.562} d_B^{0.26} Q_G^{0.057} - 0.079 v_H^{0.087}$$

$$U_B = 1.262(997)^{2.115} (0.001)^{2.211} (9.81)^{0.562} \left(\frac{2.71}{1000}\right)^{0.26} \left(\frac{20}{1000 \times 60}\right)^{0.057} - 0.079 \left(\frac{0.57}{1000}\right)^{0.087}$$

$$U_B = 0.26 \text{ m/s}$$

$$k_L = 0.767 \frac{(WL)^{0.207} d_B^{1.496} U_B^{0.654}}{D_{\text{Submerged}}^{0.234} Q_G^{0.307}} - 4.11 \times 10^{-5} \ln(v_H) + 2.10 \times 10^{-5}$$

$$k_L = 0.767 \frac{(1 \times 2.2)^{0.207} \left(\frac{2.71}{1000}\right)^{1.496} (0.26)^{0.654}}{(0.3)^{0.234} \left(\frac{20}{1000 \times 60}\right)^{0.307}} - 4.11 \times 10^{-5} \ln\left(\frac{57}{1000}\right) + 2.10 \times 10^{-5}$$

$$k_L = 9.7 \times 10^{-4} \text{ m/s}$$

$$f_B = \frac{Q_G}{V_B} = \frac{\left(\frac{20}{1000 \times 60}\right)}{\frac{\pi}{6} \times \left(\frac{2.71}{1000}\right)^3} = 32,059 \frac{1}{s}$$

$$N_B = \frac{f_B \times H_L}{U_B} = \frac{32059 \left(\frac{1}{s}\right) \times 0.3 \text{ m}}{0.26 \left(\frac{m}{s}\right)} = 37,248 \text{ bubbles}$$

$$a = \frac{N_B \times S_B}{V_{\text{Total}}} = f_B \times \frac{H_L}{U_B} \times \frac{\pi x d_B^2}{(AxH_L + N_B \times V_B)}$$

$$a = 32059 \left(\frac{1}{s}\right) \times \frac{0.3 \text{ m}}{0.26 \left(\frac{m}{s}\right)} \times \frac{\frac{22}{7} \times \left(\frac{2.71}{1000}\right)^2 \text{ (m}^2\text{)}}{0.68 \text{ m}^3} = 1.26 \frac{\text{m}^2}{\text{m}^3}$$

$$k_L a = k_L \times a = 9.7 \times 10^{-4} \left(\frac{m}{s}\right) \times 1.26 \left(\frac{m^2}{m^3}\right) = 1.2 \times 10^{-3} \left(\frac{1}{s}\right)$$

$$k_L a = 1.2 \times 10^{-3} \left(\frac{1}{s}\right) \times \left(\frac{3600 \text{ s}}{\text{h}}\right) = 4.4 \frac{1}{\text{hr}}$$

## VITA

Narapong Hongprasith is a Ph.D. student of the Department of Environmental Engineering, Faculty of Engineering, Chulalongkorn University. He completed his bachelor's degree in Environmental Engineering, Kasetsart University (Bangkhen Campus) at 2002. After that he 2 years to be an environmental engineer in the department of Thai Technology and Engineering Center (T-TEC), Ajinomoto Co., (Thailand) Ltd., Samut Prakan. Before returning to study further in master degree at the Department of Environmental Engineering, Chulalongkorn University at 2010, then he continued his study in the doctoral degree at the same department. His research is about the oxygen transfer in aeration systems, and how to improve the system efficiency that he wrote several articles about this topic. He currently resides in Bangkok with his parents, a younger brother, and a younger sister. Now he is planning to be a lecturer on his field at some university. You can reach his at [narapong\\_h@hotmail.com](mailto:narapong_h@hotmail.com).